NOTICE: When government or other drawings, specifications or other data are used for any purpose other than in connection with a definitely related government procurement operation, the U. S. Government thereby incurs no responsibility, nor any obligation whatsoever; and the fact that the Government may have formulated, furnished, or in any way supplied the said drawings, specifications, or other data is not to be regarded by implication or otherwise as in any manner licensing the holder or any other person or corporation, or conveying any rights or permission to manufacture, use or sell any patented invention that may in any way be related thereto.

ARL 62-318

LAMINAR FLOW BETWEEN TWO PARALLEL ROTATING DISKS

MARK C. BREITER
KARL POHLHAUSEN

APPLIED MATHEMATICS RESEARCH BRANCH

MARCH 1962

AERONAUTICAL RESEARCH LABORATORY
OFFICE OF AEROSPACE RESEARCH
UNITED STATES AIR FORCE

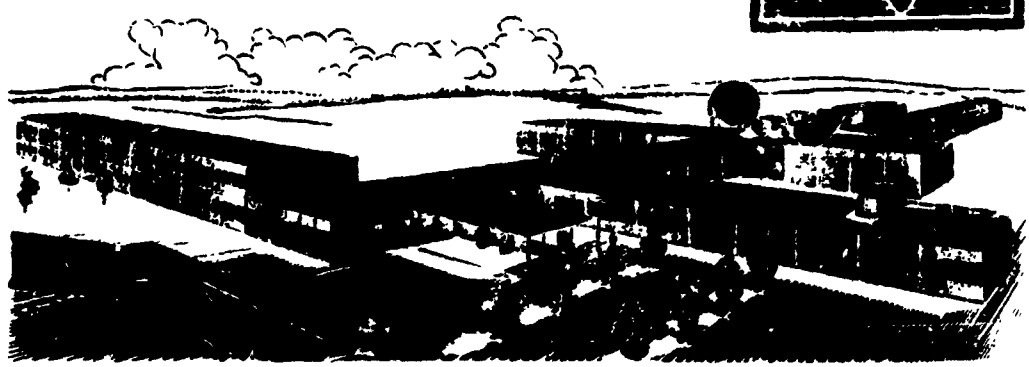

FOR ERRATA

AD 275562

THE FOLLOWING PAGES ARE CHANGES

TO BASIC DOCUMENT

ARL 62-318

March 1962

AD 275562

ERRATA - July 1962

Correct the last three lines on page 11 to read:

$$\bar{u} = \frac{u}{r_i \omega} \qquad \bar{x} = \frac{x}{r_i} \qquad \bar{r} = 1 + \bar{x}$$

$$\bar{V} = \frac{V}{r_i \omega} \qquad \bar{y} = y\sqrt{\frac{\omega}{\nu}} \qquad \bar{d} = d\sqrt{\frac{\omega}{\nu}}$$

$$\bar{w} = \frac{w}{\sqrt{\nu\omega}}$$

AERONAUTICAL RESEARCH LABORATORIES
OFFICE OF AEROSPACE RESEARCH
UNITED STATES AIR FORCE
WRIGHT-PATTERSON AIR FORCE BASE, OHIO

END CHANGE PAGES

NOTICES

When Government drawings, specifications, or other data are used for any purpose other than in connection with a definitely related Government procurement operation, the United States Government thereby incurs no responsibility nor any obligation whatsoever; and the fact that the Government may have formulated, furnished, or in any way supplied the said drawings, specifications, or other data, is not to be regarded by implication or otherwise as in any manner licensing the holder or any other person or corporation, or conveying any rights or permission to manufacture, use, or sell any patented invention that may in any way be related thereto.

Qualified requesters may obtain copies of this report from the Armed Services Technical Information Agency, (ASTIA), Arlington Hall Station, Arlington 12, Virginia.

This report has been released to the Office of Technical Services, U. S. Department of Commerce, Washington 25, D. C. for sale to the general public.

Copies of ARL Technical Reports and Technical Notes should not be returned to Aeronautical Research Laboratory unless return is required by security considerations, contractual obligations, or notices on a specific document.

ARL 62-318

LAMINAR FLOW BETWEEN TWO PARALLEL ROTATING DISKS

MARK C. BREITER
KARL POHLHAUSEN

APPLIED MATHEMATICS RESEARCH BRANCH

MARCH 1962

Project No. 7071
Task 70437

AERONAUTICAL RESEARCH LABORATORY
OFFICE OF AEROSPACE RESEARCH
UNITED STATES AIR FORCE
WRIGHT-PATTERSON AIR FORCE BASE, OHIO

300 - May 1962 - 31-1366 & 1367

FOREWORD

This report was prepared in the Applied Mathematics Research Br Aeronautical Research Laboratory, Office of Aerospace Research, Wr Patterson Air Force Base, Ohio.

The authors extend grateful acknowledgement to Dr. K. G. Guderl the Applied Mathematics Research Branch, for encouragement and mu advice.

The numerical calculations were carried out partly with the Recon graciously made available by Professor R. T. Harling of the Air Forc of Technology, and partly with the 1103A computer of the Digital Comp Branch, Systems Dynamic Analysis Division. Captain R. V. Hendon of Computation Branch rendered valuable assistance in programming.

The work was carried out un. Project 7071, "Methods of Mathen Physics", Task 70437.

FOREWORD

This report was prepared in the Applied Mathematics Research Branch of the Aeronautical Research Laboratory, Office of Aerospace Research, Wright-Patterson Air Force Base, Ohio.

The authors extend grateful acknowledgement to Dr. K. G. Guderley, Chief of the Applied Mathematics Research Branch, for encouragement and much helpful advice.

The numerical calculations were carried out partly with the Recomp computer, graciously made available by Professor R. T. Harling of the Air Force Institute of Technology, and partly with the 1103A computer of the Digital Computation Branch, Systems Dynamic Analysis Division. Captain R. V. Mendon of the Digital Computation Branch rendered valuable assistance in programming.

The work was carried out under Project 7071, "Methods of Mathematical Physics", Task 70437.

ABSTRACT

The report investigates the viscous flow between two parallel disks rotating in the same direction with the same velocity. The fluid enters the space between the two disks at a certain radius in the radial direction. Because of the shear forces, it assumes a rotating motion with about the velocity of the disks. The centrifugal forces then build up a pressure increase in the radial direction. The arrangement corresponds to a centrifugal fluid pump, which may be advantageous if cavitation is a problem.

The general equations of viscous flow are simplified by the assumption that the pressure difference normal to the disks is negligible (boundary layer assumptions). One obtains a system of parabolic partial differential equations. For large radii the deviation from rigid body rotation (with the angular velocity of the disks) is small. The linearized equations which then result are solved analytically. The velocity profiles depend upon a parameter containing the kinematic viscosity, the angular velocity and the distance of the disks, but not the radius.

The non-linearized parabolic differential equations are approximated by a difference scheme and solved numerically. The results are given in non-dimensional form with the entrance velocity and the distance of the disks as parameters. Furthermore, the efficiency of the pump is computed from the gain of the total pressure and the torque at the shaft of the rotating disks.

TABLE OF CONTENTS

Section		Page
I.	Introduction	1
II.	Statement of the Problem	3
III.	Linearized Treatment and Asymptotic Solution	5
IV.	Numerical Solution of the System of Equations (The Inlet Problem)	10
V.	Results and Conclusions	14
VI.	Appendix	17

LIST OF ILLUSTRATIONS

Figure		Page
1.	Schematic diagram of the flow between two rotating disks	21
2.	k_1 and k_2 versus αd	22
3.	$g(\alpha d)$ versus αd	23
4.	Radial velocity u and relative tangential velocity V for various values of αd	24
5.	Radial velocity $\bar{u}$ and relative tangential velocity $\bar{V}$ for $\bar{u}_0 = 1.0$ $\bar{d} = 0.5$	25
6.	Radial velocity $\bar{u}$ and relative rangential velocity $\bar{V}$ for $\bar{u}_0 = 0.5$ $\bar{d} = 0.5$	26
7.	Radial velocity $\bar{u}$ and relative tangential velocity $\bar{V}$ for $\bar{u}_0 = 0.25$ $\bar{d} = 0.5$	27
8.	Radial velocity $\bar{u}$ and relative tangential velocity $\bar{V}$ for $\bar{u}_0 = 0.1$ $\bar{d} = 0.5$	28
9.	Radial velocity $\bar{u}$ and relative tangential velocity $\bar{V}$ for $\bar{u}_0 = 1.0$ $\bar{d} = 1.0$	29
10.	Radial velocity $\bar{u}$ and relative tangential velocity $\bar{V}$ for $\bar{u}_0 = 0.5$ $\bar{d} = 1.0$	30
11.	Radial velocity $\bar{u}$ and relative tangential velocity $\bar{V}$ for $\bar{u}_0 = 0.25$ $\bar{d} = 1.0$	31
12.	Radial velocity $\bar{u}$ and relative tangential velocity $\bar{V}$ for $\bar{u}_0 = 0.1$ $\bar{d} = 1.0$	32

Figure		Page
13.	Radial velocity $\bar{u}$ and relative tangnetial velocity $\bar{V}$ for $\bar{u}_0 = 1.0$ $\bar{d} = 1.5$	33
14.	Radial velocity $\bar{u}$ and relative tangential velocity $\bar{V}$ for $\bar{u}_0 = 0.5$ $\bar{d} = 1.5$	34
15.	Radial velocity $\bar{u}$ and relative tangnetial velocity $\bar{V}$ for $\bar{u}_0 = 0.25$ $\bar{d} = 1.5$	35
16.	Radial velocity $\bar{u}$ and relative tangential velocity $\bar{V}$ for $\bar{u}_0 = 0.1$ $\bar{d} = 1.5$	36
17.	Radial velocity $\bar{u}$ and relative tangnetial velocity $\bar{V}$ for $\bar{u}_0 = 1.0$ $\bar{d} = 2.0$	37
18.	Radial velocity $\bar{u}$ and relative tangential velocity $\bar{V}$ for $\bar{u}_0 = 0.5$ $\bar{d} = 2.0$	38
19.	Radial velocity $\bar{u}$ and relative tangnetial velocity $\bar{V}$ for $\bar{u}_0 = 0.5$ $\bar{d} = 2.0$	39
20.	Radial velocity $\bar{u}$ and relative tangential velocity $\bar{V}$ for $\bar{u}_0 = 0.1$ $\bar{d} = 2.0$	40
21.	Radial velocity $\bar{u}_m$ versus r/r_i for $\bar{d} = 0.5$	41
22.	Radial velocity $\bar{u}_m$ versus r/r_i for $\bar{d} = 1.0$	41
23	Radial velocity $\bar{u}_m$ versus r/r_i for $\bar{d} = 1.5$	42
24.	Radial velocity $\bar{u}_m$ versus r/r_i for $\bar{d} = 2$	42
25.	$\bar{F}(\bar{r})$ for various values of $\bar{u}_0$ versus r/r_i for $\bar{d} = 0.5$	43

LIST OF ILLUSTRATIONS (Continued)

Figures		Page
26.	$\bar{F}(\bar{r})$ for various values of $\bar{u}_0$ versus r/r_i for $\bar{d} = 1.0$	44
27.	$\bar{F}(\bar{r})$ for various values of $\bar{u}_0$ versus r/r_i for $\bar{d} = 1.5$	44
28.	$\bar{F}(\bar{r})$ for various values of $\bar{u}_0$ versus r/r_i for $\bar{d} = 2.0$	45
29.	Moment, pressure, and efficiency versus r/r_i for $\bar{d} = 0.5$	46
30.	Moment, pressure, and efficiency versus r/r_i for $\bar{d} = 1.0$	47
31.	Moment, pressure, and efficiency versus r/r_i for $\bar{d} = 1.5$	48
32.	Moment, pressure, and efficiency versus r/r_i for $\bar{d} = 2.0$	49

I. INTRODUCTION

Investigated in this report is the viscous flow between two parallel disks, which rotate with the same constant angular velocity in the same direction. The fluid enters the space between the disks in radial direction through a cylindrical surface (Figure 1). It is set into a spiral motion whose tangential and radial velocity components are due to the friction forces and to the centrifugal forces respectively. The pressure will increase with the radius because of the centrifugal forces, thus the arrangement can serve as a centrifugal pump. One might suspect that the absence of blades leads to low values of the efficiency, but if the blades are spaced very closely and the mass flow is low, the efficiency may be quite acceptable. On the other hand, such a pump would not encounter the problem of cavitation and also its characteristics over a wide operating range might be more favorable than in a conventional turbo pump. These advantages were recognized by Mr. S. J. Hasinger, Mr. L. G. Kehrt and Dr. J. P. von Ohain of the Thermomechanics Research Branch of this laboratory. Technical details and experimental results will be published by them in a future report.

The present mathematical analysis will determine the velocity distribution between the disks, the pressures, the torque applied at the shaft and the resulting efficiency.

There exists an extensive literature on the single disk rotating in an infinite medium*. Assuming that the disk extends from radius zero to infinity, it is

---

*Advances in Applied Mathematics, Academic Press, Inc., New York, Vol IV, 1956, p. 166. F.K. Moore: Three-Dimensional Boundary Layer Theory.

possible to reduce the partial differential equations governing this problem to a system of ordinary differential equations by means of a similarity hypothesis. But an approach of this kind is not feasible in the present case because of the presence of the second disk and the fact that the flow enters the space between the disks at a radius different from zero. However, another simplification can be made here. For any practical application the distance between the disks must be very small, for otherwise the friction would not be sufficiently effective to produce a tangential flow. But then the approximations made in boundary layer theory apply reducing the original system of Navier-Stokes equations, which is elliptic, to a system of parabolic differential equations. They are derived in Section II.

A first insight into the basic characteristics of the problem is obtained if one assumes that the velocities of the fluid relative to the disks are small so that quadratic terms are negligible. This is a condition which is well satisfied for large radii; this idea is carried out in section III. It gives valuable insight into the general character of the velocity profiles; these profiles are governed by one dimensionless parameter which contains the angular velocity, the viscosity and the distance, but not the mass flow and the radius. Naturally this parameter is important for the practical design. The solutions thus obtained can be considered as an asymptotic expression for the solution of the actual non-linear system.

In the vicinity of the entrance radius the linearization is not justified, in particular the tangential velocity relative to the disks is certainly not small. This region is most critical from the point of view of cavitation, and also the principal losses are encountered there. Therefore, the system of differential equations has been integrated numerically. The methods and the results are shown in section IV and V and in an appendix.

II. STATEMENT OF THE PROBLEM

We use a system of cylindrical coordinates r and z (Figure 1), where the z axis coincides with the axis of symmetry and r is the distance from it. We denote by

- u the component of the velocity in the radial direction
- v the component of the velocity in the tangential direction measured in a system of coordinates fixed in space
- w the component of the velocity in the axial direction
- 2d the distance between the two disks
- r_i the radius of the entrance hole
- ρ the density
- μ the viscosity, $\nu = \frac{\rho}{\mu}$ the kinematic viscosity
- p the pressure
- ω the constant angular velocity.

An incompressible axi-symmetric steady viscous flow is described by the Navier-Stokes equations

$$u \frac{\partial v}{\partial r} + w \frac{\partial v}{\partial z} + \frac{u \cdot v}{r} = \nu \left(\frac{\partial^2 v}{\partial z^2} + \frac{\partial}{\partial r} \left(\frac{u}{r} + \frac{\partial^2 v}{\partial r^2} \right) \right)$$

$$u \frac{\partial w}{\partial r} + w \frac{\partial w}{\partial z} = -\frac{1}{\rho} \frac{\partial p}{\partial z} + \nu \left(\frac{\partial^2 w}{\partial z} + \frac{1}{r} \frac{\partial w}{\partial r} + \frac{\partial^2 w}{\partial r^2} \right) \qquad (2.1)$$

$$u \frac{\partial u}{\partial r} + w \frac{\partial u}{\partial z} - \frac{v^2}{r} = -\frac{1}{\rho} \frac{\partial p}{\partial r} + \nu \left(\frac{\partial^2 u}{\partial z^2} + \frac{\partial}{\partial r} \left(\frac{u}{r} + \frac{\partial^2 u}{\partial r^2} \right) \right)$$

and the equation of continuity,

$$\frac{\partial u}{\partial r} + \frac{u}{r} + \frac{\partial w}{\partial z} = 0 \qquad (2.2)$$

By applying the boundary layer approximations, this system of equations is reduced to

$$u\frac{\partial u}{\partial r} - \frac{v^2}{r} + w\frac{\partial u}{\partial z} = -\frac{1}{\rho}\frac{dp}{dr} + \nu\frac{\partial^2 u}{\partial z^2}$$

$$u\frac{\partial v}{\partial r} + \frac{u\cdot v}{r} + w\frac{\partial v}{\partial z} = \nu\frac{\partial^2 v}{\partial z^2} \qquad (2.3)$$

$$\frac{\partial u}{\partial r} + \frac{u}{r} + \frac{\partial w}{\partial z} = 0 \qquad (2.4)$$

It is convenient to introduce instead of v, which is the tangential velocity in a fixed system of coordinates, the tangential velocity V relative to the disks

$$V = v - r\omega \qquad (2.5)$$

One then obtains

$$u\frac{\partial u}{\partial r} - \frac{V^2 + 2Vr\omega + r^2\omega^2}{r} + w\frac{\partial u}{\partial z} = -\frac{1}{\rho}\frac{dp}{dr} + \nu\frac{\partial^2 u}{\partial z^2} \qquad (2.6)$$

$$u\left[\frac{\partial V}{\partial r} + \omega\right] + \frac{u[V + r\omega]}{r} + w\frac{\partial V}{\partial z} = \nu\frac{\partial^2 V}{\partial z^2} \qquad (2.7)$$

Along the disks, given by plane $z = \pm d$, one has the boundary conditions

$$u(r, \pm d) = 0$$

$$V(r, \pm d) = 0 \qquad (2.8)$$

To determine the boundary value problem completely, one must also prescribe the velocity distribution in the entrance cross section. One has

$$u(r_i, z) = u_0$$
$$V(r_i, z) = -r\omega \tag{2.9}$$

III. LINEARIZED TREATMENT AND ASYMPTOTIC SOLUTION

Omitting quadratic terms in u, V and w one obtains from Eqs (2.6) and (2.7)

$$\frac{\nu}{\omega}\frac{\partial^2 u}{\partial z^2} + 2V = \frac{1}{\rho\omega}\frac{dp}{dr} - r\omega \tag{3.1}$$

$$u = \frac{\nu}{2\omega}\frac{\partial^2 V}{\partial z^2} \tag{3.2}$$

In these equations $\frac{1}{\rho\omega}\frac{dp}{dr}$ does not depend upon z because of the boundary layer assumption that the pressure does not depend upon z. The unknown w does not appear, and so it is possible to solve these equations separately; w is determined from Eq (2.4) afterwards. It is remarkable that in these equations there appear no partial derivatives with respect to r. This means that, except for the expression

$$\frac{1}{\rho\omega}\frac{dp}{dr} - r\omega = F(r) \tag{3.3}$$

which depends upon r and is undetermined so far, the equations can be solved for each value of r independently. The expression (3.3) is the only innomogeneous term that occurs in the equations and in the boundary conditions; therefore, it will enter the solution for u and V as a factor which depends only on r. This factor

is determined by the condition that the mass flow between the disks is constant for every cross section r = const. Thus u and V as well as $\frac{1}{\rho}\frac{dp}{dr}$ can be found. After elimination of u one obtains from Eqs (3.1) and (3.2)

$$\frac{\nu^2}{2\omega^2}\frac{d^4V}{dz^4} + 2V = F(r) \tag{3.4}$$

Setting $\sqrt{\frac{\omega}{\nu}} = a$ one has finally

$$\frac{d^4V}{dz^4} + 4a^4 V = 2a^4 F(r) \tag{3.5}$$

As the most general solution of Eq (3.5) that satisfies the symmetry conditions at the plane z = 0, one finds

$$V = A_1 \sinh(az)\sin(az) + A_2 \cosh(az)\cos(az) + \frac{F(r)}{2} \tag{3.6}$$

where A_1 and A_2 are two constants which will be determined presently. The boundary conditions (2.8) together with Eq (3.2) give for $z = \pm d$

$$V = 0$$

$$u = \frac{1}{2a^2}\frac{d^2V}{dz^2} = 0 \tag{3.7}$$

Hence, by inserting Eq (3.6)

$$A_1 = -\frac{F(r)}{2} k_1 \qquad A_2 = -\frac{F(r)}{2} \cdot k_2 \tag{3.8}$$

with

$$k_1 = \frac{2 \sinh(ad) \cdot \sin(ad)}{\cosh(2ad) + \cos(2ad)}$$

$$k_2 = \frac{2 \cosh(ad) \cdot \cos(ad)}{\cosh(2ad) + \cos(2ad)} \tag{3.9}$$

Figure 2 shows k_1 and k_2 as a function of ad

The shear force at the wall is proportional to dV/dz. One finds

$$\frac{dV}{dz} = -a \frac{F(r)}{2} \left[(k_1 - k_2) \cosh(az) \sin(az) + (k_1 + k_2) \sinh(az) \cos(az) \right] \tag{3.10}$$

Let the flow of liquid (measured by volume) be given by Q. The flow through a surface r = const extending between the disks is given by

$$Q = 2\pi r \int_{-d}^{+d} u dz = \frac{\pi \cdot r}{a^2} \int_{-d}^{+d} \frac{d^2 V}{dz^2} dz = \frac{\pi \cdot r}{a^2} \cdot \frac{dV}{dz} \Bigg|_{-d}^{+d} \tag{3.11}$$

Hence with Eq (3.10)

$$Q = -\frac{\pi \cdot r}{a} \cdot F(r) \cdot g(ad) \tag{3.12}$$

where:

$$g(ad) = \frac{\sinh(2ad) - \sin(2ad)}{\cosh(2ad) + \cos(2ad)} \tag{3.13}$$

Figure 3 shows $g(ad)$ as a function of ad

From Eq (3.13) we find the function $F(r)$

$$F(r) = \pm \frac{aQ}{\pi \cdot r \cdot g(ad)} = - \frac{2q}{r} \tag{3.14}$$

where

$$q = \frac{aQ}{2\pi \cdot g(ad)} \tag{3.15}$$

One thus obtains finally for the velocity components, expressed in terms of the mass flow

$$V = \frac{q}{r}\left[k_1 \sinh(az) \sin(az) + k_2 \cosh(az) \cos(az) - 1\right] \tag{3.16}$$

$$u = \frac{q}{r}\left[k_1 \cosh(az) \cos(az) - k_2 \sinh(az) \sin(az)\right] \tag{3.16}$$

Inserting these expressions into the continuity equation Eq (2.4) one finds $w = 0$.

The velocities in the middle plane between the two disks are found by setting $z = 0$.

$$V_{z=0} = \frac{q}{r} \cdot \left[k_2 - 1\right]$$

$$u_{z=0} = \frac{q}{r} \cdot k_1 \tag{3.17}$$

Figure 4 shows the radial velocity component for different values of αd as a function of z/d for $q/r = 1$. For small values of αd, the profiles have a near parabolic shape with maximum velocity in the middle ($z = 0$). For $\alpha d = \pi/2$ the profile is flat in the middle, for higher value of αd the flow is more and more concentrated in the neighborhood of the disks.

The tangential velocity V is represented in Figure 4 for $q/r = 1$. For small values of αd it also has a parabolic shape, but with increasing αd the slope in the vicinity of the disks becomes steeper and the relative velocity in the middle plane approaches -1.

Actually the profiles for high values of αd must be viewed with considerable caution. One sees that in this case the velocity u may become negative in the middle; i.e. for such cases one has a radial outflow close to the disks with a radial inflow in the middle. Obviously it would take a rather special arrangement to produce such a flow pattern physically. These results ought to be disregarded for technical applications. Important in any case is the role played by the dimensionless parameter αd which determines the character of the profiles. This character is neither influenced by the mass flow Q nor by the radius r. For a given ω and a given ν, i.e., a given fluid, the only quantity that can be influenced in this parameter is the distance of the disks. If one wants to use high angular velocities, one must try to lower the value of d by skillful design.

The pressure distribution is obtained from the function F(r) in Eq (3.5). Inserting Eq (3.14) into (3.3).

one finds

$$\frac{dp}{dr} = \rho\omega \left[r\omega - \frac{2q}{r} \right] \qquad (3.18)$$

and by integration

$$p = \rho\omega \left[\frac{r^2\omega}{2} - 2q\ln r + \text{const} \right] \tag{3.19}$$

The momentum required at the shaft of the rotor can be determined in two different ways, either from the moment of the shearing forces on the inner side of two disks, or by applying the law of conservation for the moment of momentum. One has in the first case

$$M = 2 \cdot 2\pi \cdot \mu \int_{r_i}^{r} r^2 \left(\frac{dV}{dz} \right)_{z=d} dr \tag{3.20}$$

in the second

$$M = 2\pi r^2 \rho \int_{-d}^{+d} u \cdot v \, dz \tag{3.21}$$

For the numerical evaluation the second one is preferable.

IV. NUMERICAL SOLUTION OF THE SYSTEM OF EQUATIONS (THE INLET PROBLEM)

The approximation shown in the previous section is unsatisfactory in the vicinity of the entrance, where the velocity components are certainly not small. Moreover, the linearization causes all r-derivatives to vanish, i. e. it introduces such a strong change of the character of the flow equations, that it becomes impossible to satisfy the boundary conditions at the inlet. But the inlet is important for it accounts for most of the losses.

As was mentioned above, the introduction of the boundary layer assumption gives us a parabolic system of differential equations where lines r = const are the characteristics, therefore, it is possible to proceed in the numerical solutions from one line r = const to the next one without any need to go back. Thus, we may adopt a numerical scheme for the integration of the parabolic differential equations.

For our computations we assumed that the rotating disks lie in horizontal planes, and introduce a new system of coordinates x, y, whose origin lies in the entrance cross section at the lower disk. Thus the x-axis coincides with the lower disk. We have

$$x = r - r_i$$

$$y = z + d$$

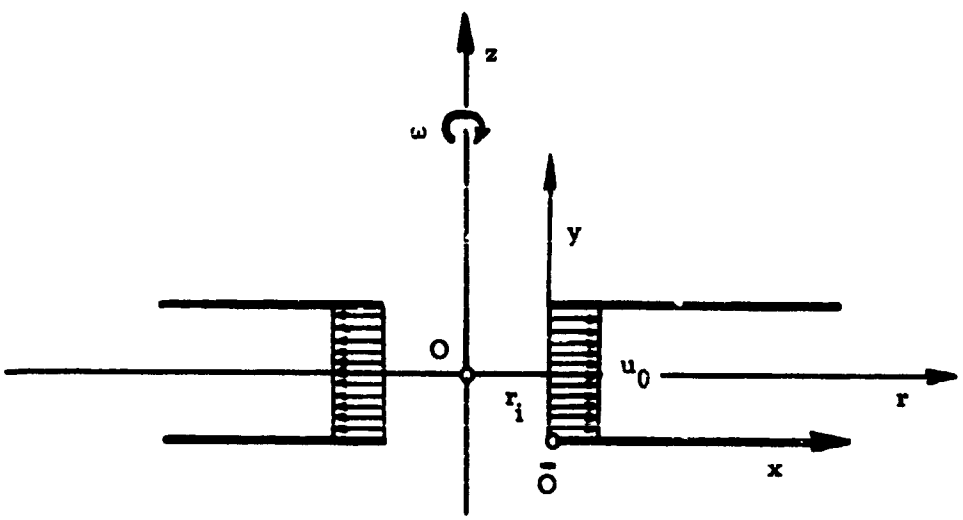

We introduce dimensionless variables in the system of differential equations (2.6), (2.7), and (2.4)

$$\bar{u} = u \frac{\omega}{r_i} \qquad \bar{x} = \frac{x}{r_i} \qquad \bar{r} = 1 + \bar{x}$$

$$\bar{V} = V \frac{\omega}{r_i} \qquad \bar{y} = y \cdot \frac{\omega}{r} \qquad \bar{d} = d\sqrt{\frac{\omega}{\nu}}$$

$$\bar{w} = \frac{w}{\sqrt{\nu \omega}}$$

One thus obtains

$$\bar{u}\,\frac{\partial \bar{u}}{\partial \bar{x}} - \bar{V}\left[\frac{\bar{V}}{1+\bar{x}} + 2\right] + \bar{w}\,\frac{\partial \bar{u}}{\partial \bar{y}} = \bar{F}(\bar{r}) + \frac{\partial^2 \bar{u}}{\partial \bar{y}^2}$$

$$u\left[\frac{\partial \bar{V}}{\partial \bar{x}} + \frac{\bar{V}}{1+\bar{x}} + 2\right] + \bar{w}\,\frac{\partial \bar{V}}{\partial \bar{y}} = \frac{\partial^2 \bar{V}}{\partial \bar{y}^2} \qquad (4.2)$$

$$\frac{\partial \bar{u}}{\partial \bar{x}} + \frac{\bar{u}}{1+\bar{x}} + \frac{\partial \bar{w}}{\partial \bar{y}} = 0$$

where for abbreviation

$$F(r) = r - \frac{1}{\rho\omega^2 r^2}\,\frac{dp}{dr} \qquad (4.3)$$

The functions $\bar{u}$ and $\bar{V}$ and $\bar{w}$ are given at the entrance ($\bar{x} = 0$). The channel extends from $\bar{y} = 0$ to $\bar{y} = 2\bar{d}$. The boundary condition at $\bar{y} = 2\bar{d}$ can be replaced by a symmetry condition at $\bar{y} = \bar{d}$. Thus, one has as boundary conditions

$$\bar{u}(\bar{x}, 0) = 0 \qquad \frac{\partial \bar{u}(\bar{x}, \bar{d})}{\partial \bar{y}} = 0$$

$$\bar{V}(\bar{x}, 0) = 0 \qquad \frac{\partial \bar{V}(\bar{x}, \bar{d})}{\partial \bar{y}} = 0 \qquad (4.4)$$

$$\bar{w}(\bar{x}, 0) = 0 \qquad \bar{w}(\bar{x}, \bar{d}) = 0$$

The natural method of solving such a system numerically is the introduction of a difference scheme. Here caution is needed from the point of view of stability.

The coefficients of the derivatives with respect to $\bar{x}$, in Eq (4.2) may become very small for large values of $\bar{x}$ and it also is small in the vicinity of $\bar{y} = \bar{d}$, but then it is necessary to use a very fine mesh size in the $\bar{x}$ direction, if one applies a "direct" difference scheme where the derivatives with respect to $\bar{y}$ are computed along the line $\bar{x}$ = const which is already known. Otherwise the procedure would become unstable.

For this reason it was decided to use an "inverse" difference procedure where the derivatives are formed along the line $\bar{x}$ = const for which the state is to be computed. This brings about a rather severe complication, for the state along the new line $\bar{x}$ = const is determined by a system of simultaneous equations. Since the original differential equations are non-linear, this system of equations is also non-linear. At first the non-linear system was solved directly by an iteration method. Since this method proved to be inconvenient, approach was modified in the following manner: In going from one line $\bar{x}$ = const to the next one we computed the changes of $\bar{\rho}$, $\bar{V}$ and $\bar{w}$ rather than the values themselves. If a difference procedure is admissible at all, these changes ought to be small and second order terms in these changes are negligible. In other words we use a linearization which considers as a basic approximation the values at the line $\bar{x}$ = const which has been computed previously.

The state along the new line can then be obtained by a suitable super-position of particular solutions of the linear equation which arises in this manner. The linear system of equation which arises in this process has a rather simple structure insofar as the matrix of systems has elements that are different from zero on only a few lines that are parallel to the main diagonal. This brings about certain simplifications in the inversion of the matrix. For further details of the

numerical analysis see the appendix.

V. RESULTS AND CONCLUSIONS

The numerical procedure described above gives a nearly complete description of the flow pattern. Assuming constant velocity $\bar{u}_0$ at the entrance, we give the results for a set of four initial radial velocities $\bar{u}_0 = 1.0,\ 0.5,\ 0.25$ and 0.1. The initial tangential velocity $\bar{V}_0$ is always $\bar{V}_0 = -1$ because of Eq (2.5). For the dimensionless distance between the disks we choose $\bar{d} = 0.5,\ 1.0,\ 1.5$, and 2.

Figures 5 thru 20 show the dimensionless velocity profiles versus z/d with r/r_i as parameter. These profiles have a common characteristic: at the wall the inlet velocities $\bar{u}_0$ and $\bar{v}_0$, which are constant over the cross section, are immediately reduced to zero because of the boundary conditions. The reduction of the radial velocities at the wall causes the velocities in the middle to increase. Therefore the radial velocity in the profiles close to the entrance cross section overshoots the entrance profile in the middle. The effect decreases with increasing r because of the increase of the available cross section with r, finally the profile approaches the form given by the linearized theory. Figures 21 thru 24 show this behavior again; here the radial velocities $\bar{u}_m$ in the median plane of the disks ($z = 0$) are plotted versus r/r_i. The average radial velocities are obviously determined by the condition of continuous flow.

The average tangential velocity is directly connected with the moment M of the shear forces and thus with the work that must be performed to drive the pump. Furthermore it gives the main contribution to the dynamic pressure of the fluid particles as they leave the pump, thus it influences strongly the efficiency. As mentioned before shear forces can be obtained from the slope of the velocity

profiles at the wall Eq (3.18); but it appears to be preferable (from the numerical point of view) to compute it from the radial and tangential velocities Eq (3.19).

The pressure distribution is computed from the function $\bar{\bar{F}}(\bar{r})$ which is found in the numerical procedure as a function of r/r_i. Here an integration in the direction of r is required. In our figures the contribution to p due to the term $\bar{r}$ in Eq (4.3) is shown separately, (as a straight line). The pressures are given by the difference of the curve $\bar{F}(\bar{r})$ from this straight line.

Properly speaking the dynamic pressure varies from streamline to streamline. For technical purposes only the average velocity can be utilized. The dynamic pressure for the average velocity is slightly lower than the average of the dynamic pressures; in other words in defining the dynamic pressure with average velocities one takes into account the mixing losses. Thus, we have according to Bernoulli's equation

$$p_d = \frac{\rho}{2}\left[u_{av}^2 + v_{av}^2\right]$$

The efficiency η of the process in the pump is best defined by

$$\eta = \frac{p_s + p_d}{M \cdot \omega} \cdot Q$$

where $Q = 2\pi r_i \cdot 2du_0$ denotes the amount of fluid entering at r_i. Figures 29 thru 31 show, for $\omega = \rho = 1$, the moment M, the total pressure $p_s + p_d$ and the efficiency versus $\frac{r}{r_i}$ for the chosen values of $\bar{u}_0$ and $\bar{d}$.

According to the linearized approach the profiles at large values of r do not depend upon the flow field at smaller radii, thus dynamic pressure and torque are determined only by the exit cross section. However the static pressure arises by

an integration over the pressure gradient in the radial direction. The losses encountered appear in this analysis as losses in static pressure.

The exit cross section does not play a special role in the computation; in other words, each value of r can be considered as the other radius of the rotor.

In the vicinity of the entrance, one has always a slight pressure drop, for large volume flow the pressure drop is more pronounced, and this fact is of interest from the point of view of computations. High mass flows are also detrimental from the point of view of efficiency.

APPENDIX

For the numerical solution of the system of equations (4.2) we set up a network of lines $\bar{x}$ = constant and $\bar{y}$ = constant with a spacing of h and ℓ respectively along the $\bar{x}$ and $\bar{y}$ axes. The length ℓ is chosen as one twentieth of the distance from the wall to the median plane of the disks. The derivatives in Eqs (4.2) are replaced by difference quotients, e.g.

$$\frac{\partial \bar{u}}{\partial \bar{x}} = \frac{\bar{u}_{i+1,k} - \bar{u}_{i,k}}{h}, \quad \frac{\sigma \bar{w}}{\sigma \bar{y}} = \frac{\bar{w}_{i+1,k+1} - \bar{w}_{i+1,k-1}}{2\ell}$$

$$\frac{\partial^2 \bar{u}}{\partial \bar{y}^2} = \frac{\bar{u}_{i+1,k+1} - 2\bar{u}_{i+1,k} + \bar{u}_{i+1,k-1}}{\ell^2} \tag{A1}$$

Here i and i+1 correspond to successive lines $\bar{x}$ = constant and k - 1, k, and k+1 to successive lines $\bar{y}$ = constant with k = 0 at the wall. Starting with given values of $\bar{u}$, $\bar{V}$, $\bar{w}$ at the line x = const (i = 0) corresponding to the inlet, we determine the unknown values of $\bar{u}$, $\bar{V}$, $\bar{w}$ on the (i+1)st line from the known values on the i-th line.

It is convenient to introduce as new unknowns the differences $\Delta\bar{u}_k$, $\Delta\bar{V}_k$, $\Delta\bar{w}_k$, defined by

$$\Delta \bar{u}_k = \bar{u}_{i+1,k} - \bar{u}_{i,k},$$

and similarly for $\Delta\bar{V}_k$, and $\Delta\bar{w}_k$, and neglect all terms in the equations of higher order in the Δ's. (Naturally these Δ's will also depend on i, but only one value of i is needed at a time).

Equations (4.2) then lead to the following linear difference equations in the unknown differences $\Delta\bar{u}$, $\Delta\bar{V}$, and $\Delta\bar{w}$ and the unknown pressure function $f(\bar{x})$.

$$(1-\frac{\ell}{2}\bar{w}_{i,k})\Delta\bar{u}_{k+1} = -\bar{u}_{i,k+1}(1-\frac{\ell}{2}\bar{w}_{i,k})+2\bar{u}_{i,k}-\bar{u}_{i,k-1}(1+\frac{\ell}{2}\bar{w}_{i,k})$$

$$-\ell^2\bar{V}_{i,k}(\frac{\bar{V}_{i,k}}{\bar{x}}+2)+(2+\frac{\ell^2}{h}\bar{u}_{i,k})\Delta\bar{u}_k$$

$$-(1+\frac{\ell}{2}\bar{w}_{i,k})\Delta\bar{u}_{k-1}+\frac{\ell}{2}(\bar{u}_{i,k+1}-\bar{u}_{i,k-1})\Delta\bar{w}_k$$

$$-2\ell^2(\frac{\bar{V}_{ik}}{\bar{x}}+1)\Delta\bar{V}_k-\ell^2 f(\bar{x}),$$

$$(1-\frac{\ell}{2}\bar{w}_{ik})\Delta\bar{V}_{k+1} = -\bar{V}_{i,k+1}(1-\frac{\ell}{2}\bar{w}_{i,k})+2\bar{V}_{i,k}+\frac{\ell^2}{h}\bar{V}\quad\bar{u}_{i,k}(1+\frac{h}{\bar{x}}) \qquad (A2)$$

$$-\bar{V}_{i,k-1}(1+\frac{\ell}{2}\bar{w}_{i,k})+(2\ell^2-\frac{\ell^2}{h}\bar{V}_{i,k-1})\bar{u}_{i,k-1}$$

$$+\frac{\ell}{2}(\bar{V}_{i,k+1}-\bar{V}_{i,k-1})\Delta\bar{w}_k+\ell^2(\frac{\bar{V}_{i,k}}{\bar{x}}+2)\Delta\bar{u}_k$$

$$+[2+\frac{\ell^2}{h}\bar{u}_{i,k}(1+\frac{h}{x})]\Delta\bar{V}_k-(1+\frac{\ell}{2}\bar{w}_{i,k})\Delta\bar{V}_{k-1},$$

$$\Delta\bar{w}_{k+1} = \Delta\bar{w}_{k-1}-\frac{2\ell}{h}(1+\frac{h}{\bar{x}})\Delta u_k-\frac{2\ell}{\bar{x}}\bar{u}_{i,k}-\bar{w}_{i,k+1}+\bar{w}_{i,k-1}.$$

In addition to Eqs (A2) the complete specification of the problem requires Eqs (A3), (A4), and (A5) resulting from boundary conditions.

Since $\bar{u} = \bar{V} = \bar{w} = 0$ along the wall, one has

$$\Delta \bar{u}_0 = \Delta \bar{V}_0 = \Delta \bar{w}_0 = 0. \tag{A3}$$

Since $\bar{u}$ and $\bar{V}$ are symmetric and $\bar{w}$ antisymmetric with respect to the median plane of the disks,

$$\begin{aligned} \Delta \bar{u}_{21} - \Delta \bar{u}_{19} &= 0, \\ \Delta \bar{V}_{21} - \Delta \bar{V}_{19} &= 0, \\ \Delta \bar{w}_{20} &= 0. \end{aligned} \tag{A4}$$

In the continuity equation there appear only first derivatives with respect to $\bar{y}$, while the other equations contain second derivatives. One will notice that in Eq (A1) the first derivative of $\bar{w}$ with respect to $\bar{y}$ has not been formed from values $\bar{w}$ at adjacent points. This was done in order to obtain a central difference formula for $\frac{\partial \bar{w}}{\partial \bar{y}}$, just as for $\frac{\partial^2 \bar{u}}{\partial \bar{y}^2}$ and $\frac{\partial^2 \bar{V}}{\partial \bar{y}^2}$. As a consequence one equation is lost. Therefore, the following approximation is made in the vicinity of the wall. In the last of equations (4.2) the term $\frac{\partial \bar{u}}{\partial \bar{x}}$ is zero at the wall; $\bar{u}$ may be approximated by its linear term. Thus

$$\begin{aligned} \bar{u} &= f(\bar{x}) \cdot \bar{y}, \\ \frac{\partial \bar{u}}{\partial \bar{x}} &= f'(\bar{x}) \cdot \bar{y}, \\ \frac{\partial \bar{w}}{\partial \bar{y}} &= -f'(\bar{x})\bar{y} - \frac{f'(\bar{x})}{1+\bar{x}}\bar{y} = A(\bar{x})\bar{y}, \\ \bar{w} &= A(\bar{x})\frac{\bar{y}^2}{2}. \end{aligned} \tag{A5}$$

From the last equation one finds

$$\bar{w}_{i+1,\,1} = \frac{1}{4}\ \bar{w}_{i+1,\,2}$$

$$\bar{w}_{i,\,1} = \frac{1}{4}\ \bar{w}_{i,\,2}$$

and so

$$\Delta \bar{w}_1 = \frac{1}{4}\ \Delta \bar{w}_2$$

An alternate form is

$$\Delta \bar{w}_1 = \frac{1}{4}\ \Delta \bar{w}_2 + \left(\frac{\bar{w}_{i,\,2}}{4} - \bar{w}_{i,\,1} \right)$$

Here the second term ought to be zero, but by proceeding in this fashion we are more sure that the [illegible] equation of (A5) is not violated because of error accumulation.

By numerically integrating the radial velocity $\bar{u}$ with respect to $\bar{y}$ for any fixed value of $\bar{x}$, we obtain the total fluid volume passing through the cylindrical surface characterized by $\bar{x}$, and comparison with input volume provides some check of the numerical results.

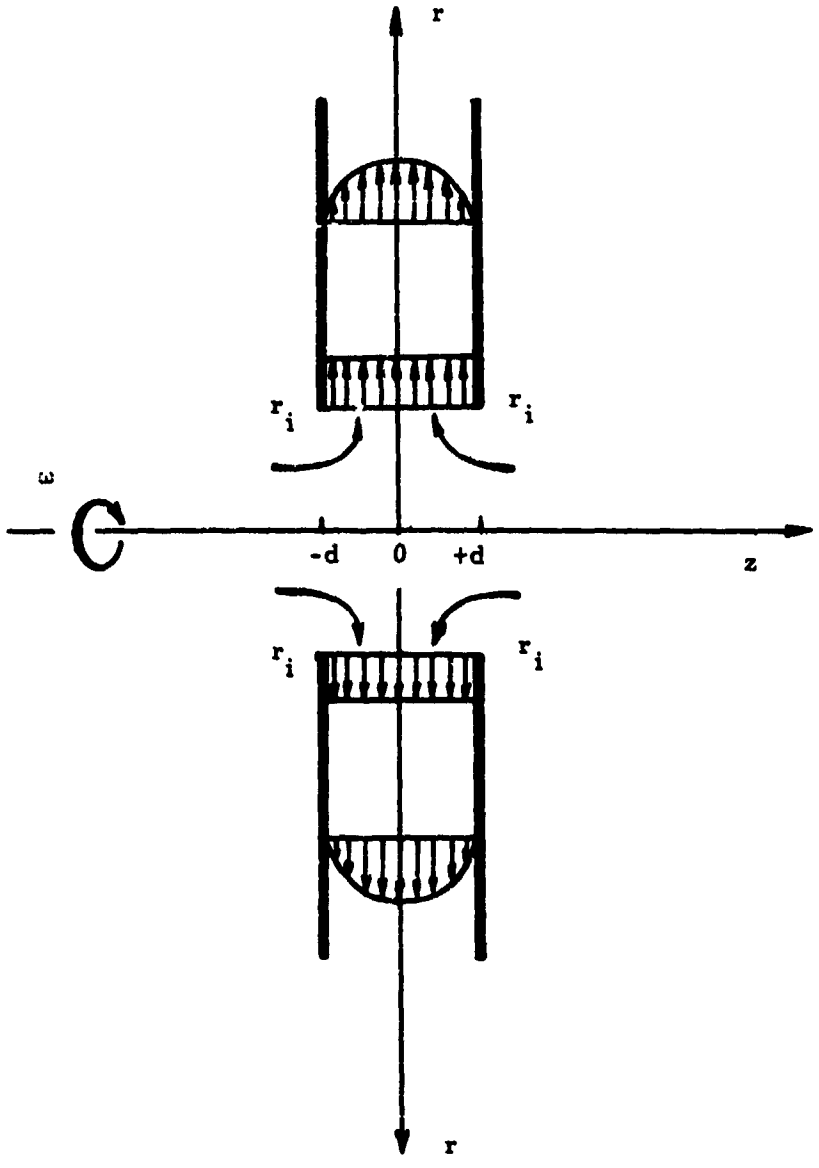

Fig 1. Schematic diagram of the flow between two rotating disks

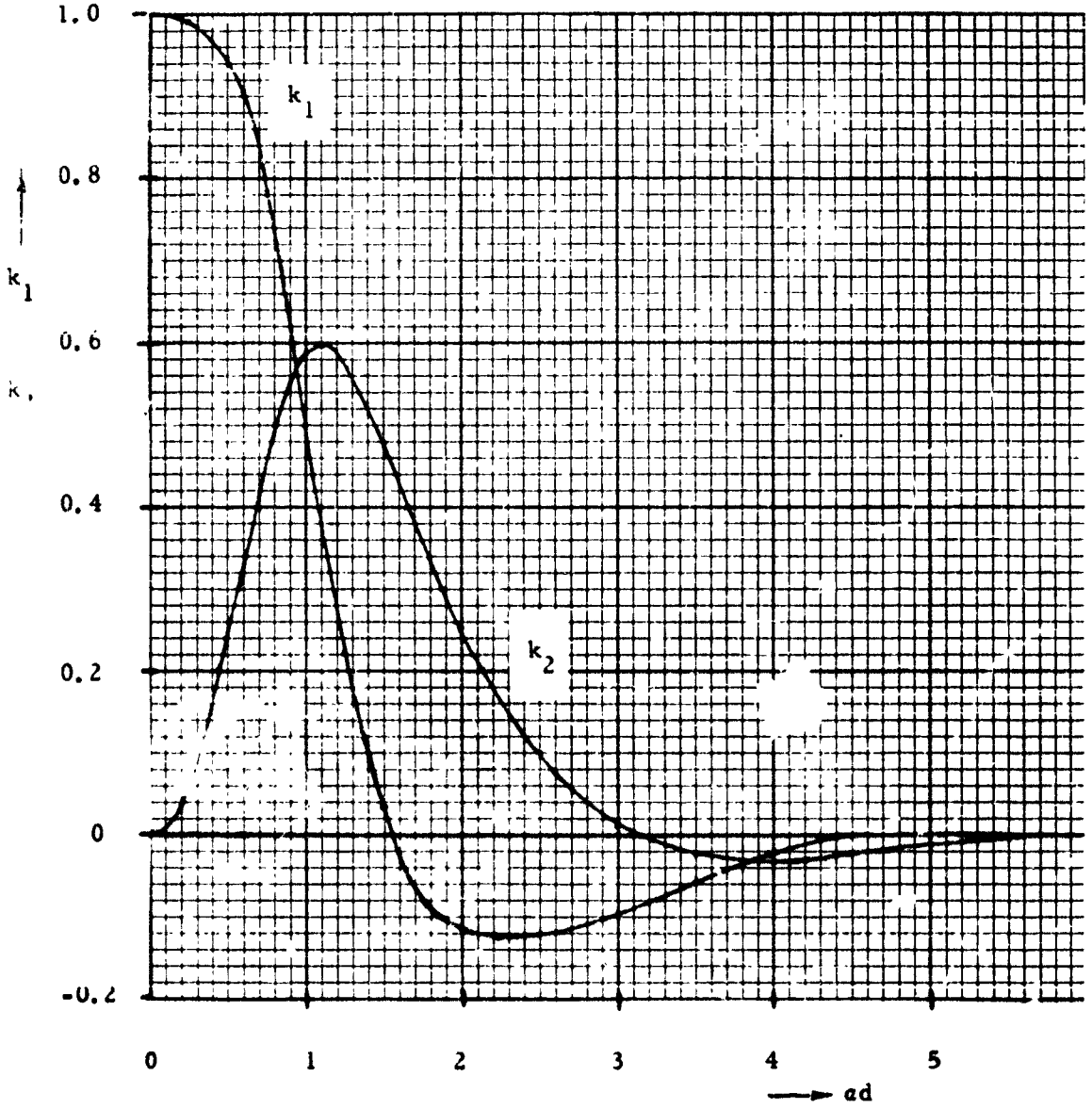

Fig. 2 k_1 and k_2 versus αd

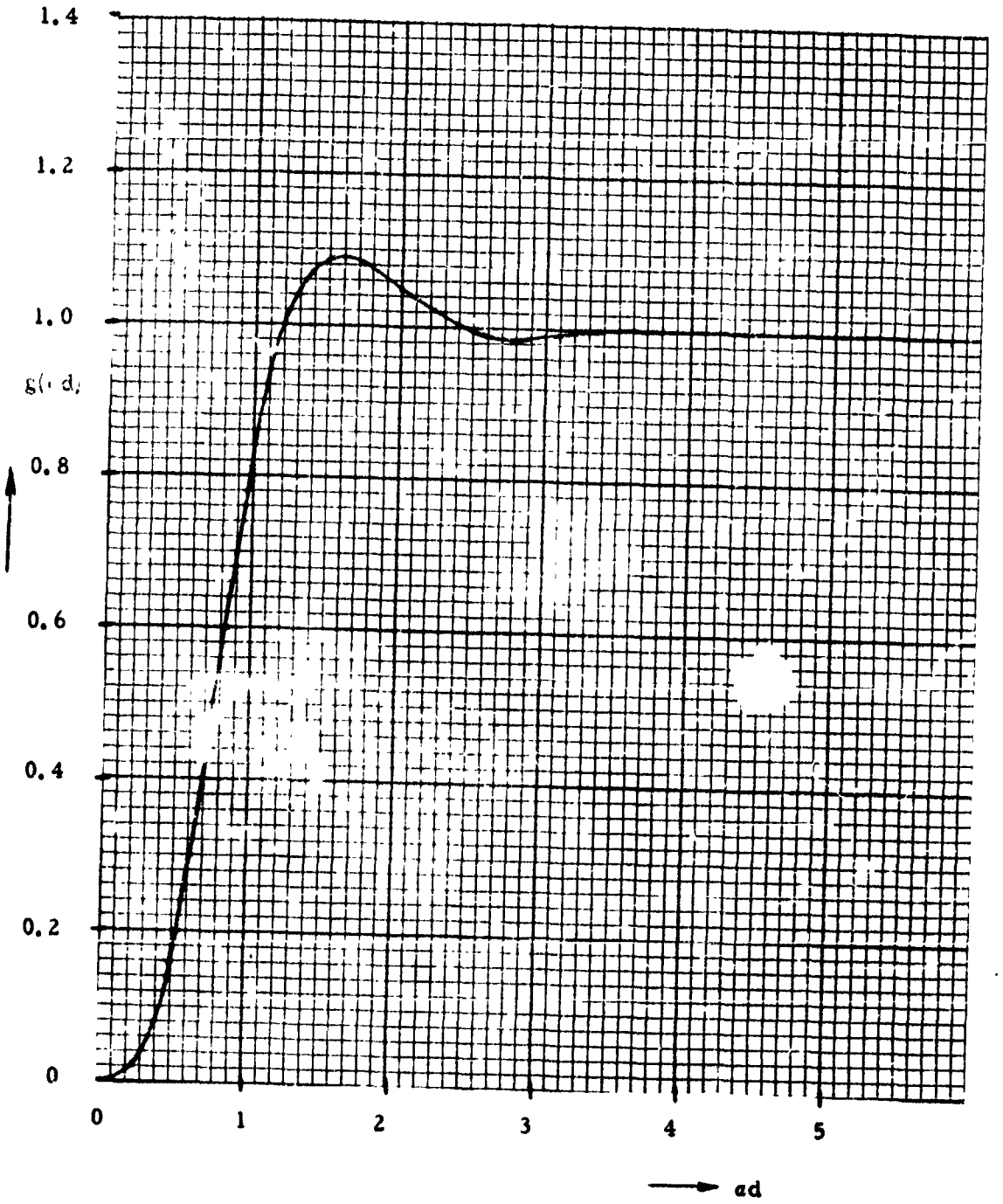

Fig. 3 g(*ad*) versus *ad*

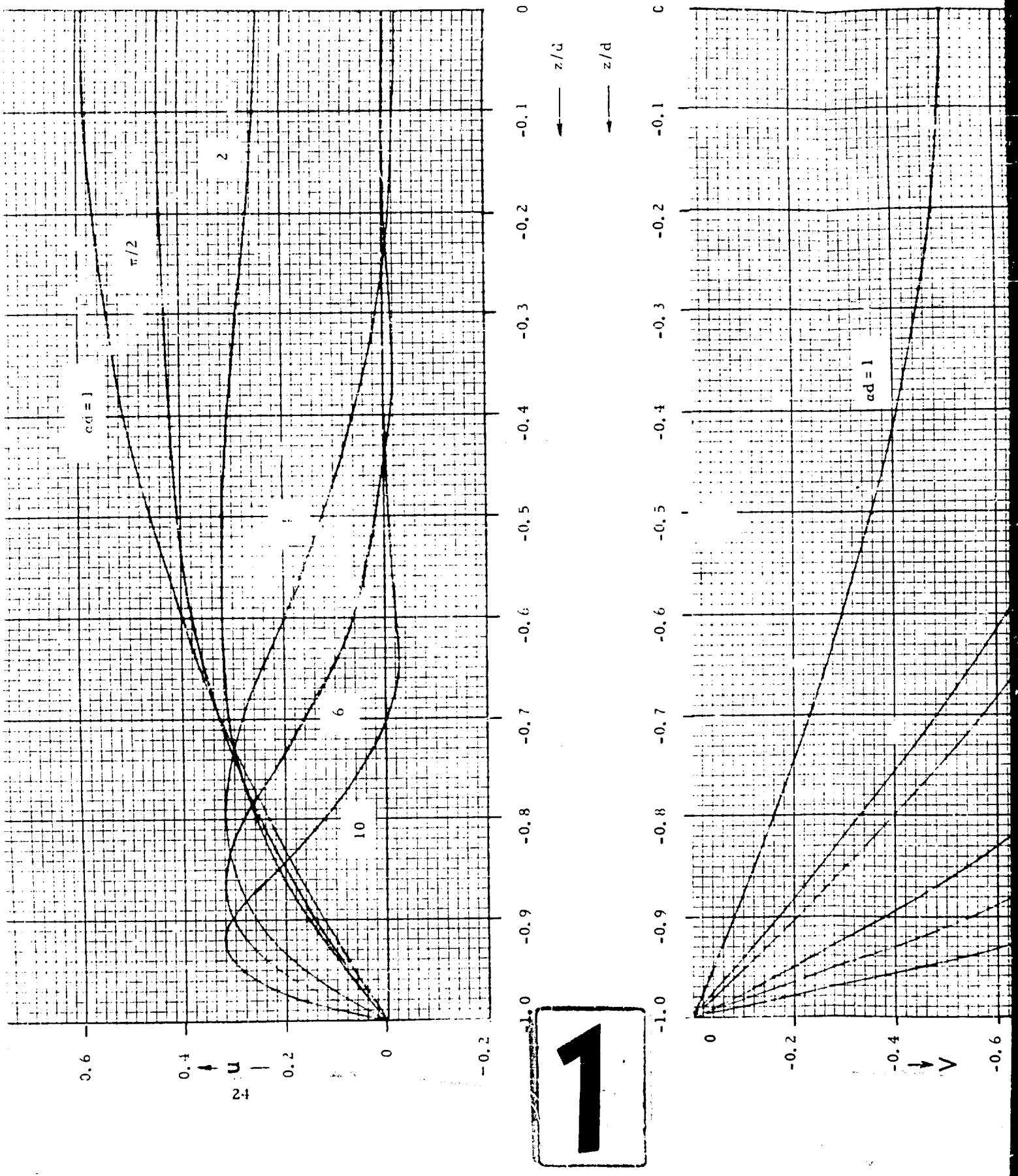

1

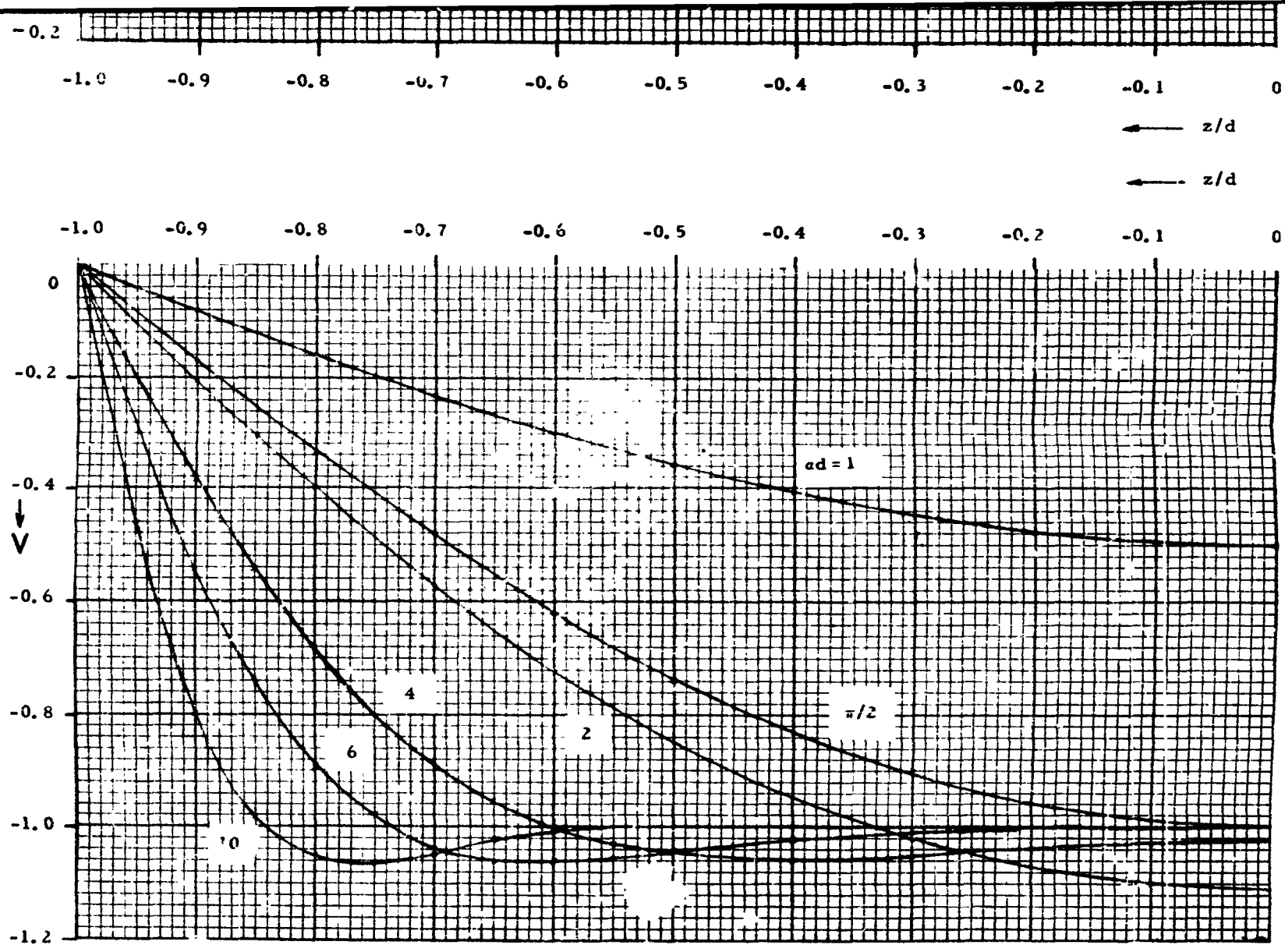

Fig. 4 Radial velocity u and relative tangential velocity V for various values of αd

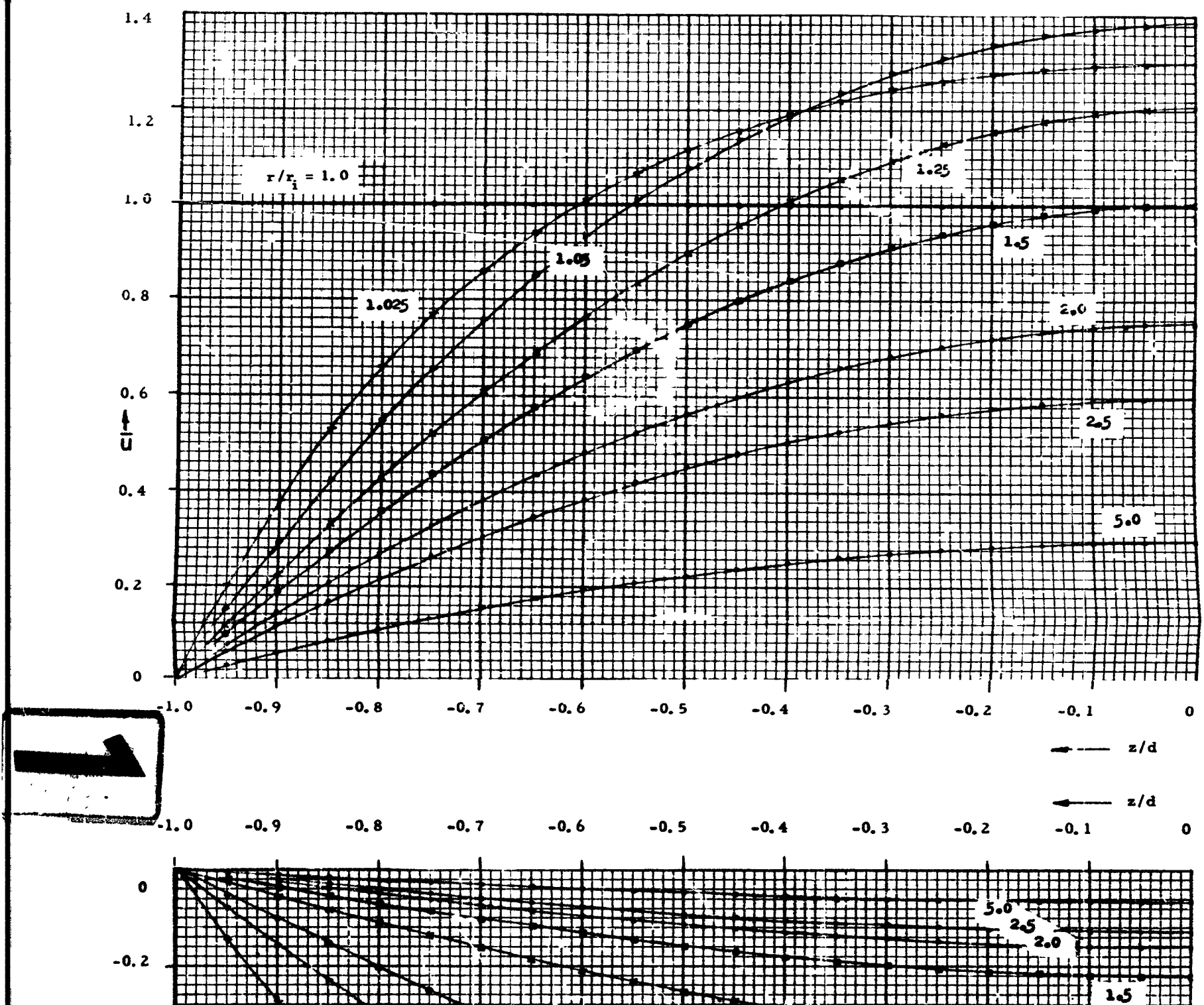
1.4
1.2
1.0
0.8
0.6
0.4
0.2
0
$\frac{v}{U}$
$r/r_i = 1.0$
1.025
1.05
1.25
1.5
2.0
2.5
5.0
-1.0
-0.9
-0.8
-0.7
-0.6
-0.5
-0.4
-0.3
-0.2
-0.1
0
z/d
z/d
-1.0
-0.9
-0.8
-0.7
-0.6
-0.5
-0.4
-0.3
-0.2
-0.1
0
0
-0.2
5.0
2.5
2.0
1.5

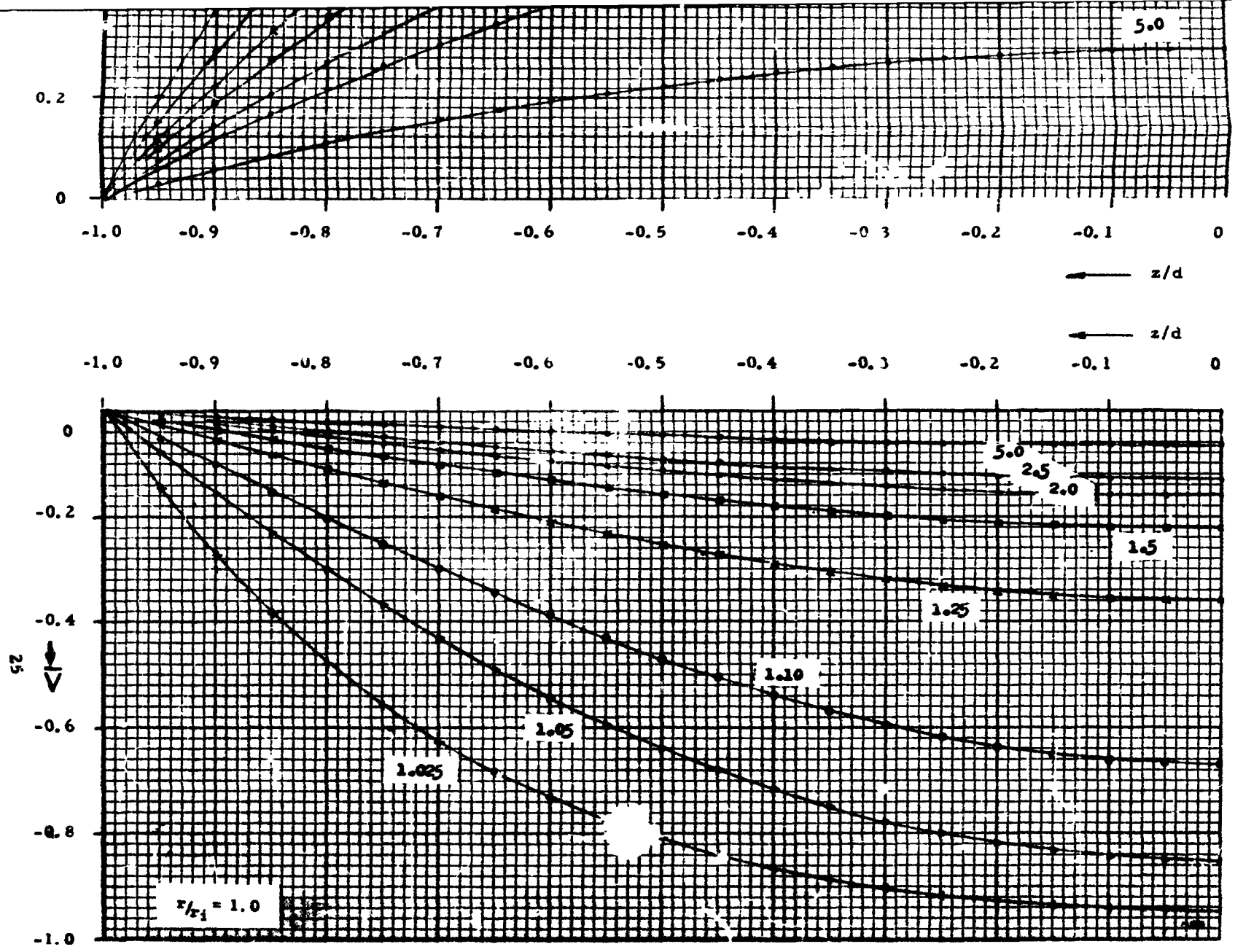

Fig. 5 Radial velocity $\bar{u}$ and relative tangential velocity $\bar{V}$ for $\bar{u}_0 = 1.0$ $\bar{d} = 0.5$

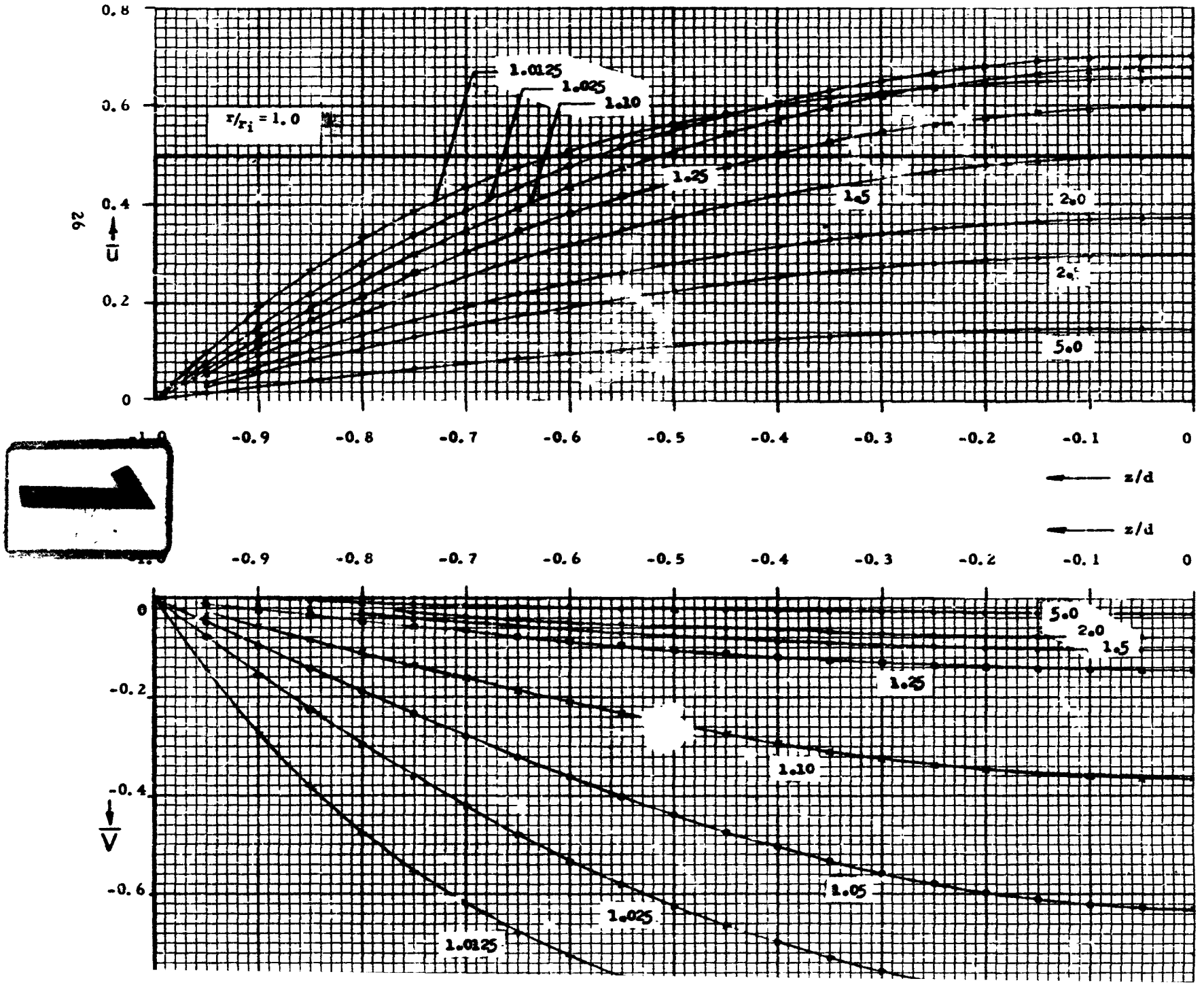
0.8
0.6
0.4
0.2
0
$r/r_i = 1.0$
1.0125
1.025
1.10
1.25
1.5
2.0
5.0
$\frac{U}{2a}$
-0.9
-0.8
-0.7
-0.6
-0.5
-0.4
-0.3
-0.2
-0.1
0
z/d
-0.2
-0.4
-0.6
$\frac{V}{2a}$

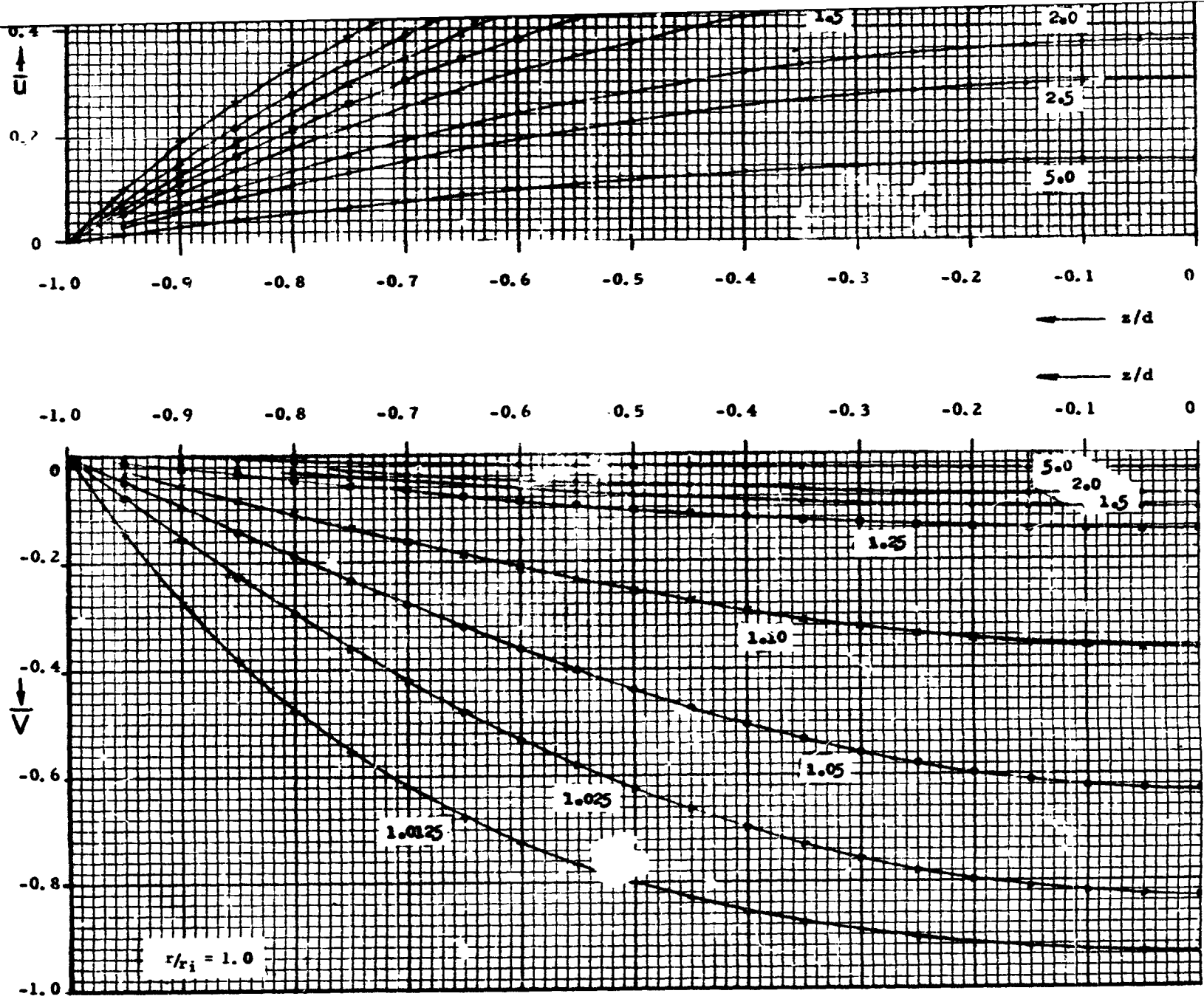

Fig. 6 Radial velocity $\bar{u}$ and relative tangential velocity $\bar{V}$ for $\bar{u}_0 = 0.5$ $\bar{d} = 0.5$

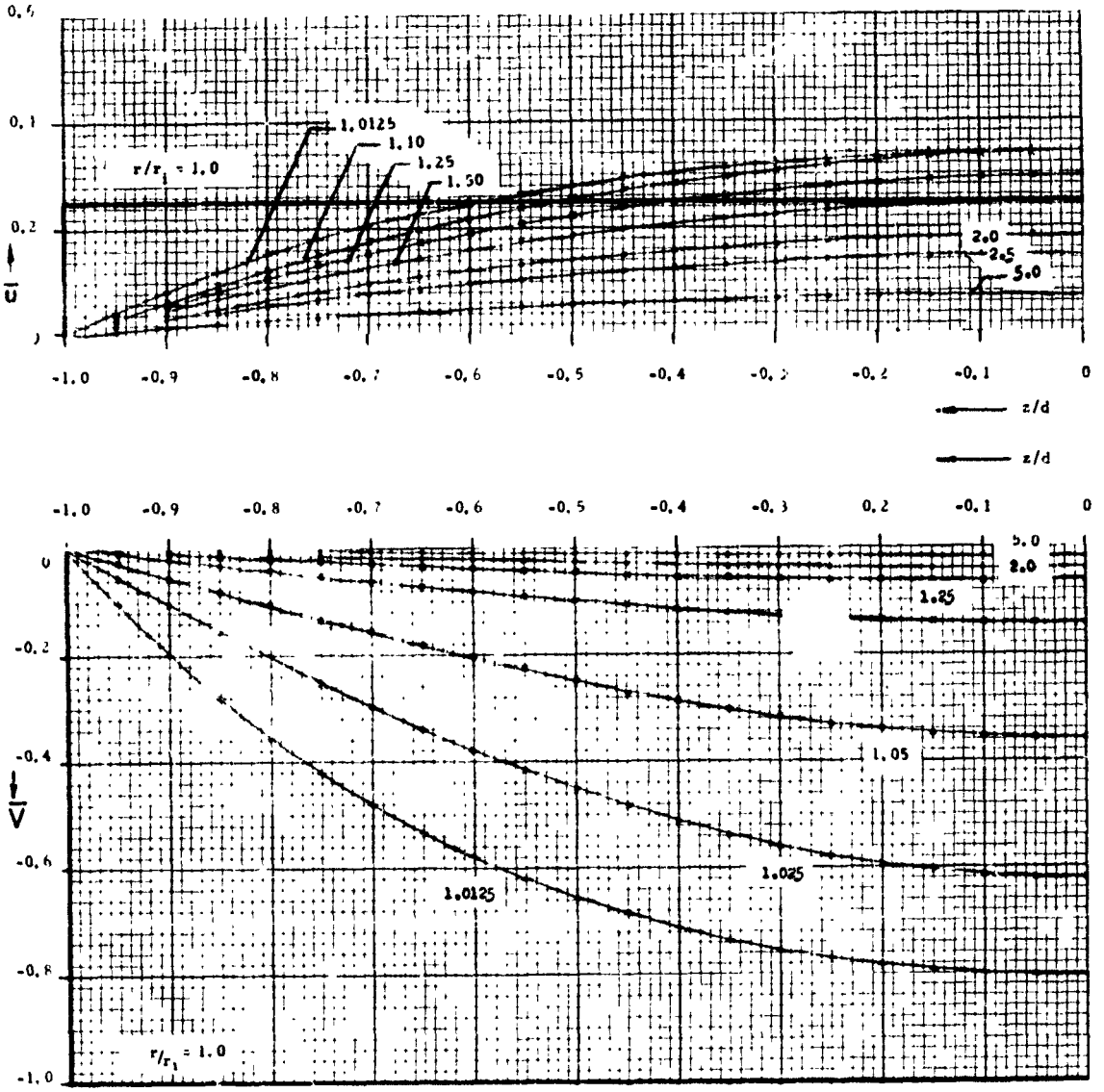

Fig. 7. Radial velocity u and relative tangential velocity V for $u_0 = 0.25$
$\bar{d} = 0.5$

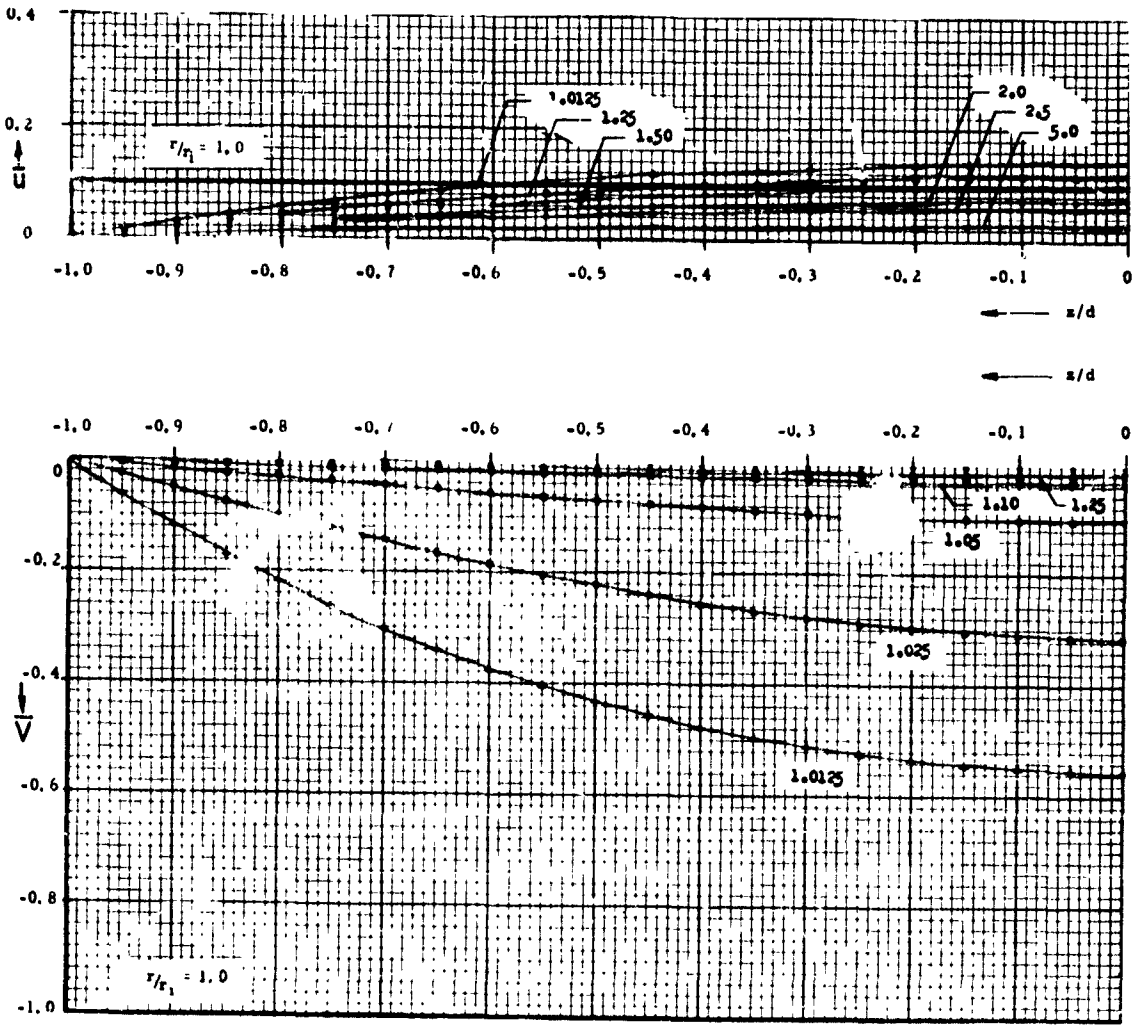

Fig. 8 Radial velocity $\bar{u}$ and relative tangential velocity $\bar{V}$ for $\bar{u}_0 = 0.1$ $\bar{d} = 0.5$

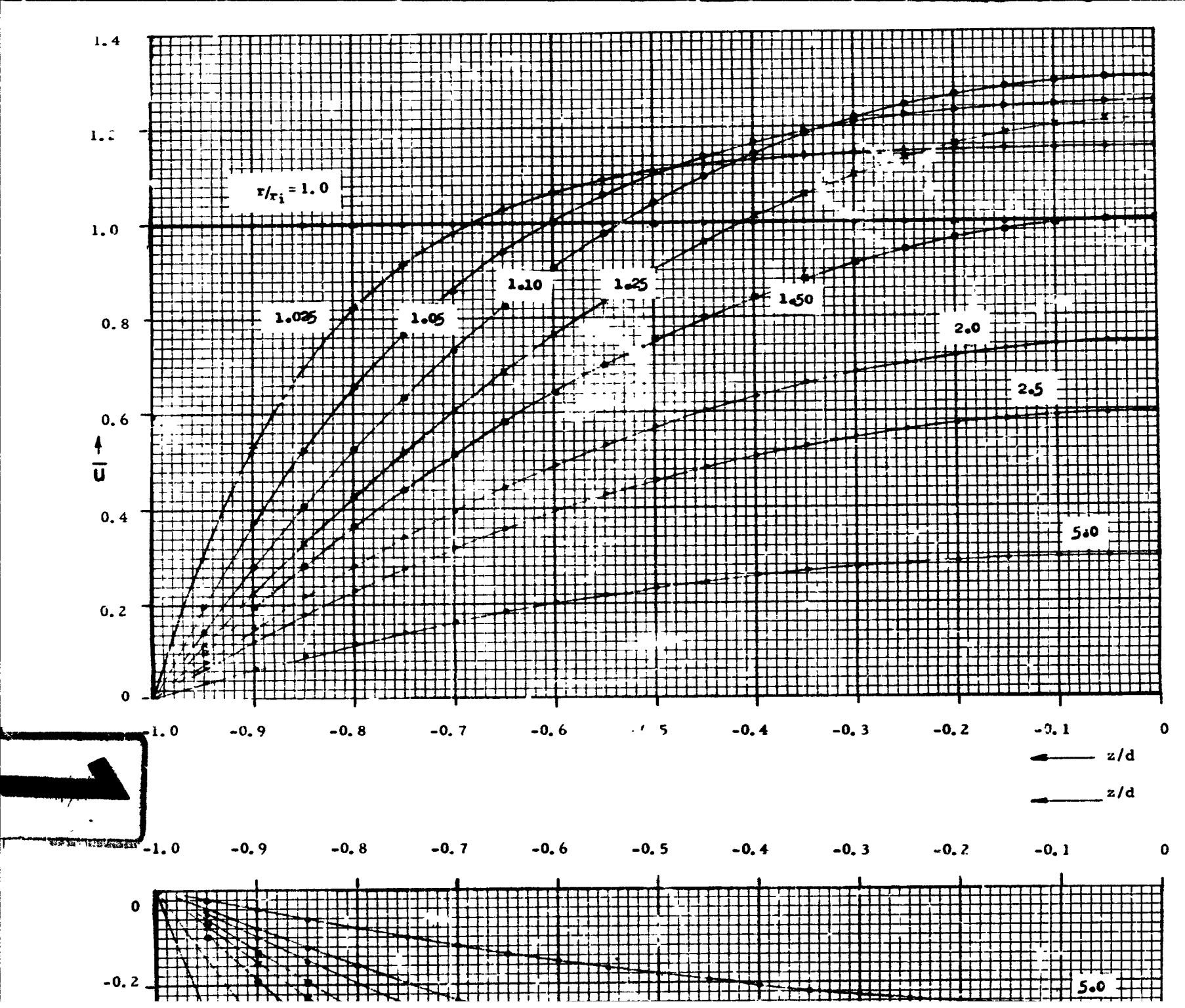
1.4
1.2
1.0
0.8
0.6
0.4
0.2
0
$\bar{u}$
$r/r_i = 1.0$
1.025
1.05
1.10
1.25
1.50
2.0
2.5
5.0
-1.0
-0.9
-0.8
-0.7
-0.6
-0.5
-0.4
-0.3
-0.2
-0.1
0
z/d
z/d
-1.0
-0.9
-0.8
-0.7
-0.6
-0.5
-0.4
-0.3
-0.2
-0.1
0
0
-0.2
5.0

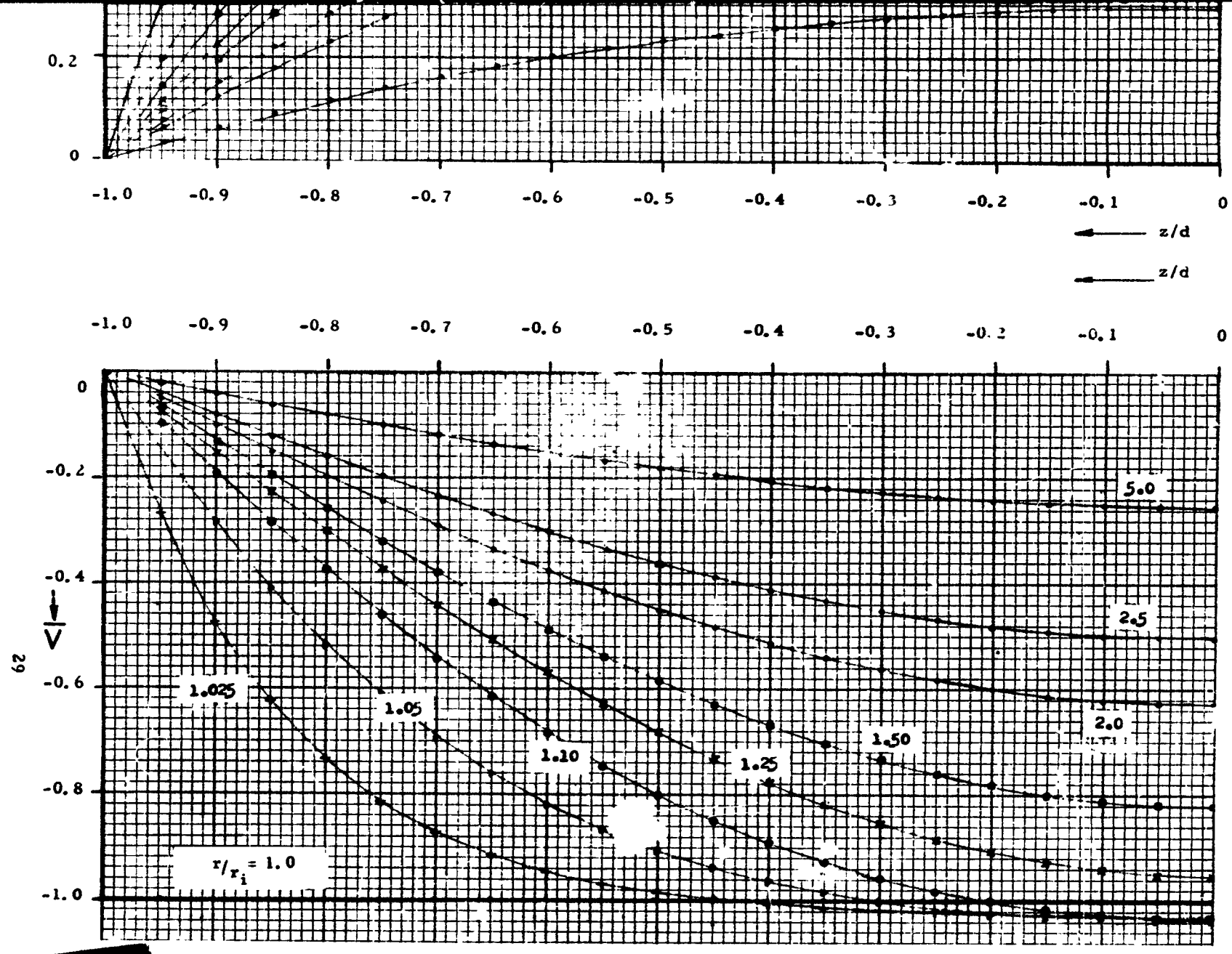

Fig. 9 Radial velocity $\bar{u}$ and relative tangential velocity $\bar{V}$ for $\bar{u}_0 = 1.0$ $\bar{d} = 1.0$

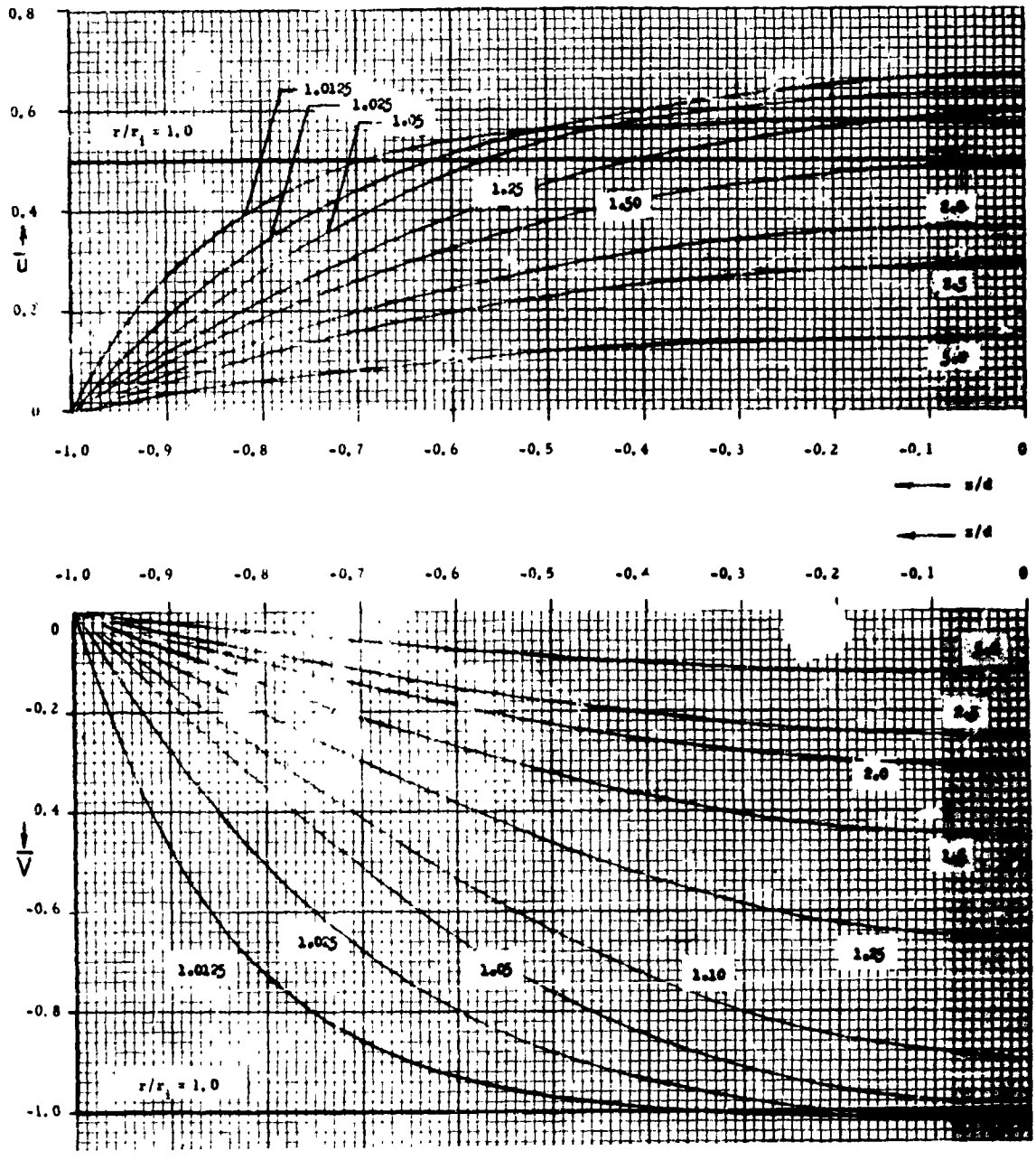

Fig. 10 Radial velocity $\bar{u}$ and relative tangential velocity $\bar{V}$ for $\bar{u}_0 = 0.5$ $\bar{d} = 1.0$

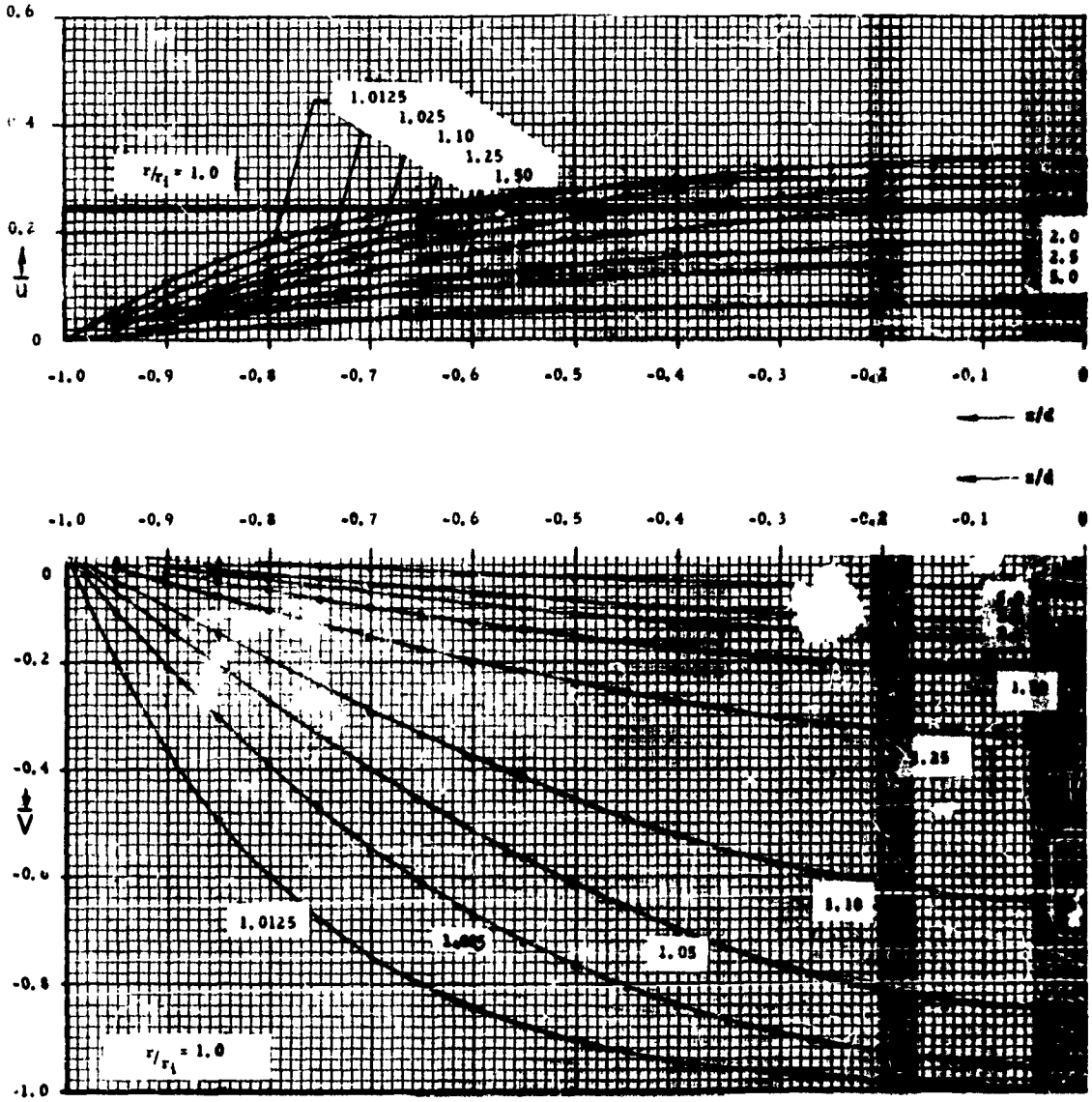

Fig. 11 Radial velocity $\bar{u}$ and relative tangential velocity $\bar{V}$ for $\bar{u}_0 = 0.25$ $\bar{d} = 1.0$

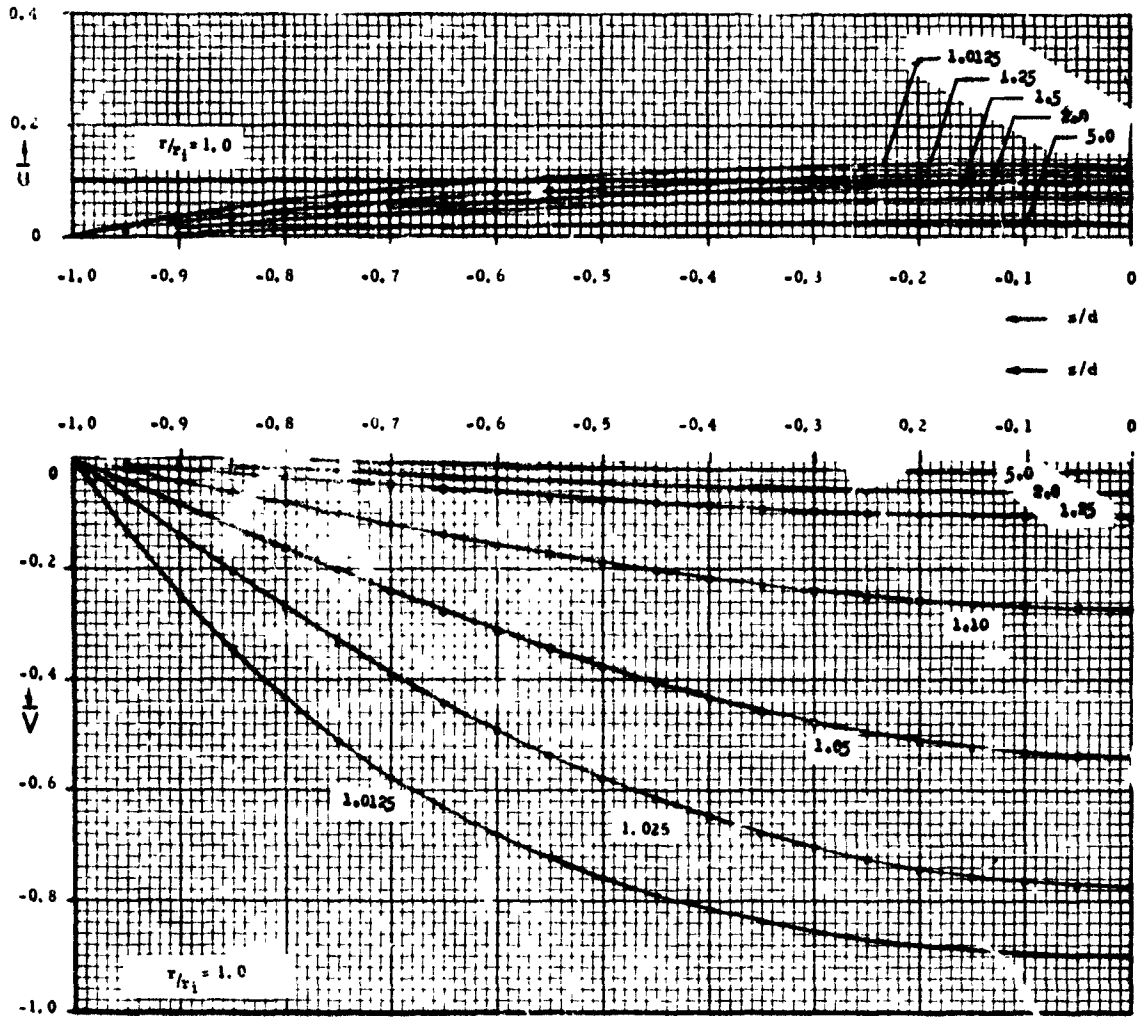

Fig. 12 Radial velocity $\bar{u}$ and relative tangential velocity $\bar{V}$ for $\bar{u}_0 = 0.1$ $\bar{d} = 1.0$

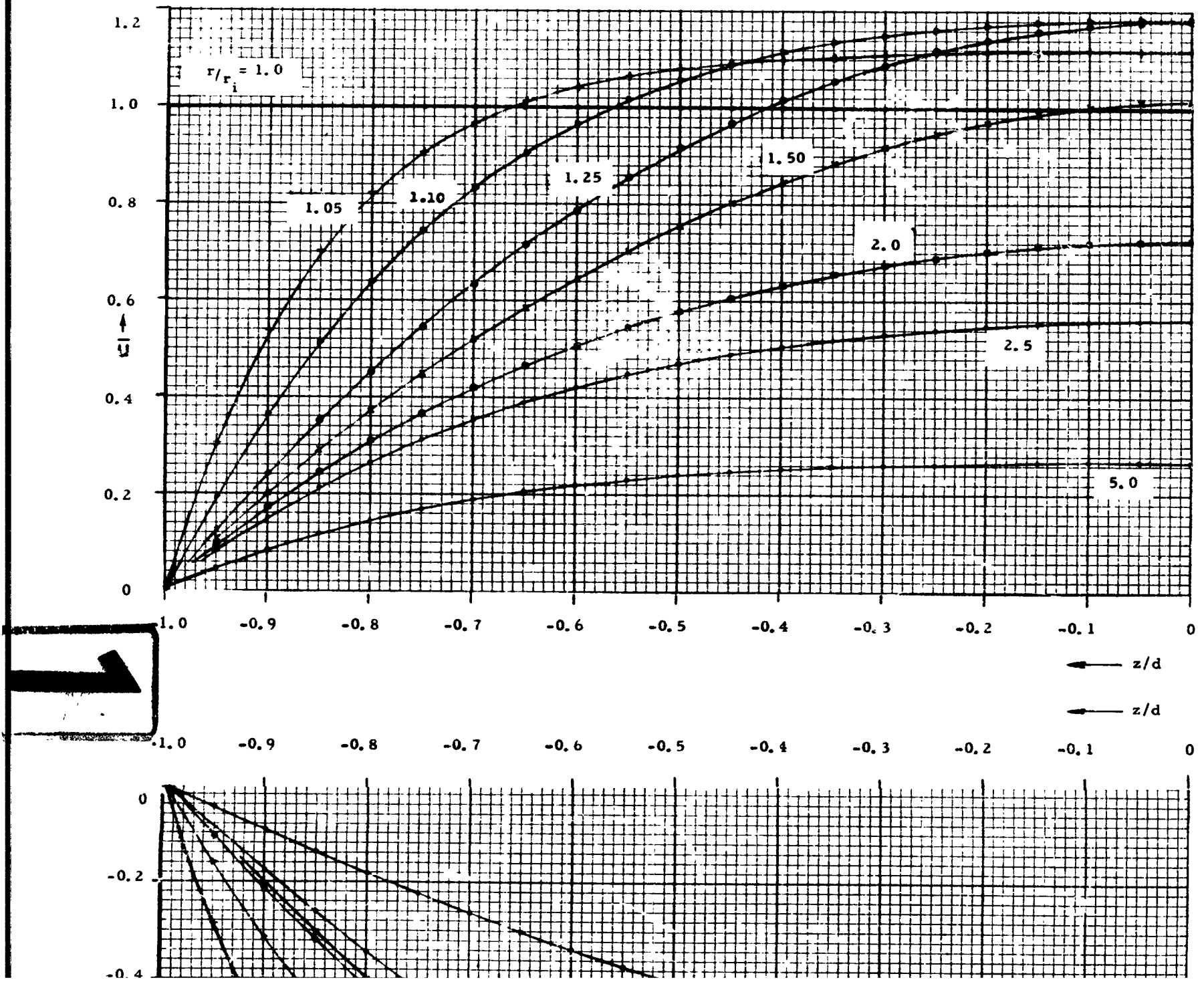
1.2
1.0
0.8
0.6
0.4
0.2
0
$\bar{u}$
$r/r_i = 1.0$
1.05
1.10
1.25
1.50
2.0
2.5
5.0
-1.0
-0.9
-0.8
-0.7
-0.6
-0.5
-0.4
-0.3
-0.2
-0.1
0
z/d
z/d
-1.0
-0.9
-0.8
-0.7
-0.6
-0.5
-0.4
-0.3
-0.2
-0.1
0
0
-0.2
-0.4

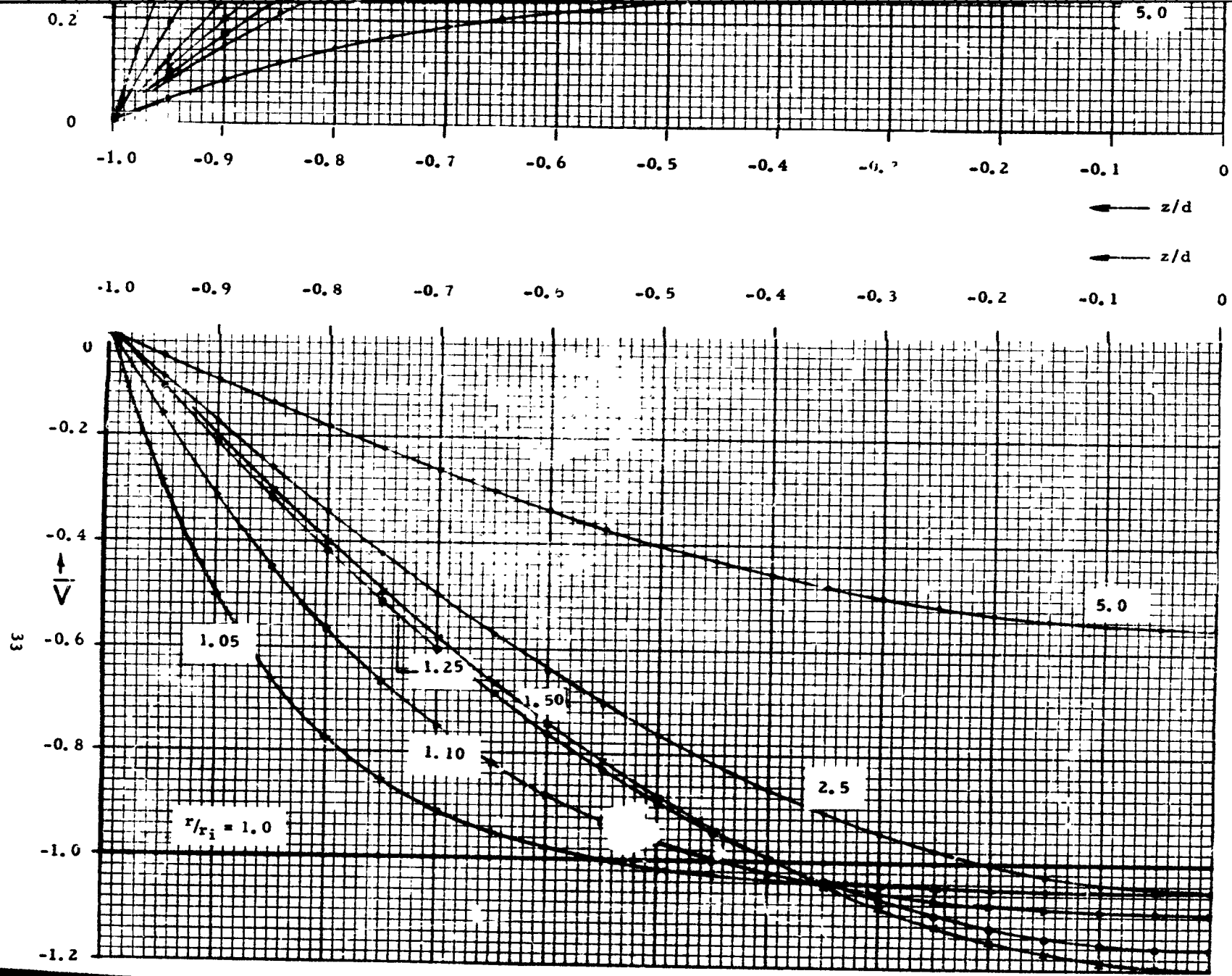

Fig. 13 Radial velocity $\bar{u}$ and relative tangential velocity $\bar{V}$ for $\bar{u}_0 = 1.0$ $\bar{d} = 1.5$

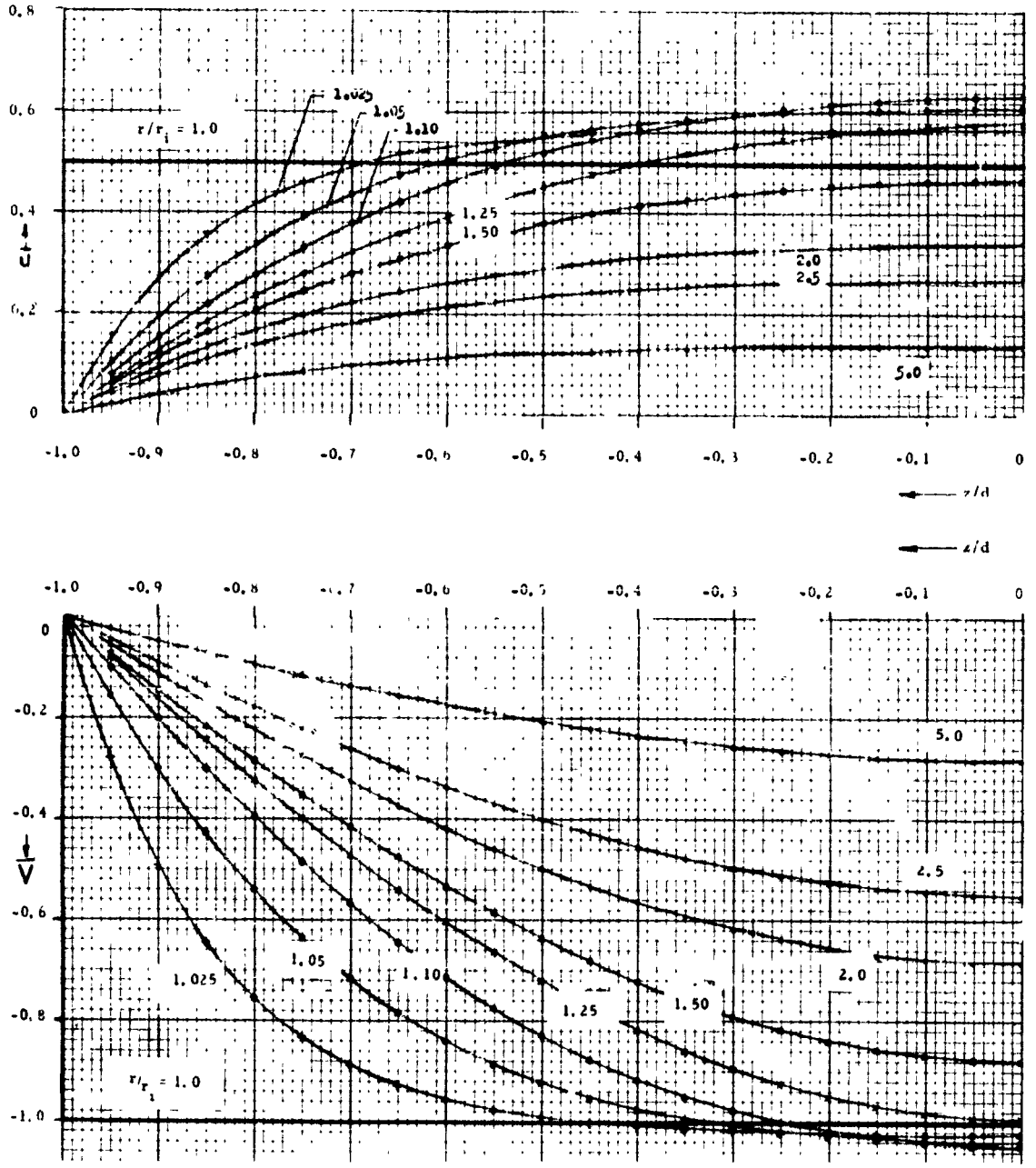

Fig. 14 Radial velocity $\bar{u}$ and relative tangential velocity $\bar{V}$ for $\bar{u}_0 = 0.5$ $\bar{d} = 1.5$

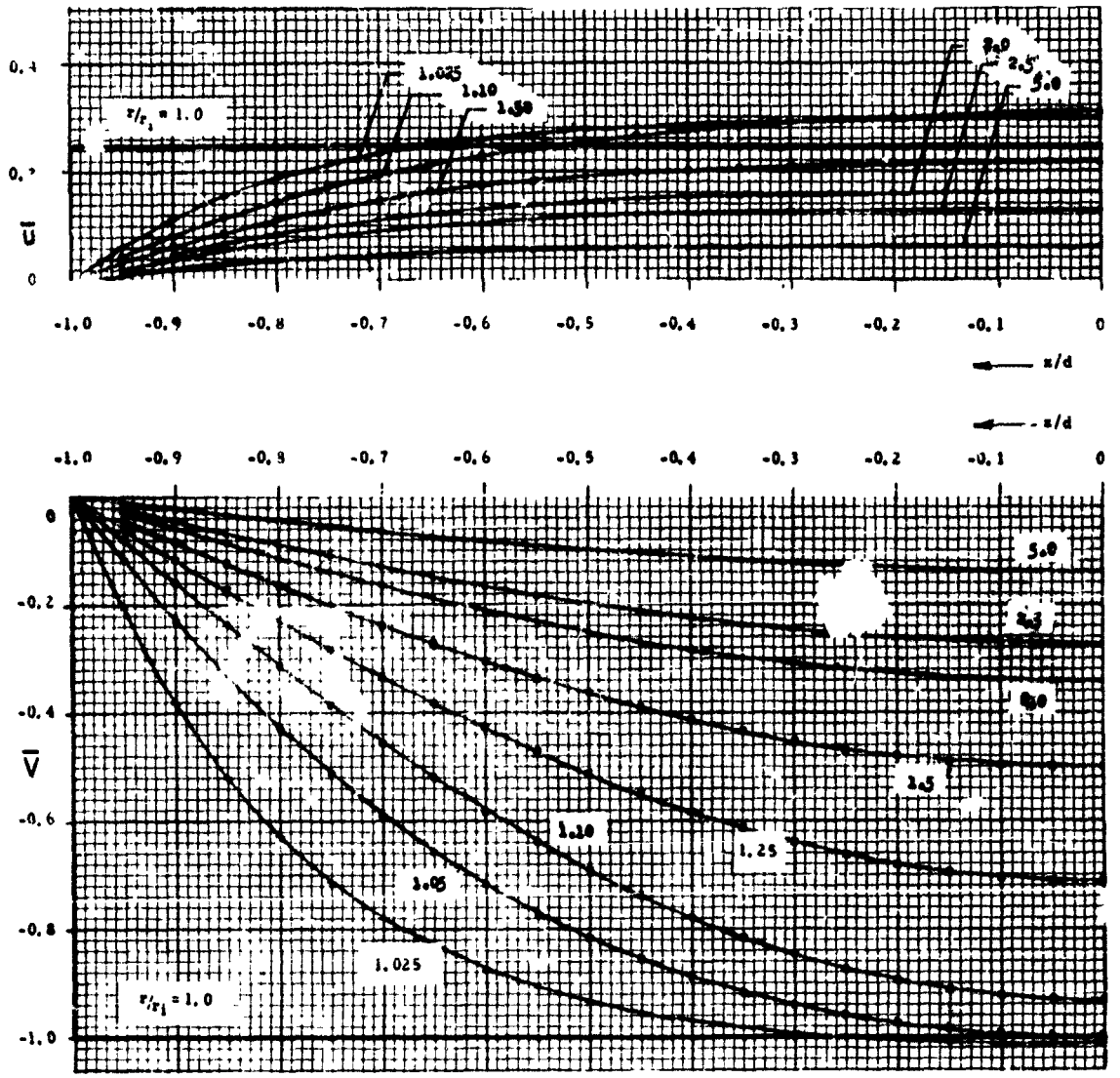

Fig. 15 Radial velocity $\bar{u}$ and relative tangential velocity $\bar{V}$ for $\bar{u}_0 = 0.25$ $\bar{d} = 1.5$

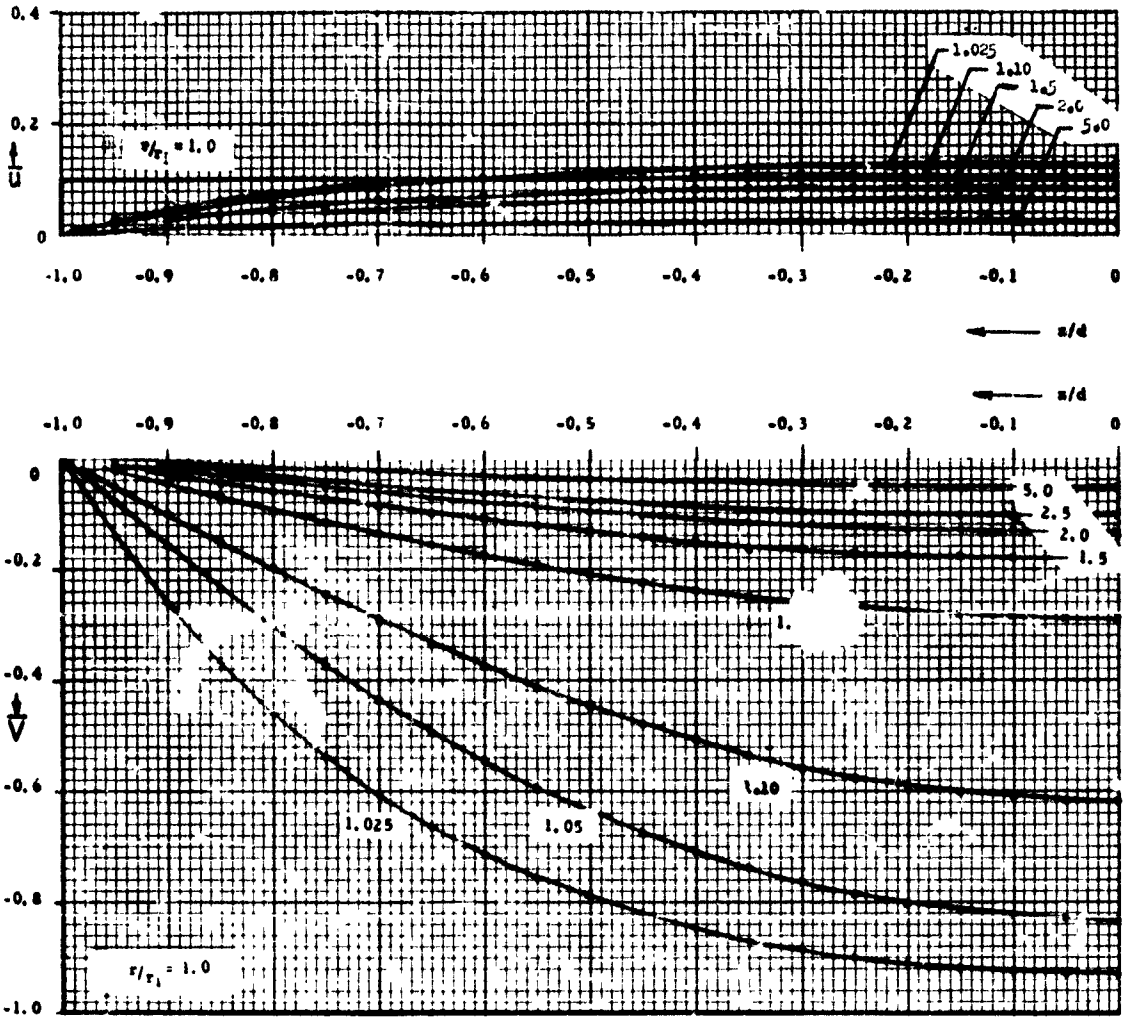

Fig. 16 Radial velocity $\bar{u}$ and relative tangential velocity $\bar{V}$ for $\bar{u}_0 = 0.1$ $\bar{d} = 1.5$

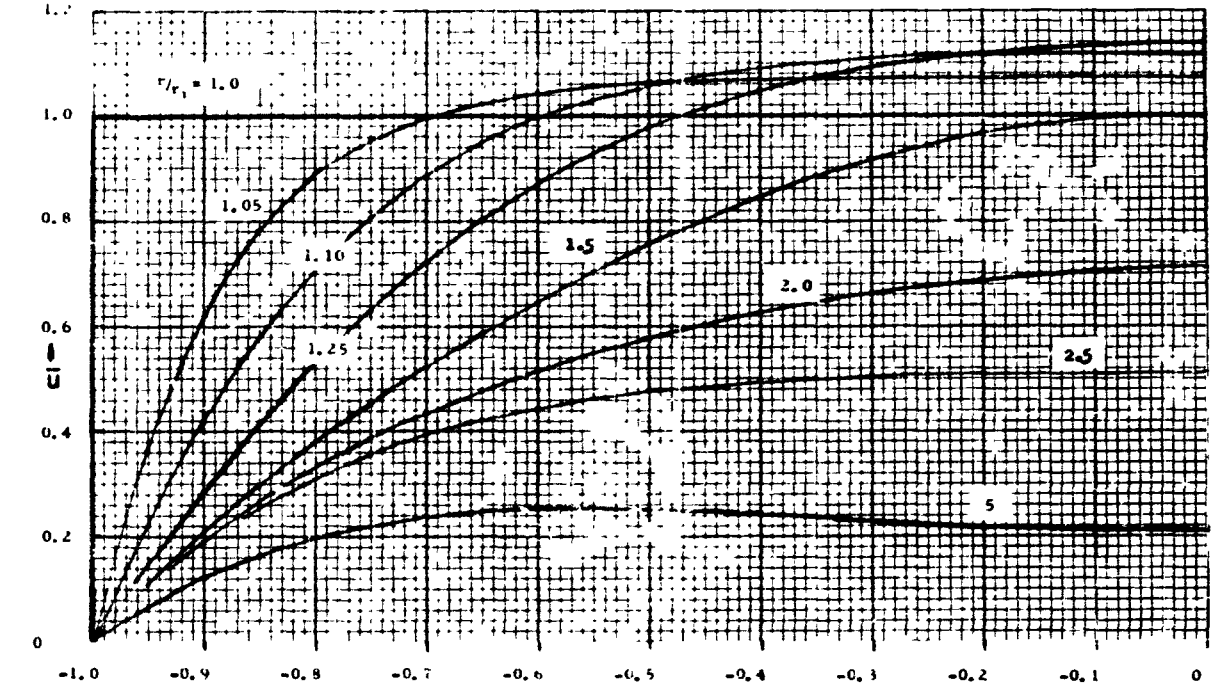
r/r1 = 1.0
1.05
1.10
1.25
1.5
2.0
2.5
5
U
1.0
0.8
0.6
0.4
0.2
0
-1.0
-0.9
-0.8
-0.7
-0.6
-0.5
-0.4
-0.3
-0.2
-0.1
0
z/d

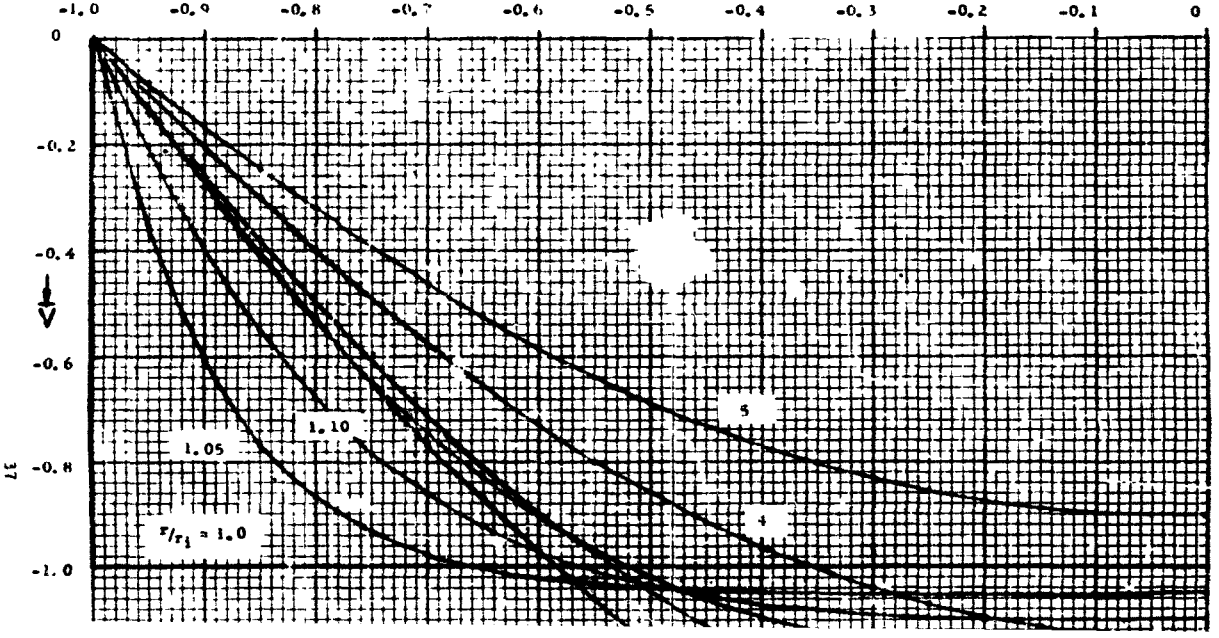
-1.0
-0.9
-0.8
-0.7
-0.6
-0.5
-0.4
-0.3
-0.2
-0.1
0
-0.2
-0.4
V
-0.6
-0.8
-1.0
1.05
1.10
r/r1 = 1.0
5
4
z/d

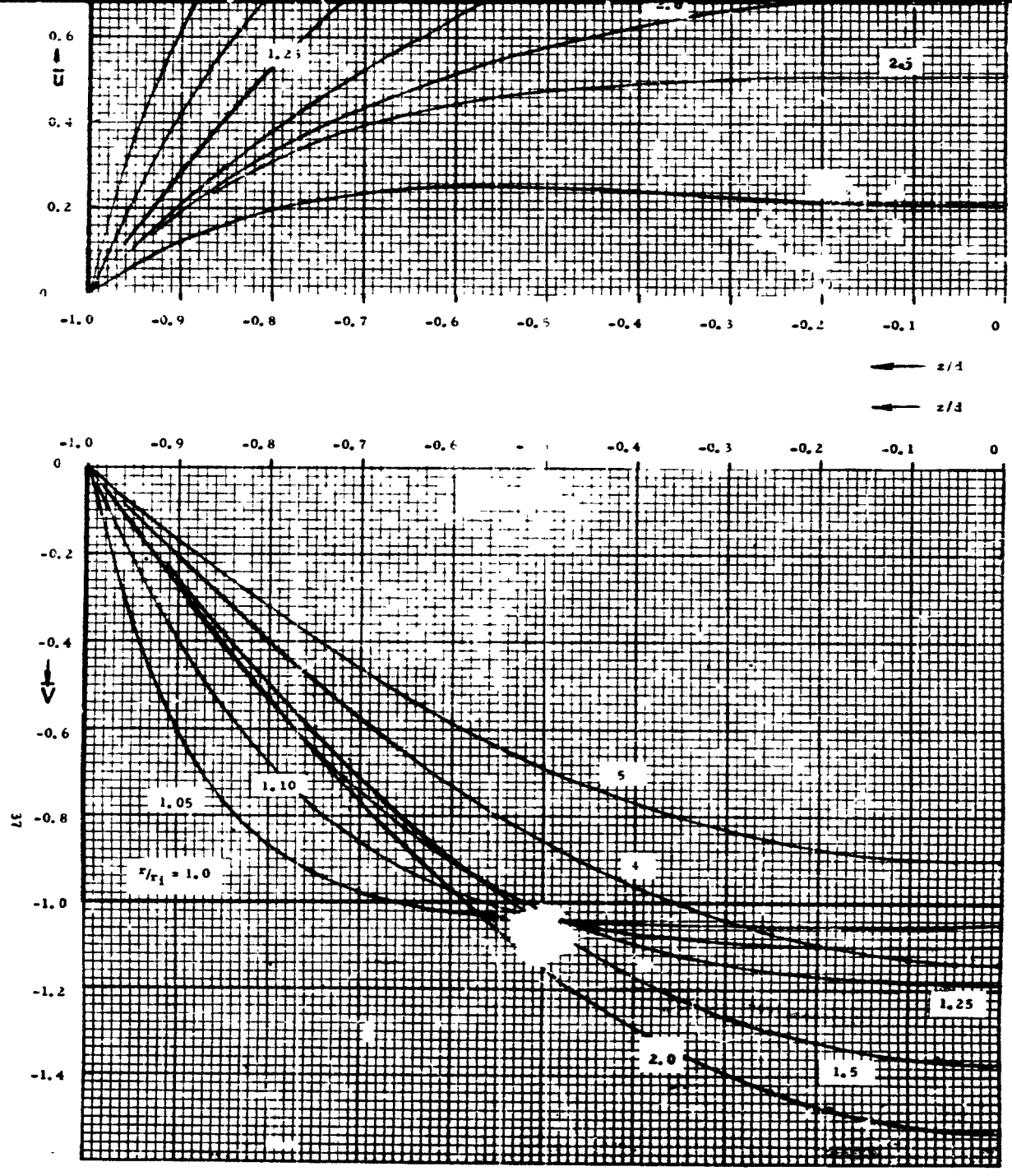

Fig. 17 Radial velocity $\bar{u}$ and relative tangential velocity $\bar{V}$ for $\bar{u}_0 = 1.0$ $\bar{d} = 2.0$

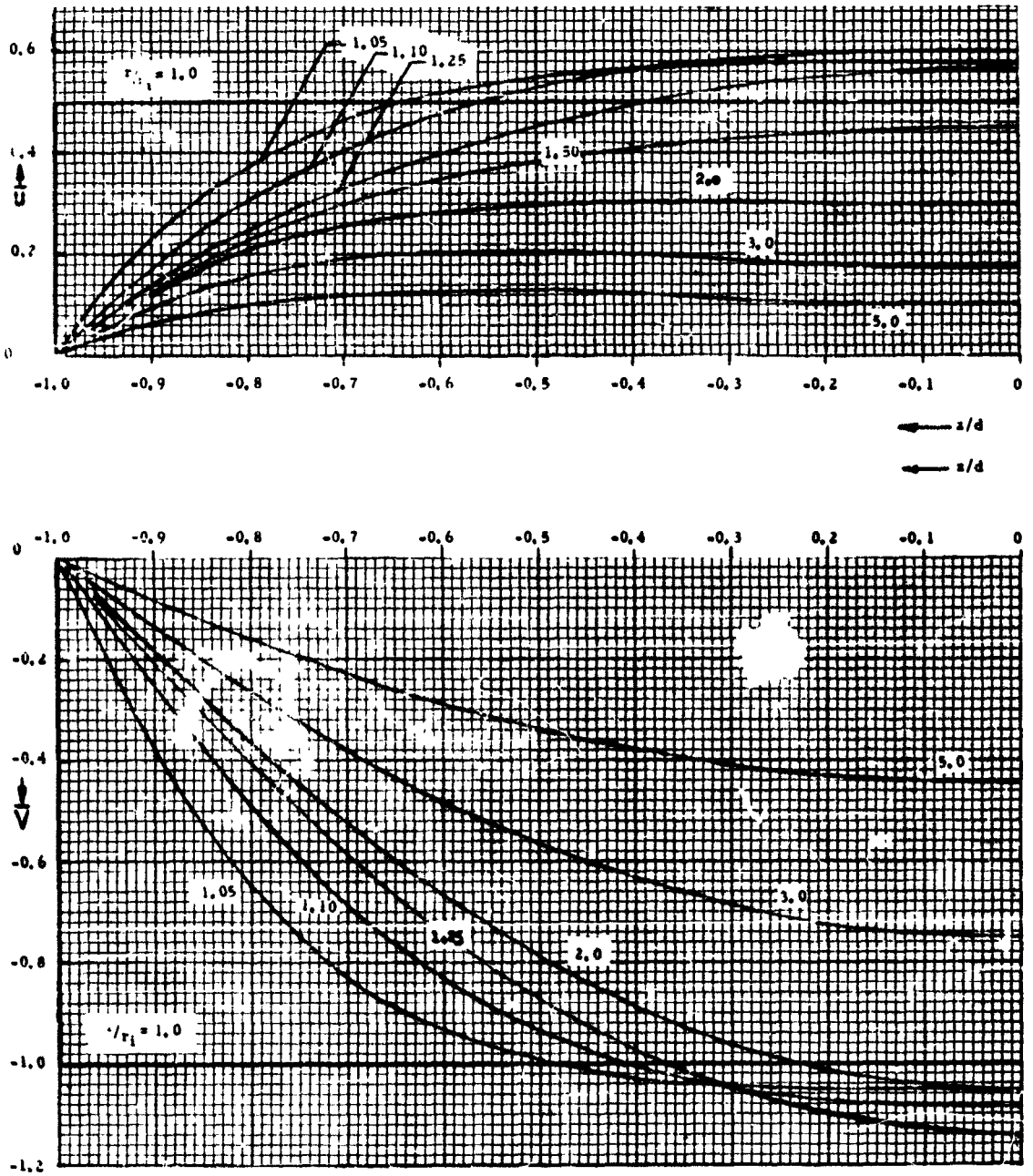

Fig. 18 Radial velocity $\bar{u}$ and relative tangential velocity $\bar{V}$ for $\bar{u}_0 = 0,5$ $\bar{d} = 2,0$

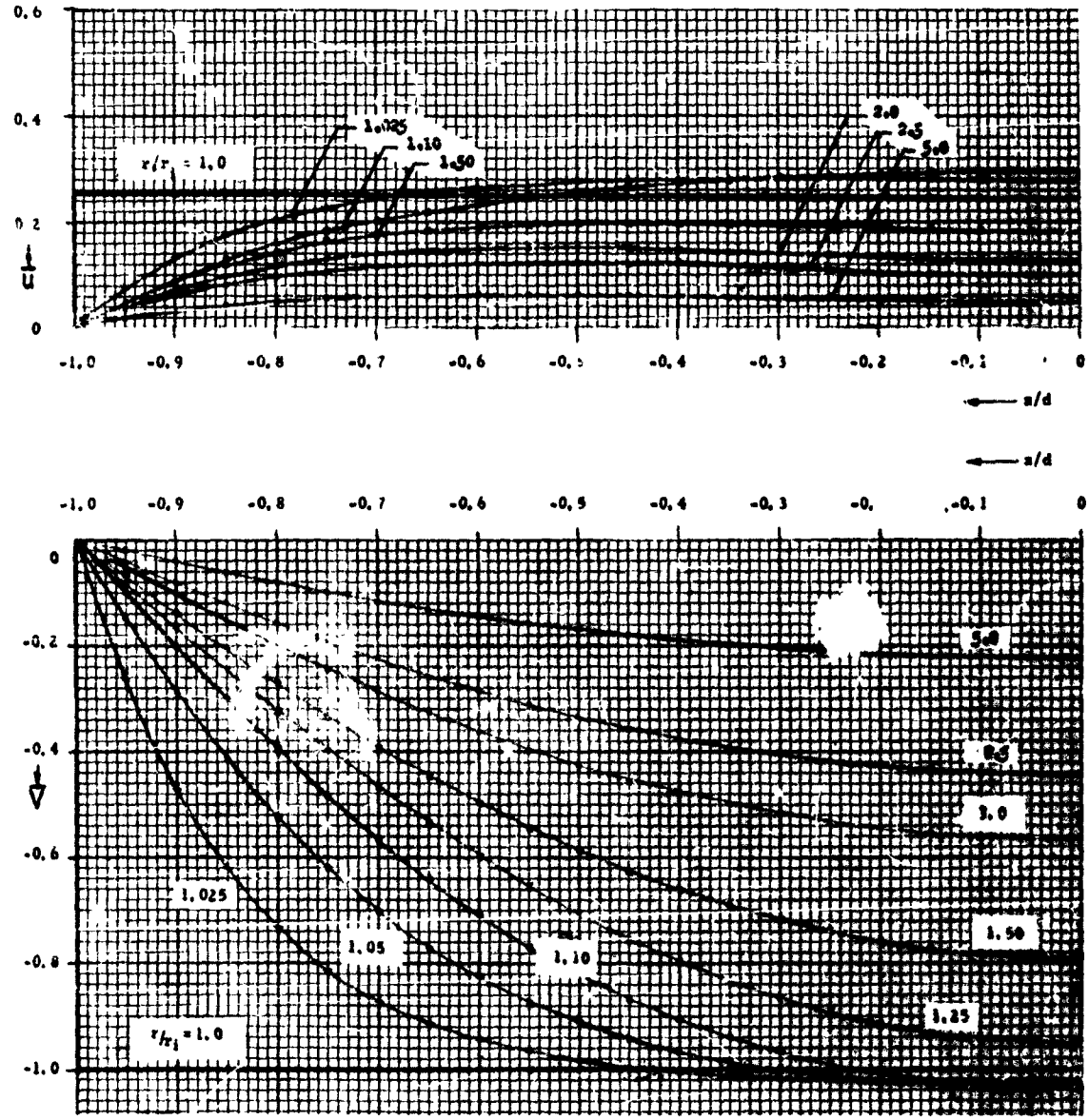

Fig. 19 Radial velocity $\bar{u}$ and relative tangential velocity $\bar{V}$ for $\bar{u}_0 = 0.25$ $\bar{d} = 2.0$

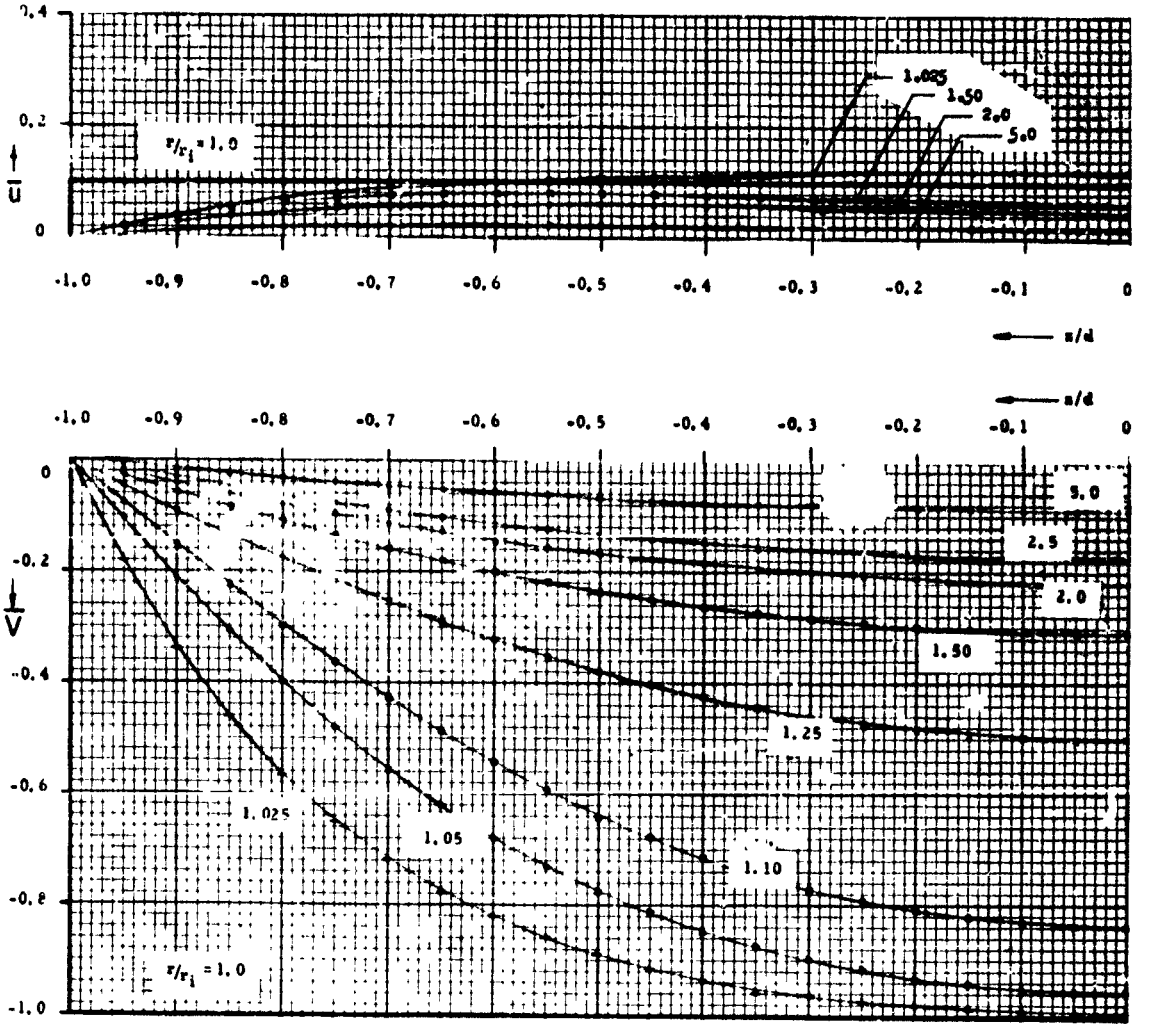

Fig. 20 Radial velocity $\bar{U}$ and relative tangential velocity $\bar{V}$ for $\bar{n}_0 = 0.1$ $\bar{d} = 2.0$

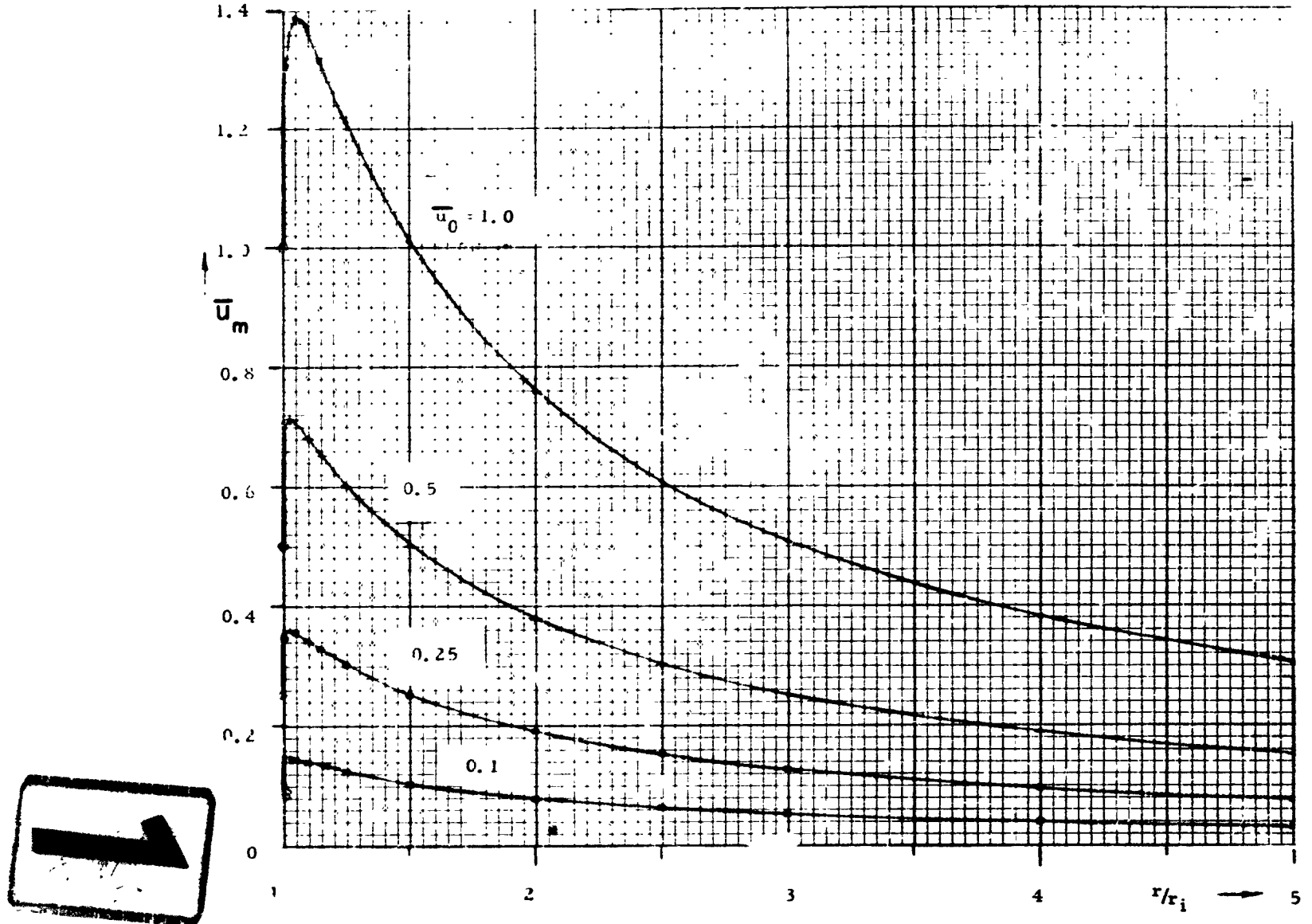

Fig. 21 Radial velocity $\bar{u}_m$ versus r/r_i for $\bar{d} = 0.5$

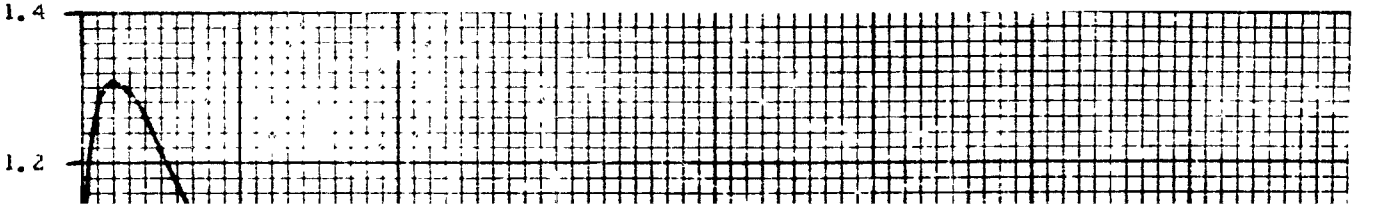

Fig. 21 Radial velocity $\bar{u}_m$ versus r/r_i for $\bar{d} = 0.5$

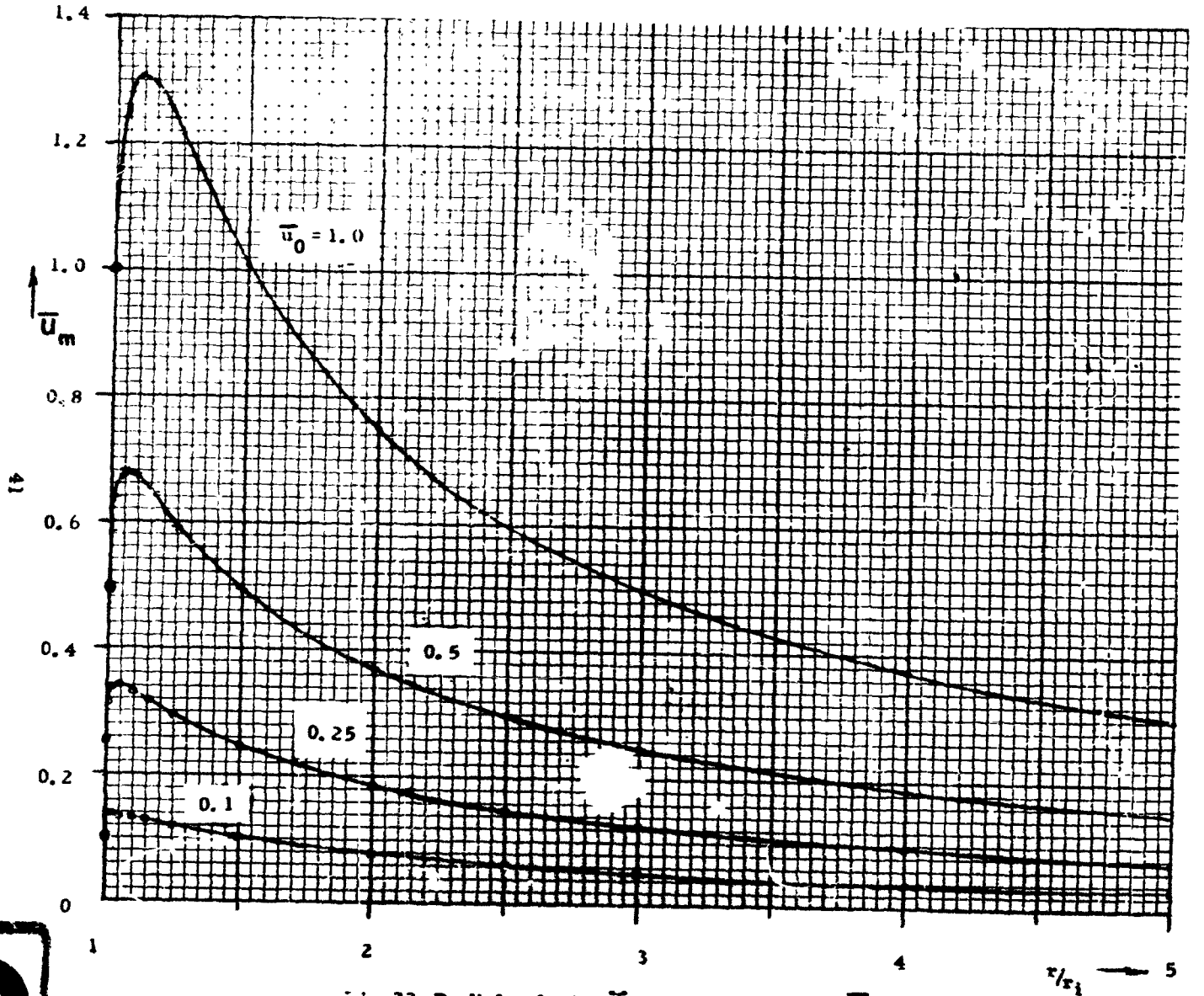

Fig. 22 Radial velocity $\bar{u}_m$ versus r/r_i for $\bar{d} = 1.0$

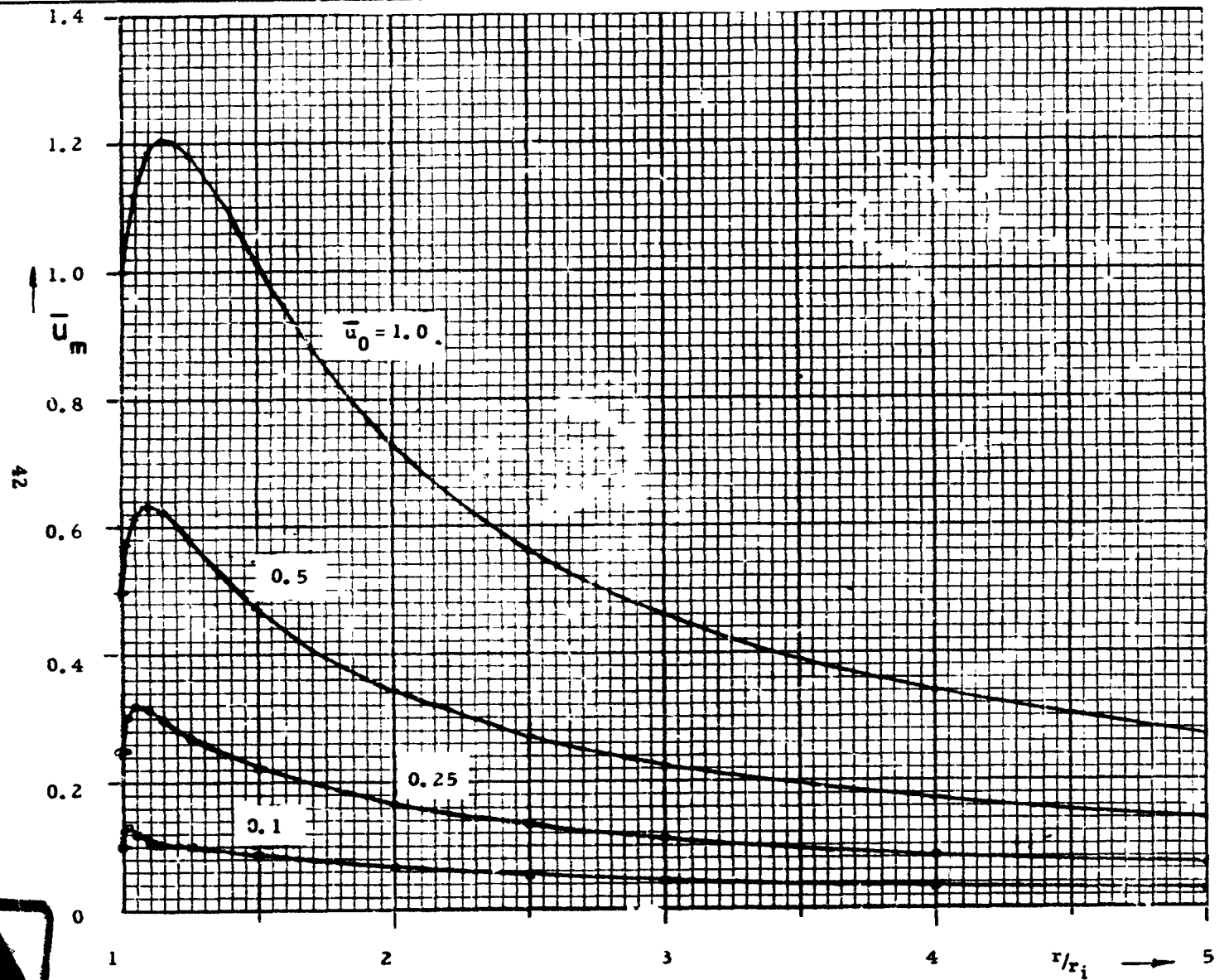

Fig. 23 Radial velocity $\bar{u}_m$ versus r/r_i for $\bar{d} = 1.5$

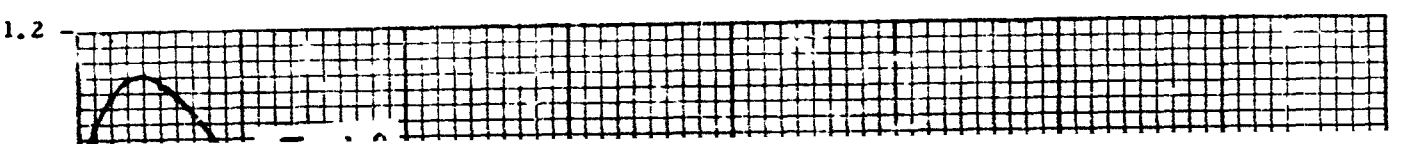

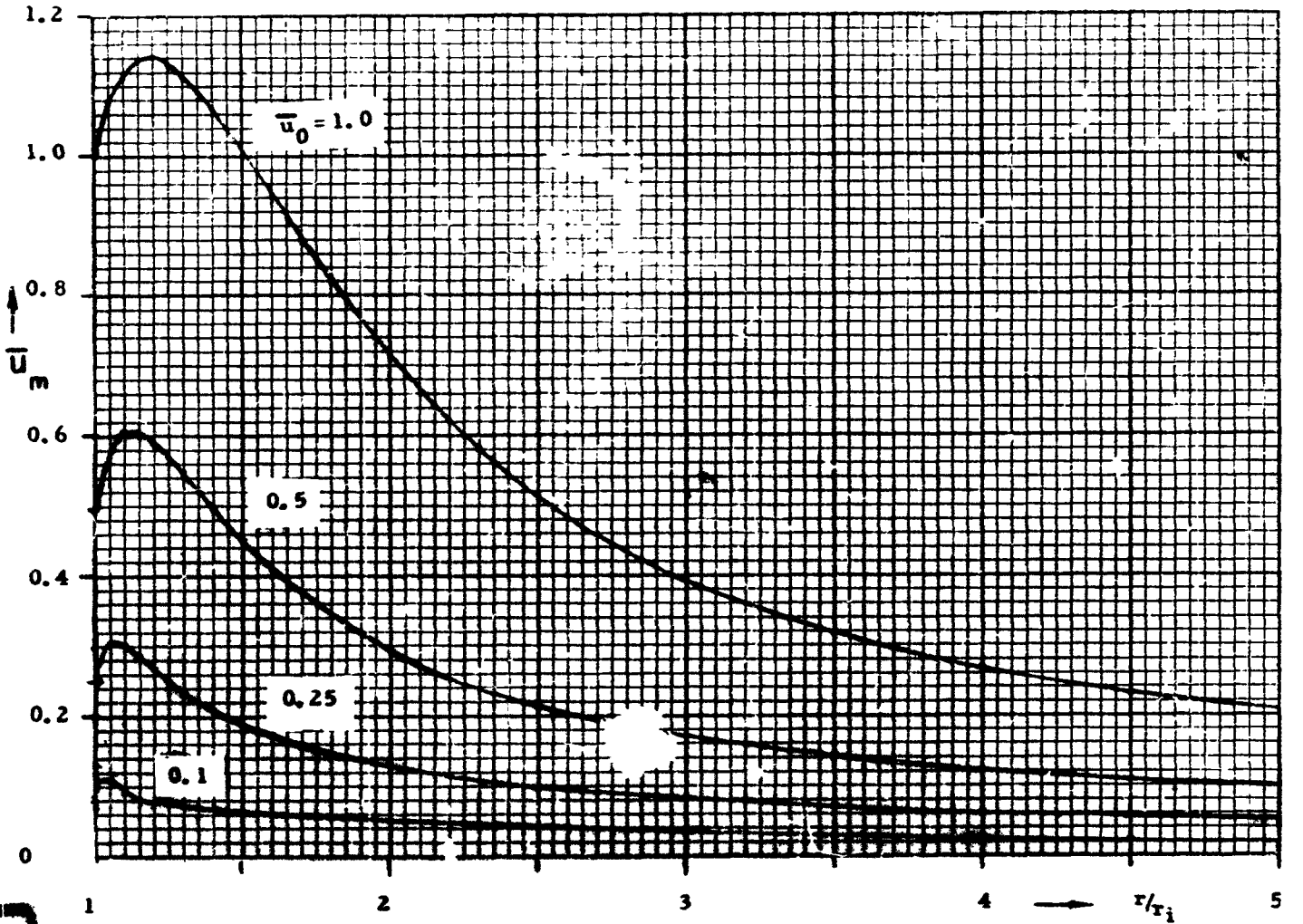

Fig. 24 Radial velocity $\bar{u}_m$ versus r/r_i for $\bar{d} = 2$

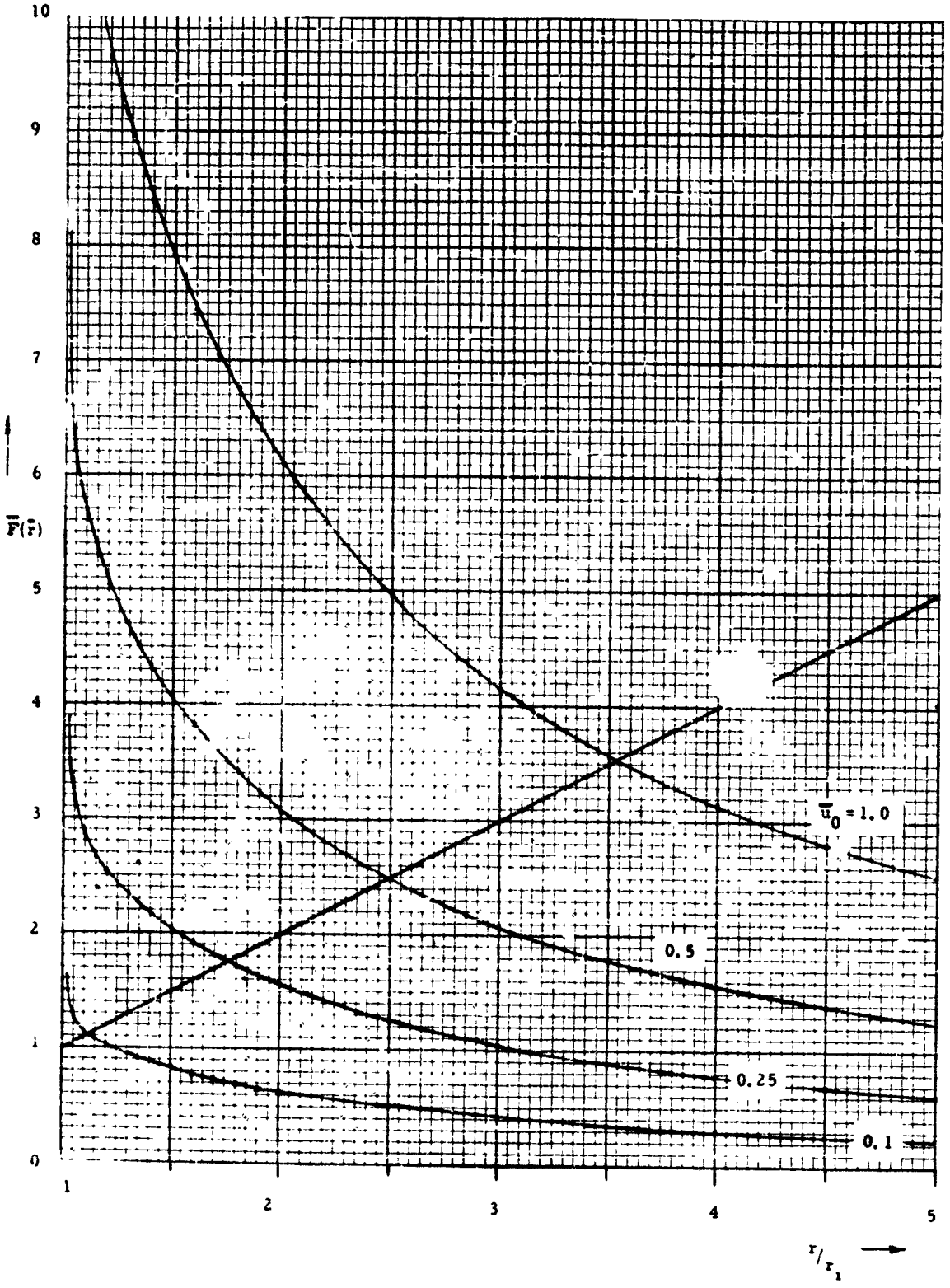

Fig. 25 $F(\bar{r})$ for various values of $\bar{u}_0$ versus r/r_1 for $\bar{d} = 0.5$

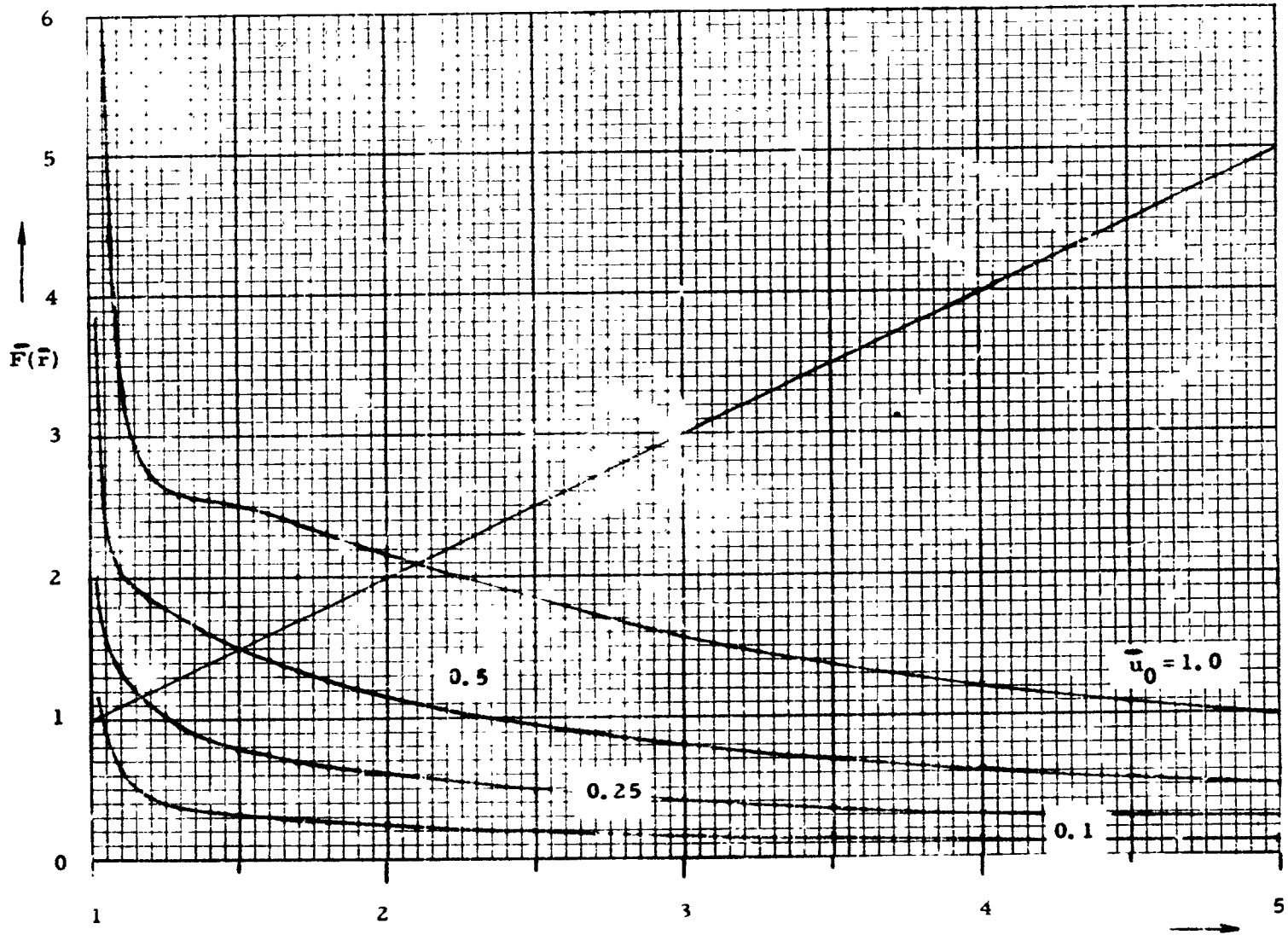

Fig. 26 $\bar{F}(\bar{r})$ for various values o $_0$ versus r/r_i for $\bar{d} = 1.0$ r/r_i

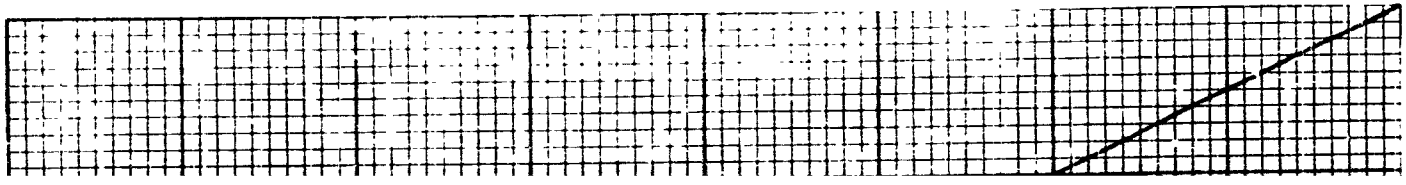

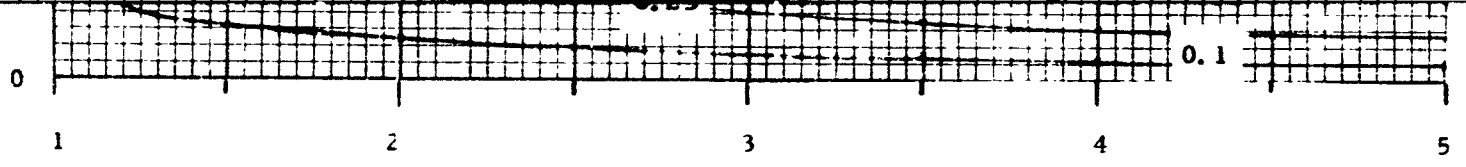

Fig. 26 $\bar{F}(\bar{r})$ for various values of $\bar{u}_0$ versus r/r_i for $\bar{d} = 1.0$

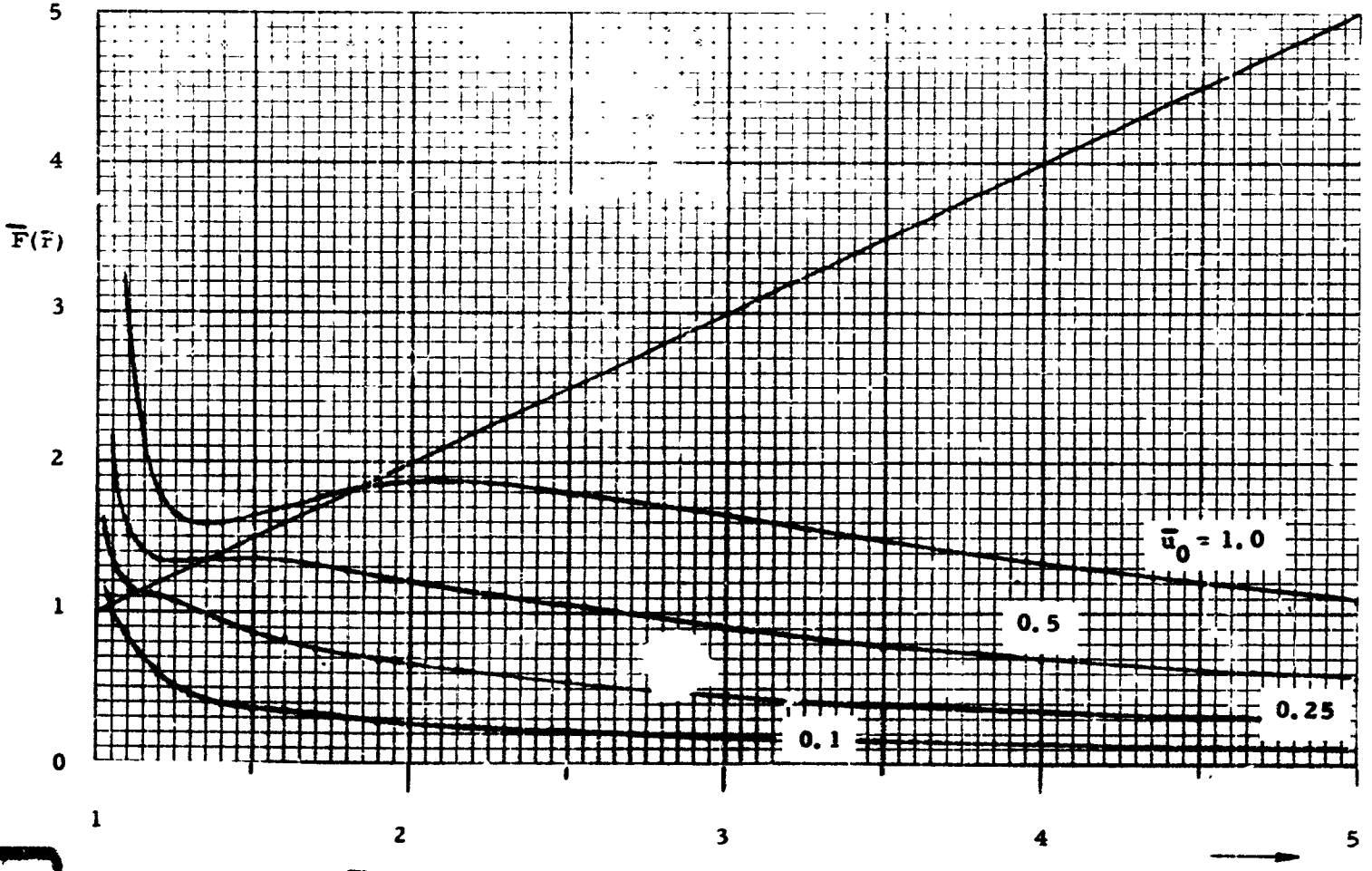

Fig. 27 $\bar{F}(\bar{r})$ for various values of $\bar{u}_0$ versus r/r_i for $\bar{d} = 1.5$

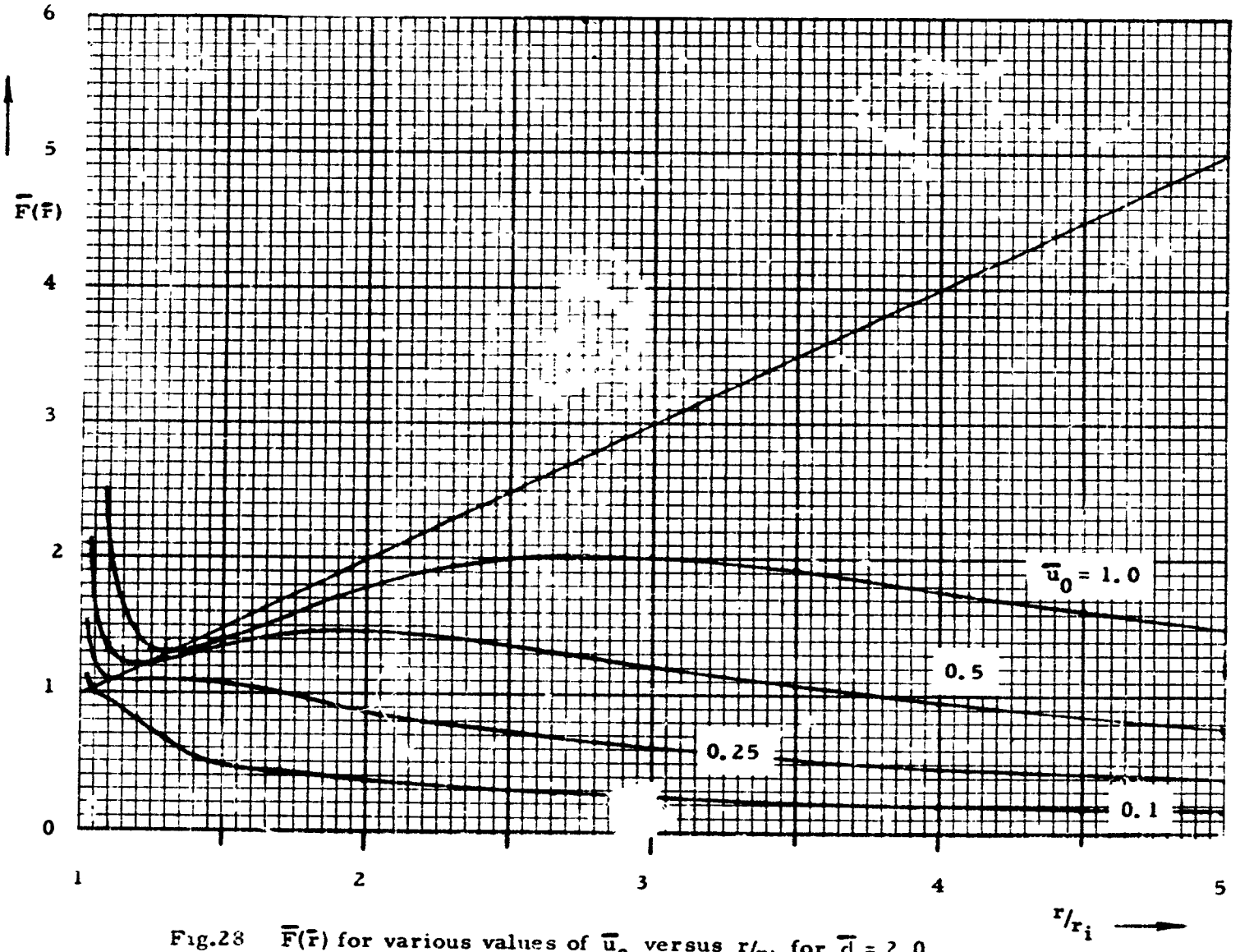

Fig.28 $\bar{F}(\bar{r})$ for various values of $\bar{u}_0$ versus r/r_i for $\bar{d} = 2.0$

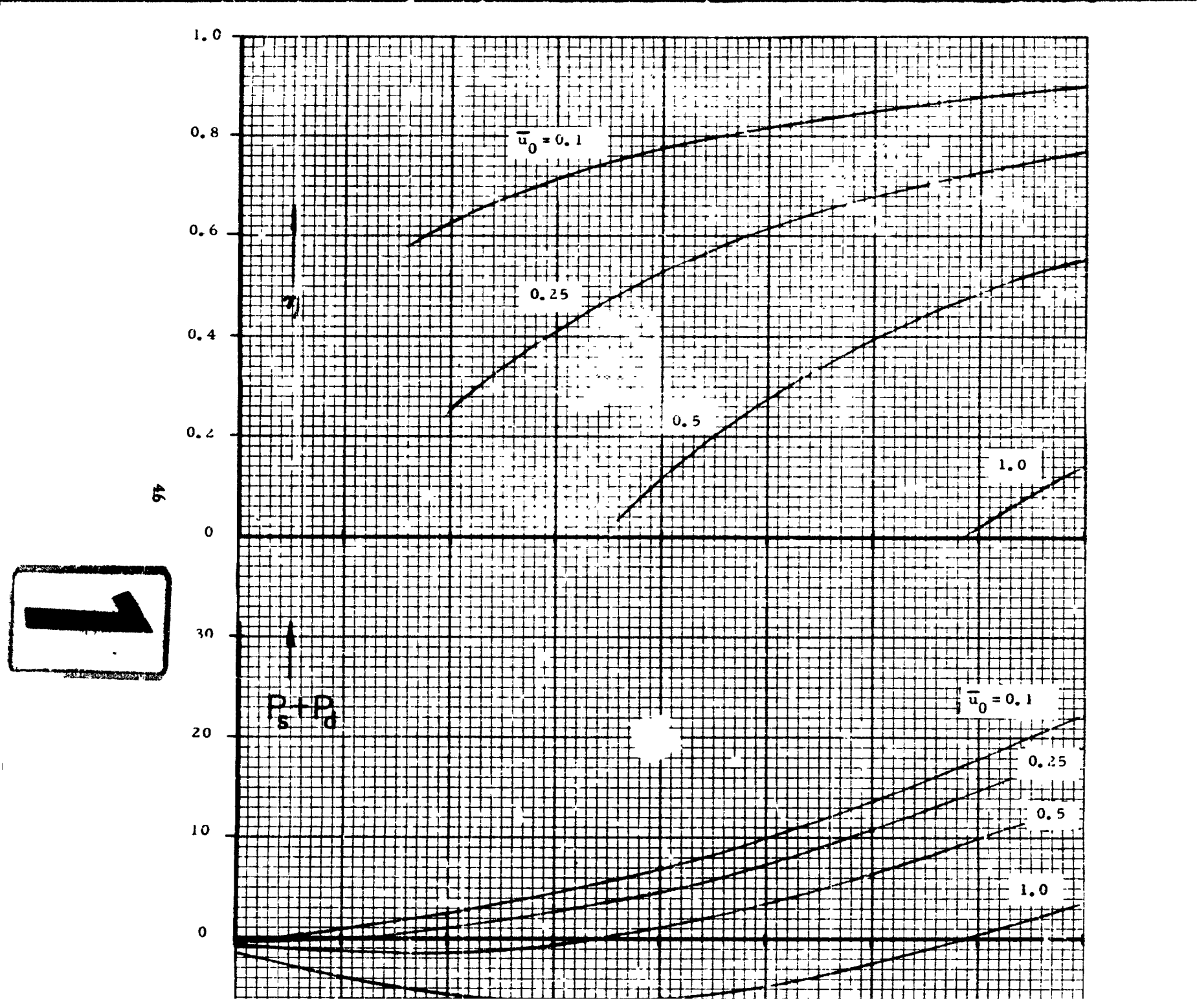
1.0
0.8
0.6
0.4
0.2
0
$\bar{u}_0 = 0.1$
0.25
0.5
1.0
$\frac{y}{\delta}$
30
20
10
0
$P_s + P_d$
$\bar{u}_0 = 0.1$
0.25
0.5
1.0

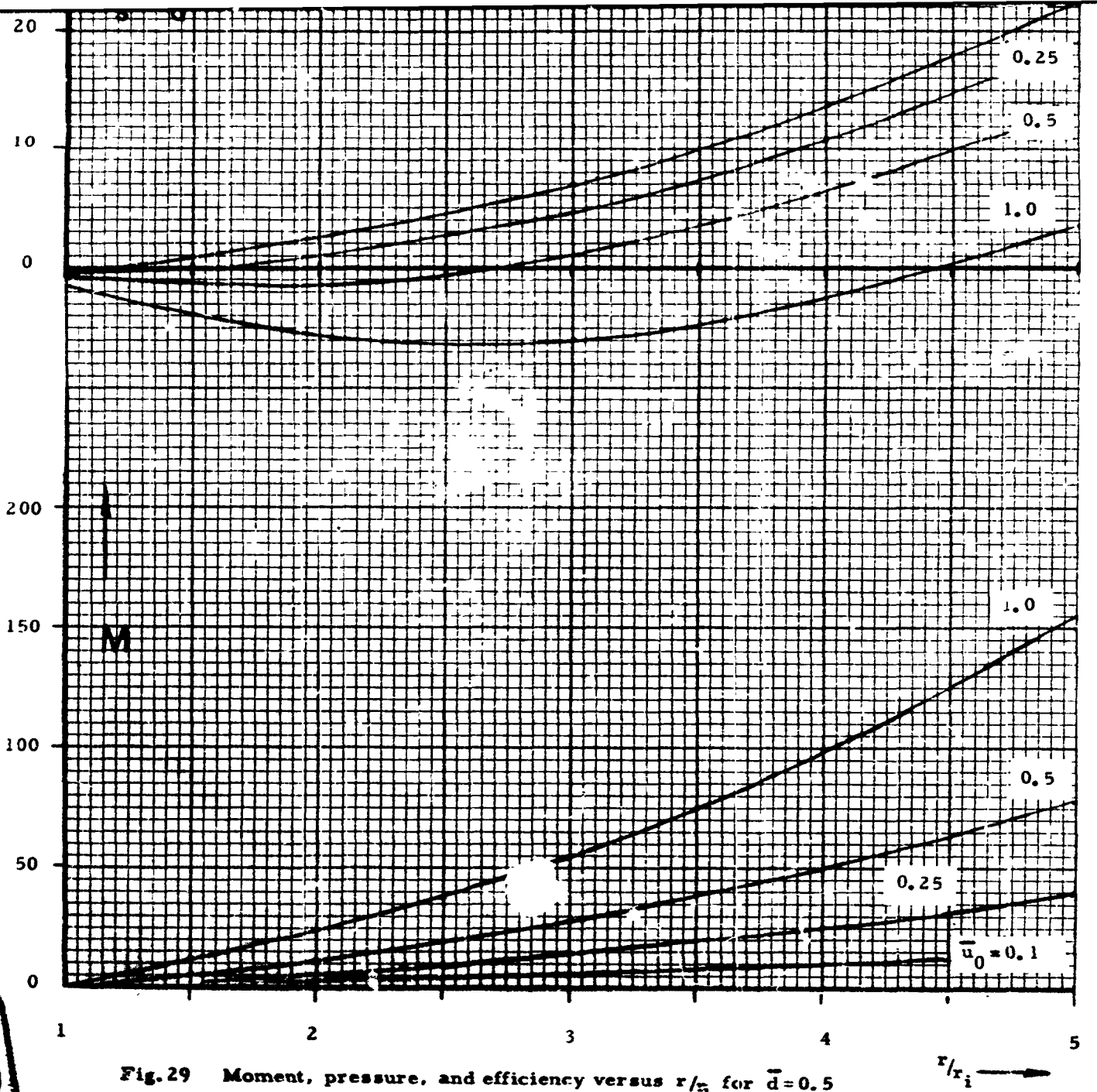

Fig. 29 Moment, pressure, and efficiency versus r/r_i for $\bar{d} = 0.5$

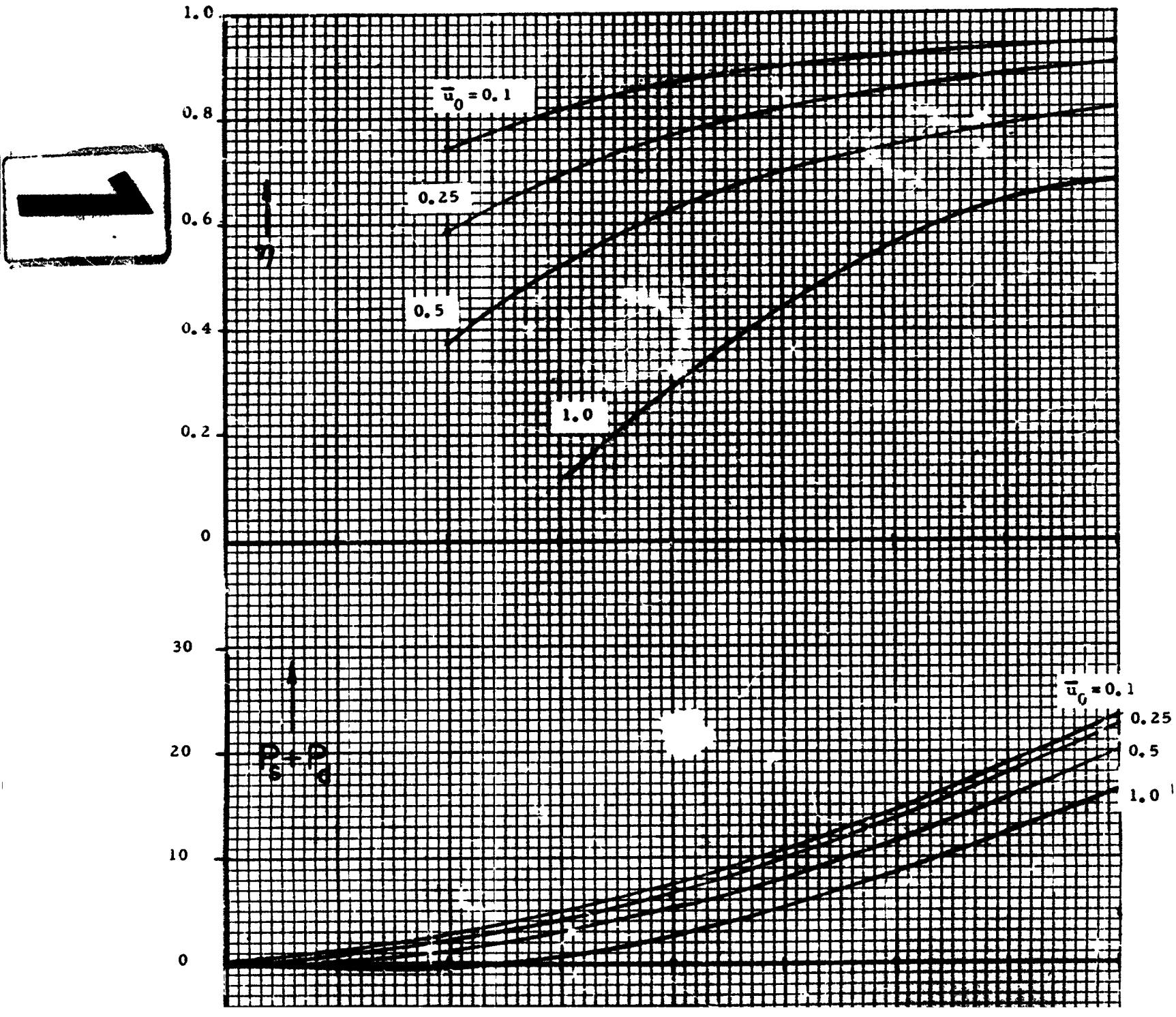
1.0
0.8
0.6
0.4
0.2
0
$\frac{q}{\gamma}$
$\bar{u}_0 = 0.1$
0.25
0.5
1.0
30
20
10
0
$P_s + P_d$
$\bar{u}_0 = 0.1$
0.25
0.5
1.0

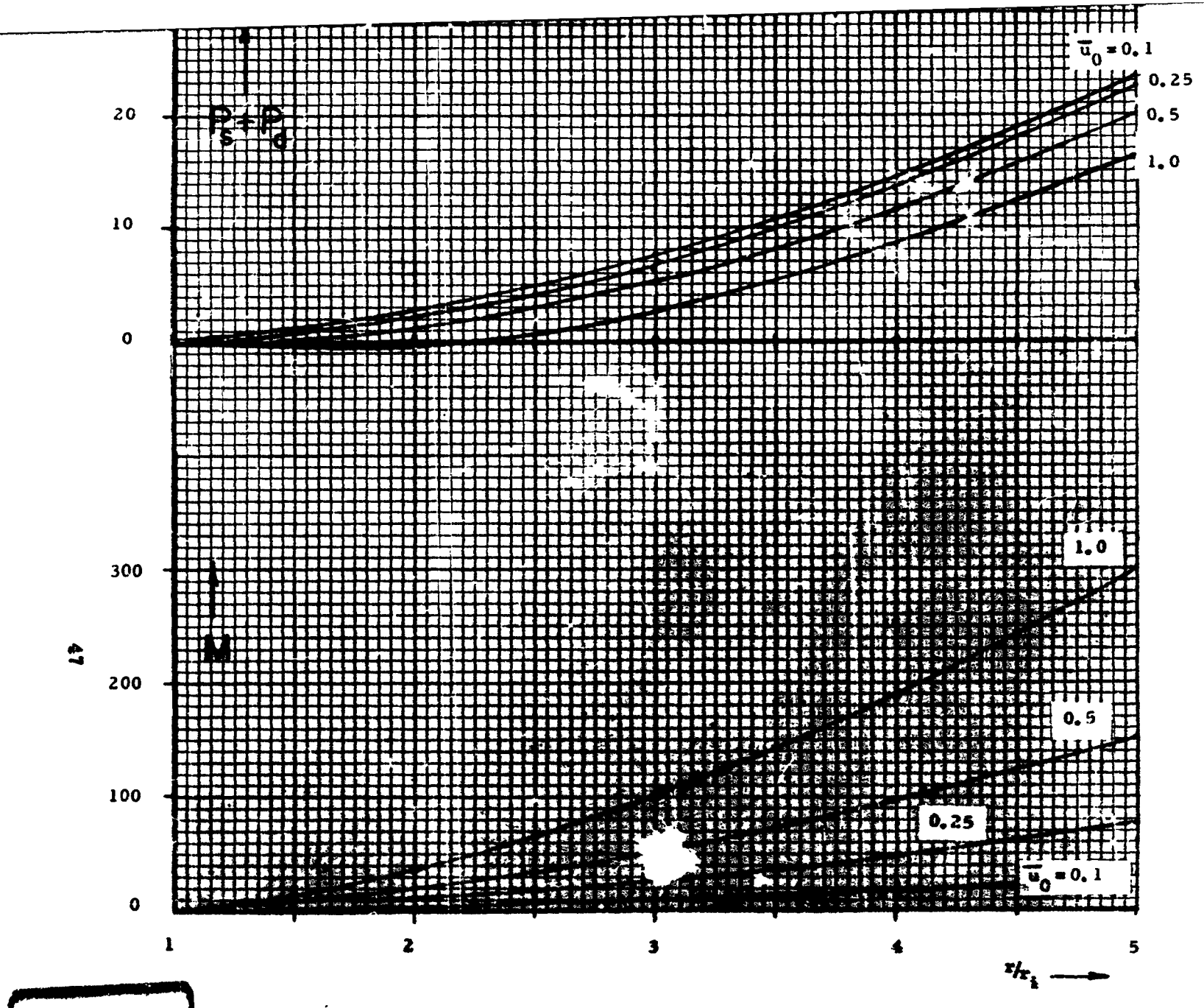

Fig. 30 Moment, pressure, and efficiency versus r/r_i for $\bar{d} = 1.0$

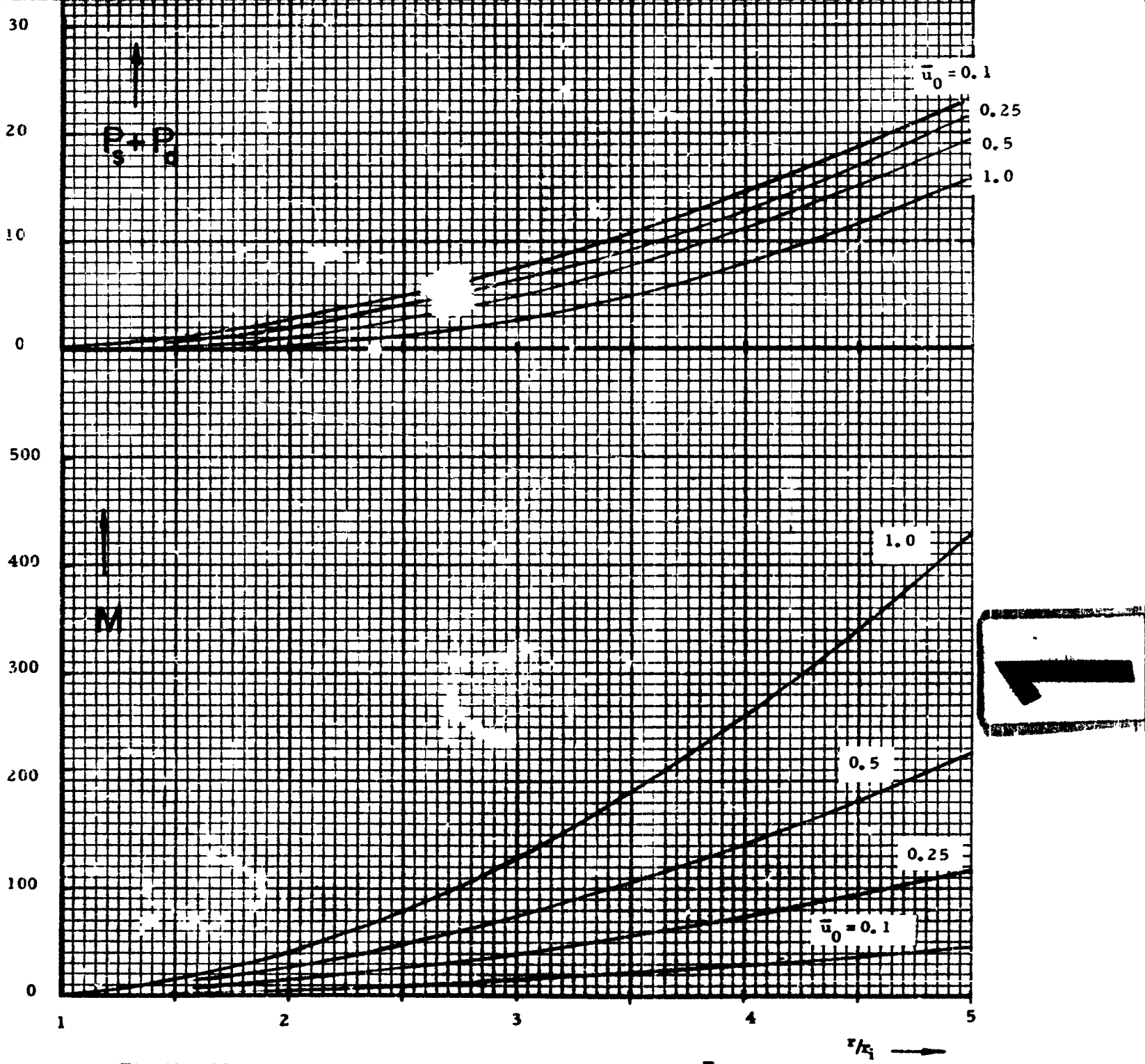

Fig. 31 Moment, pressure, and efficiency versus r/r_i for $\bar{q} = 1.5$

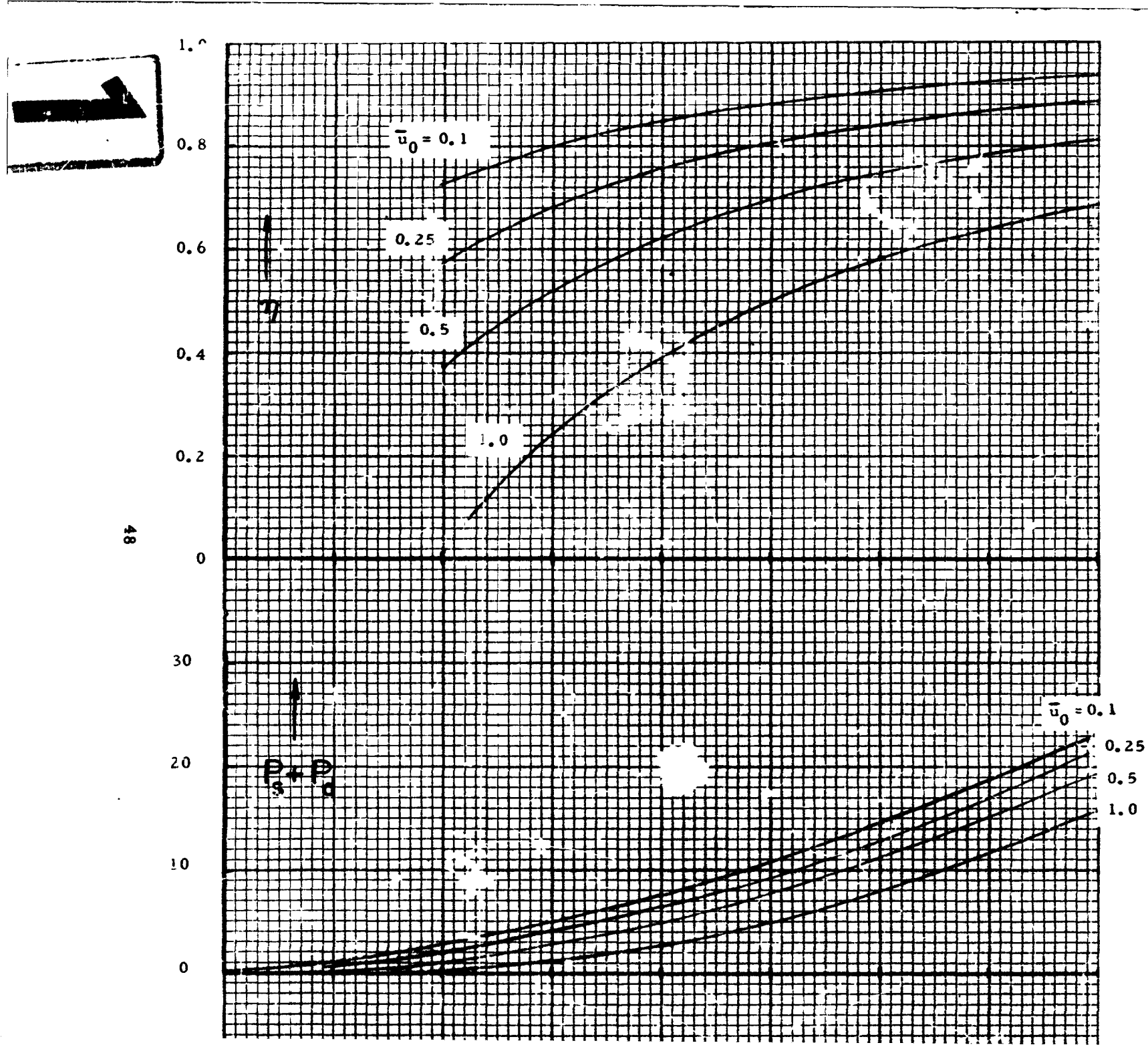
1.0
0.8
0.6
0.4
0.2
0
30
20
10
0
$\bar{u}_0 = 0.1$
0.25
0.5
1.0
η
$P_s + P_d$
$\bar{u}_0 = 0.1$
0.25
0.5
1.0

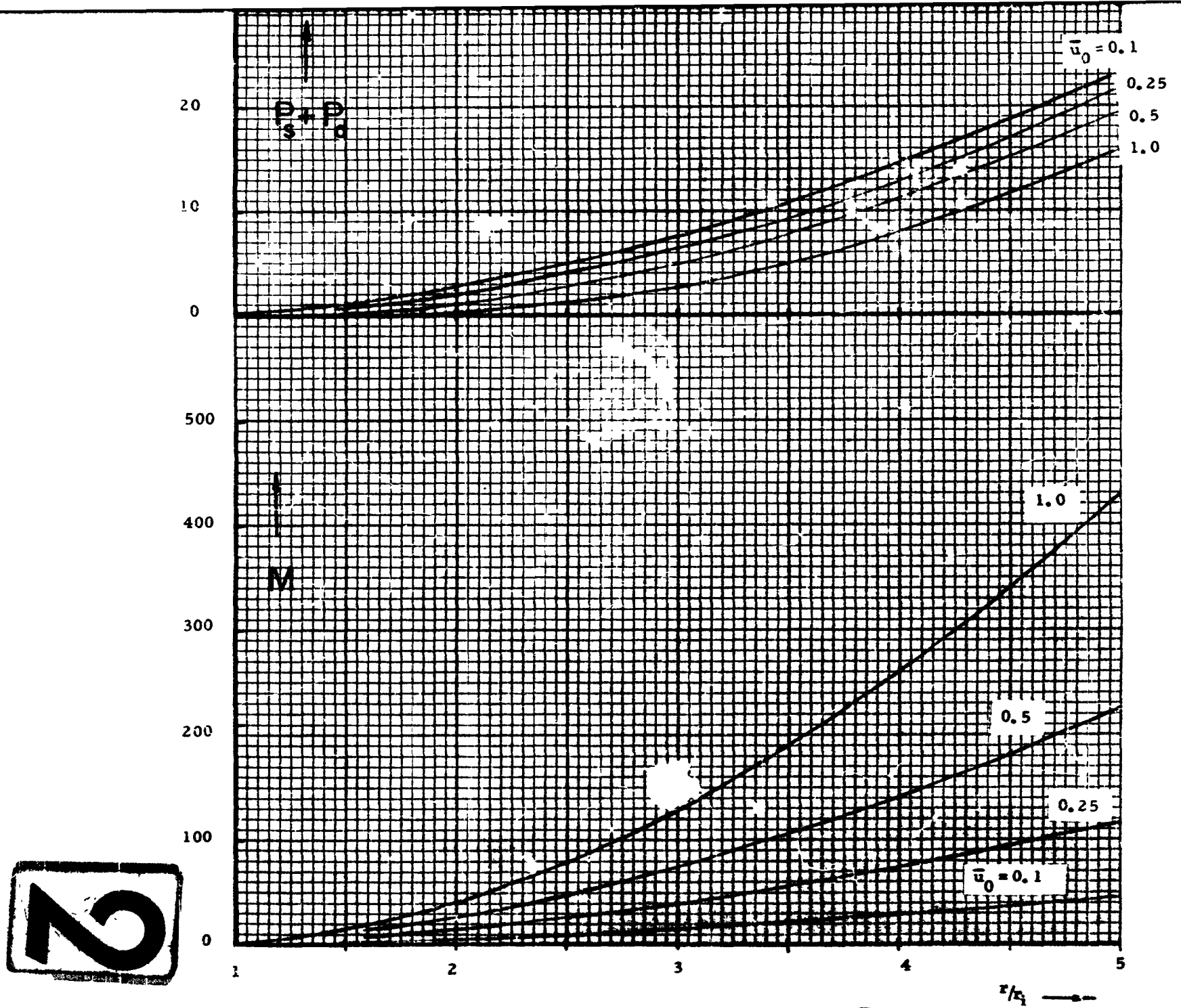

Fig. 31 Moment, pressure, and efficiency versus r/r_i for $\bar{d} = 1.5$

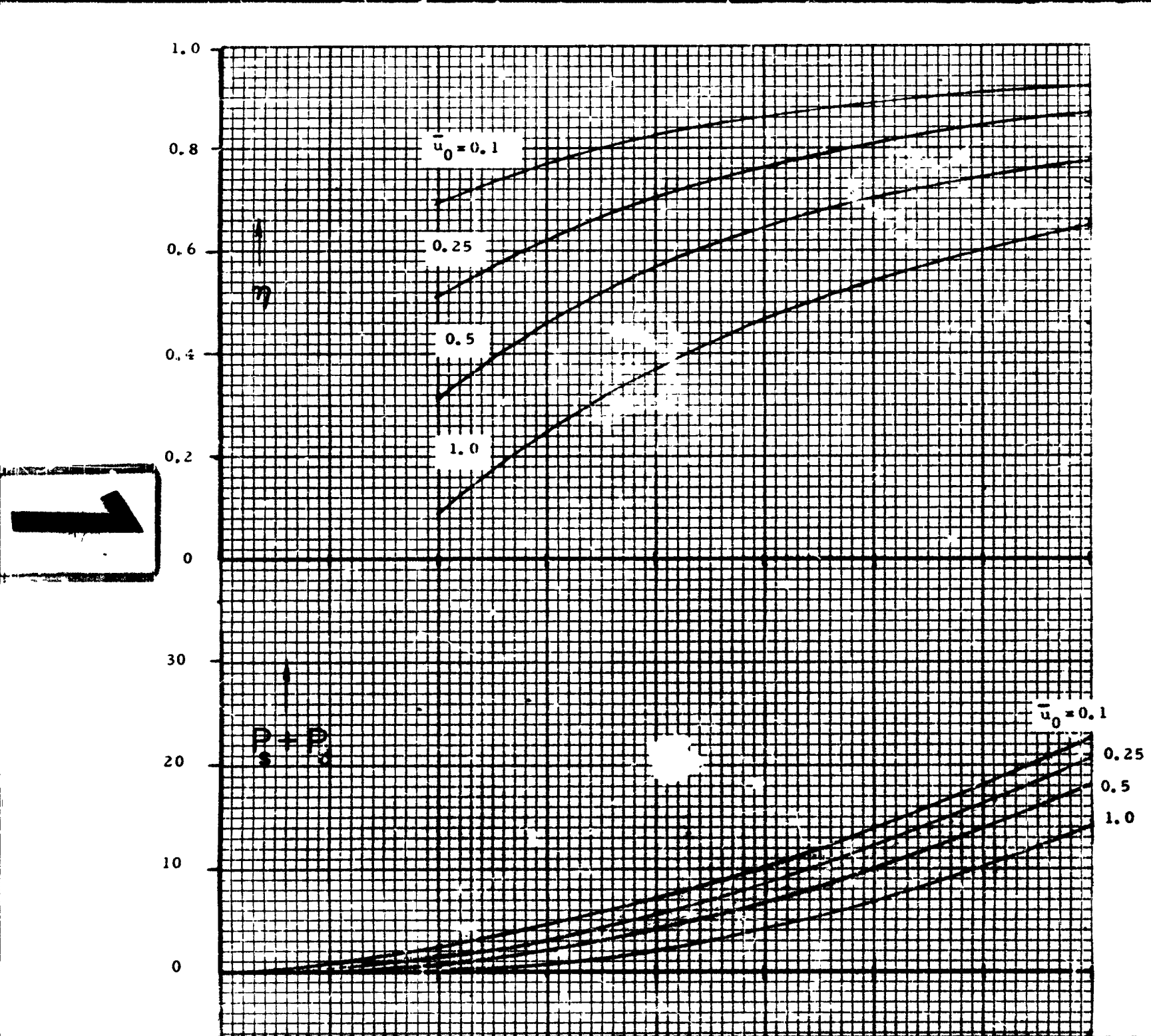
1.0
0.8
0.6
0.4
0.2
0
$\bar{u}_0 = 0.1$
0.25
0.5
1.0
η
30
20
10
0
$\frac{P}{S} \div P_d$
$\bar{u}_0 = 0.1$
0.25
0.5
1.0

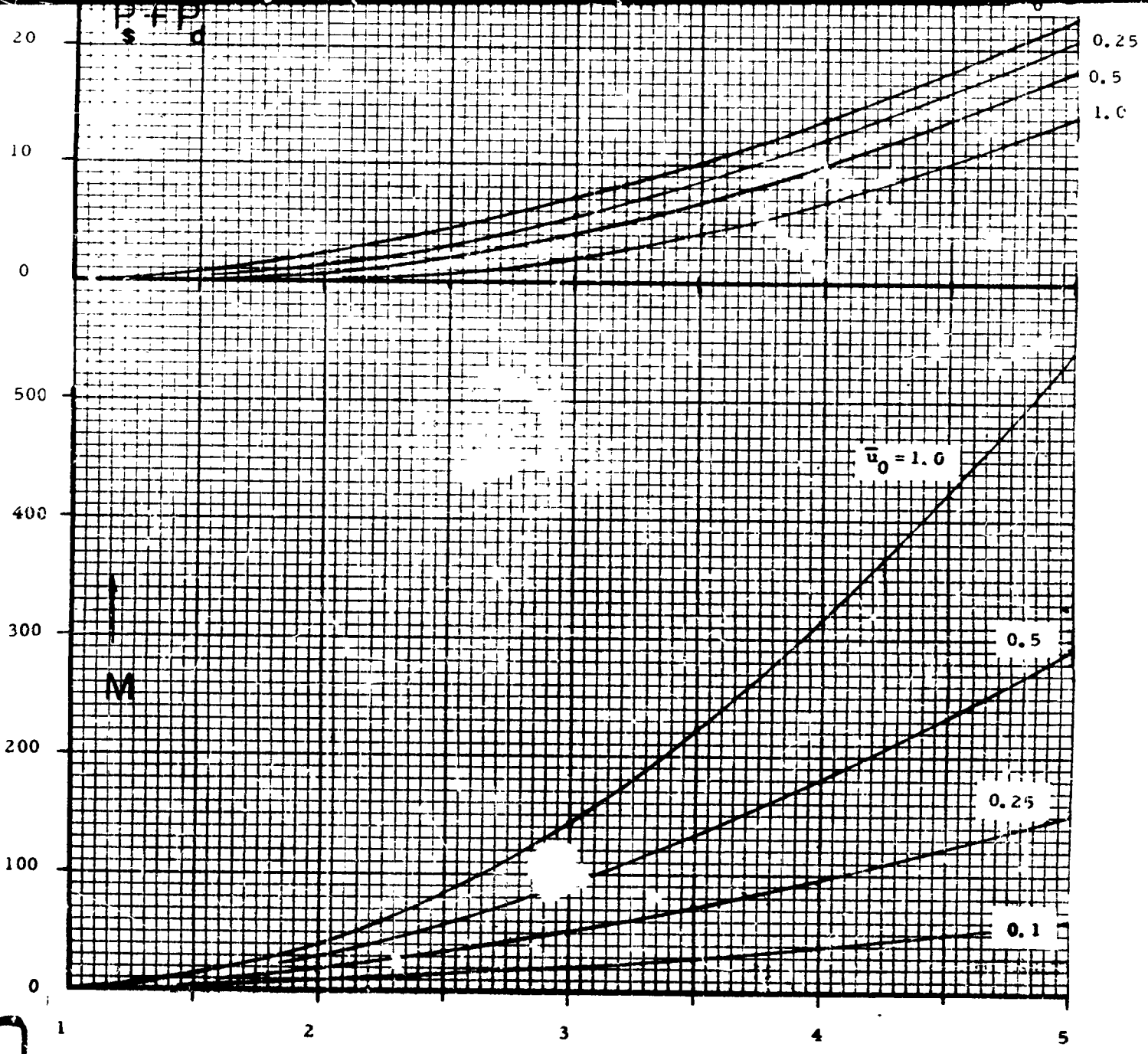

Fig. 32 Moment, pressure, and efficiency versus r/r_i for $\bar{d} = 2.0$

Aeronautical Research Laboratory, Wright Patterson Air Force Base, Ohio. LAMINAR FLOW BETWEEN TWO PARALLEL ROTATING DISKS, by M.C. Breiter and Karl Pohlhausen, March 1962. 49pp. incl. illus. (Project 7071, Task 70437) (ARL 62-318)

Unclassified Report

The report investigates the viscous flow between two parallel disks rotating in the same direction with the same velocity. The fluid enters the space between the two disks at a certain radius in the radial direction. Because of the shear forces, it assumes a rotating motion. The centrifugal forces then build up a pressure increase in the radial direction. The arrangement corresponds to a centrifugal fluid pump, which may be advantages if cavitation is a problem.

The general equations of viscous flow are simplified by boundary layer assumptions and the linearized equations are solved analytically. The velocity profiles depend upon a parameter containing the kinematic viscosity, the angular velocity and the distance of the disks, but not the radius.

The non-linearized parabolic differential equations are approximated by a difference scheme and solved numerically. Furthermore, the efficiency of the pump is computed from the gain of the total pressure and the torque at the shaft of the rotating disks.

(over)

UNCLASSIFIED

I. Project 7071
II. Task 70437
III. Internal Report
IV. Aeronautical Research Laboratory Wright-Patterson AFB, Ohio
V. Breiter, Mark C.
IV. Pohlhausen, Karl

UNCLASSIFIED

Aeronautical Research Laboratory, Wright Patterson Air Force Base, Ohio. LAMINAR FLOW BETWEEN TWO PARALLEL ROTATING DISKS, by M.C. Breiter and Karl Pohlhausen, March 1962. 49pp. incl. illus. (Project 7071, Task 70437) (ARL 62-318)

Unclassified Report

The report investigates the viscous flow between two parallel disks rotating in the same direction with the same velocity. The fluid enters the space between the two disks at a certain radius in the radial direction. Because of the shear forces, it assumes a rotating motion. The centrifugal forces then build up a pressure increase in the radial direction. The arrangement corresponds to a centrifugal fluid pump, which may be advantages if cavitation is a problem.

The general equations of viscous flow are simplified by boundary layer assumptions and the linearized equations are solved analytically. The velocity profiles depend upon a parameter containing the kinematic viscosity, the angular velocity and the distance of the disks, but not the radius.

The non-linearized parabolic differential equations are approximated by a difference scheme and solved numerically. Furthermore, the efficiency of the pump is computed from the gain of the total pressure and the torque at the shaft of the rotating disks.

(over)

UNCLASSIFIED

I. Project 7071
II. Task 70437
III. Internal Report
IV. Aeronautical Research Laboratory Wright-Patterson AFB, Ohio
V. Breiter, Mark C.
IV. Pohlhausen, Karl

UNCLASSIFIED

Aeronautical Research Laboratory, Wright Patterson Air Force Base, Ohio. LAMINAR FLOW BETWEEN TWO PARALLEL ROTATING DISKS, by M.C. Breiter and Karl Pohlhausen, March 1962. 49pp. incl. illus. (Project 7071, Task 70437) (ARL 62-318)

Unclassified Report

The report investigates the viscous flow between two parallel disks rotating in the same direction with the same velocity. The fluid enters the space between the two disks at a certain radius in the radial direction. Because of the shear forces, it assumes a rotating motion. The centrifugal forces then build up a pressure increase in the radial direction. The arrangement corre-

(over)

UNCLASSIFIED

I. Project 7071
II. Task 70437
III. Internal Report
IV. Aeronautical Research Laboratory, Wright-Patterson AFB, Ohio
V. Breiter, Mark C.
IV. Pohlhausen, Karl

UNCLASSIFIED

UNCLASSIFIED

sponds to a centrifugal fluid pump, which may be advantages if cavitation is a problem.

The general equations of viscous flow are simplified by boundary layer assumptions and the linearized equations are solved analytically. The velocity profiles depend upon a parameter containing the kinematic viscosity, the angular velocity and the distance of the disks, but not the radius.

The non-linearized parabolic differential equations are approximated by a difference scheme and solved numerically. Furthermore, the efficiency of the pump is computed from the gain of the total pressure and the torque at the shaft of the rotating disks.

UNCLASSIFIED

Aeronautical Research Laboratory, Wright Patterson Air Force Base, Ohio. LAMINAR FLOW BETWEEN TWO PARALLEL ROTATING DISKS, by M.C. Breiter and Karl Pohlhausen, March 1962. 49pp. incl. illus. (Project 7071, Task 70437) (ARL 62-318)

Unclassified Report

The report investigates the viscous flow between two parallel disks rotating in the same direction with the same velocity. The fluid enters the space between the two disks at a certain radius in the radial direction. Because of the shear forces, it assumes a rotating motion. The centrifugal forces then build up a pressure increase in the radial direction. The arrangement corre-

(over)

I. Project 7071
II. Task 70437
III. Internal Report
IV. Aeronautical Research Laboratory Wright-Patterson AFB, Ohio
V. Breiter, Mark C.
IV. Pohlhausen, Karl

UNCLASSIFIED

UNCLASSIFIED

sponds to a centrifugal fluid pump, which may be advantages if cavitation is a problem.

The general equations of viscous flow are simplified by boundary layer assumptions and the linearized equations are solved analytically. The velocity profiles depend upon a parameter containing the kinematic viscosity, the angular velocity and the distance of the disks, but not the radius.

The non-linearized parabolic differential equations are approximated by a difference scheme and solved numerically. Furthermore, the efficiency of the pump is computed from the gain of the total pressure and the torque at the shaft of the rotating disks.

UNCLASSIFIED